Hungarian University of Agriculture and Life Sciences

Pathogenesis and biological control of fungal pathogens in garlic (*Allium sativum* L.), with a comparative analysis of host defense responses in garlic and okra (*Abelmoschus esculentus* (L.) Moench)

Doctoral Dissertation (PhD.)

Samara Ounis

Gödöllő

2025

The PhD School

Name	Doctoral School of Agriculture and Food Sciences
Discipline	Integrated Plant Protection
Head	Prof. Dr. Melinda Kovács, Professor, MHAS, Head of the Doctoral School of Agriculture and Food Sciences, Hungarian University of Agriculture and Life Sciences
Doctoral Program	Prof. Dr. Zoltán Pék, Professor, Head of Doctoral Program of Plant Science Hungarian University of Agriculture and Life Sciences
Supervisor	Dr. Turóczi György Associate Professor, Plant Protection Institute, Department of Integrated Plant Protection, Hungarian University of Agriculture

.....	.....
Approval of the Head of the Doctoral Program	Approval of the Supervisor
Prof. Dr. Zoltán Pék	Dr. Turóczi György

.....
Approval of the Head of the Doctoral School

Prof. Dr. Melinda Kovács

TABLE OF CONTENTS

LIST OF ABBREVIATIONS

ROS	Reactive oxygen species
PPO	Polyphenol oxidase
POX	Guaiacol peroxidase
PDA	Potato Dextrose Agar
SDA	Sabouraud Dextrose Agar
CDA	Czapek-Dox Agar
MEA	Malt Extract Agar
NA	Nutrient Agar
Df	Distance *Fusarium* grows towards *Stromatinia*
Cf	Mean radial growth of *Fusarium* control plates
Ds	Distance *Stromatinia* grows towards *Fusarium*
Cs	Mean radial growth of *Stromatinia* control plates
DI	Disease incidence
cv.	Cultivar
D1	Pathogen growth in absence of antagonist
D2	Pathogen growth in presence of antagonist
Tris-HCl	Tris(hydroxymethyl)aminomethane hydrochloride
EDTA-Na_2	Ethylenediaminetetraacetic acid disodium salt
PVP K25	Polyvinylpyrrolidone K25
PVPP	Polyvinylpolypyrrolidone
BLAST	Basic Local Alignment Search Tool
ITS	Internal Transcribed Spacer sequencing
ANOVA	Analysis of Variance
SE	Standard Error
SD	Standard Deviation
C	Control
TF	*Trichoderma* × *Fusarium*
BF	*Bacillus* × *Fusarium*

TBF	*Trichoderma* + *Bacillus* × *Fusarium*
TS	*Trichoderma* × *Stromatinia*
BS	*Bacillus* × *Stromatinia*
TBS	*Trichoderma* + *Bacillus* × *Stromatinia*
FS	*Fusarium* × *Stromatinia*
Sc	*Sclerotinia*
TSc	*Trichoderma* + *Sclerotinia*
BSc	*Bacillus* + *Sclerotinia*
TBSc	*Trichoderma* + *Bacillus* + *Sclerotinia*
ScR	*Sclerotinia* × *Rhizoctonia*
TR	*Trichoderma* × *Rhizoctonia*
BR	*Bacillus* × *Rhizoctonia*
TBR	*Trichoderma* + *Bacillus* × *Rhizoctonia*
IPM	Integrated Pest Management

CHAPTER 1: INTRODUCTION

Garlic (*Allium sativum* L.) is one of the most important vegetables and spice crops worldwide. It is renowned for its extensive use in cuisines around the world and its medicinal properties, attributed to compounds such as allicin (Amarakoon and Jayasekara, 2017). The global cultivation of garlic, along with onion, underscores its economic and nutritional value with an annual production exceeding 28 million tons in 2021, with China leading in production, followed by India (FAOSTAT, 2021). Although the crop is mainly cultivated for its cloves for culinary use, it also exhibits a wide spectrum of human health benefits, including antioxidant, antimicrobial and anticancer activities (Kovarovič et al., 2019). When extracted and isolated, the bioactive compounds of garlic show a wide range of beneficial human health effects to treat various infectious diseases, non-communicable diseases, as well as metabolic and genetic disorders (Amarakoon and Jayasekara, 2017). Beyond culinary and medicinal applications, garlic's allelochemicals show promise as sustainable agricultural biostimulants, enhancing crop quality and resistance against pathogens (Hayat et al., 2018).

Similarly, okra (*Abelmoschus esculentus* L.) is another valuable crop vulnerable to fungal pathogens. It is widely cultivated for its nutritional value and economic importance in tropical and subtropical regions. Globally, okra production has expanded significantly, rising from 1.8 million tonnes in 1972 to 11.2 million tonnes in 2022, with India alone accounting for more than 60% of the total (FAOSTAT, 2022). Other major producers include Nigeria, Mali, Pakistan, Sudan, and Côte d'Ivoire. Its young fruits are consumed as a vegetable rich in vitamins, minerals, and fibre, while its seeds and leaves are valued for their antidiabetic, antioxidant, and antimicrobial properties (Adebooye and Oputa, 1996, Ardestani et al., 2020). However, like garlic, its productivity is constrained by soil-borne fungal diseases that severely reduce yield and postharvest quality (Ounis et al., 2025).

Soil-borne fungal pathogens are particularly destructive in garlic production, with *Stromatinia cepivora* Berk. 1841 and *Fusarium proliferatum* (Matsush.) Nirenberg ex Gerlach & Nirenberg (1982) being the most significant. *Stromatinia cepivora* (anamorpha *Sclerotium cepivorum*) is an economically significant pathogen that causes white rot disease in garlic and other *Allium* species (Hanci, 2018). This disease was first reported in Hungary in 2011 (Bakonyi et al., 2011). *Stromatinia cepivora* is a major limiting pathogen for onion and garlic production worldwide due to its ability to cause large yield and quality losses (Coley-Smith, 1987, Crowe et al., 1980). This pathogen is distinguished by its sclerotia, which can survive in the soil for several years, thus limiting the use of infected fields in a rotation system (Coley-Smith, 1987, Crowe et al., 1980, Wu

et al., 2010). These sclerotia germinate in response to volatile organic compounds from *Allium* root exudates, initiating infection (King and Coley-Smith, 1969). White rot symptoms typically appear from mid-season to harvest, starting with yellowing and wilting of the leaves, followed by white mycelial growth on the bulb surface or at the crown of seedlings (Fullerton and Stewart, 1991). As the infestation progresses, the root system is destroyed, leading to plant collapse. Infected bulbs often exhibit white, fluffy fungal growth, similar to cotton wool, with small black sclerotia interspersed (Sammour et al., 2011). The pathogen's resilience and long dormancy of the sclerotia, enabling them to persist in the soil until a suitable host becomes available, make it extremely difficult to manage (Wu et al., 2010).

Among soil-borne fungal pathogens of garlic, *Fusarium proliferatum* (Matsushima) Nirenberg is of particular concern due to its widespread occurrence and significant impact on *Allium* crop production (Llamas et al., 2013). This species is associated with basal plate rot and bulb rot in garlic, leading to substantial economic losses both in the field and during post-harvest storage (Leyronas et al., 2018, Tonti et al., 2012). Other *Fusarium* species, including *F. oxysporum*, *F. culmorum*, and *F. solani*, have also been reported on garlic (Matuo et al., 1986, Moharam et al., 2013, Rengwalska and Simon, 1986), but *F. proliferatum* is of greater concern due to its broader host range and adaptability across diverse climatic zones. It infects not only garlic but also other *Allium* crops such as onions and leeks, reflecting its capacity to persist and spread in different agro-ecological systems (Medina et al., 2017, Palmero et al., 2010).

The pathogen was first reported as the causal agent of garlic bulb rot in 1999 in Hungary during winter storage (Simay, 1990). Since then, *F. proliferatum* has been identified in garlic crops across multiple regions, including Germany (Seefelder et al., 2002), Serbia (Stankovic et al., 2007), Spain (Palmero et al., 2010), and Italy (Tonti et al., 2012). The symptoms of garlic rot caused by *F. proliferatum* include dry, brown necrotic spots that develop on the surface of the cloves and can progress inward. In severe cases, white mycelium and water-soaked lesions can also occur (Tonti et al., 2012, Wang et al., 2022). The pathogen often colonises garlic roots during the growing season and remains latent, causing substantial postharvest losses as rot develops in storage (Leyronas et al., 2018, Llamas et al., 2013, Tonti et al., 2012), where conditions such as temperature significantly influence the progression of the disease (Moharam et al., 2023). Furthermore, *F. proliferatum* is a significant mycotoxigenic species, producing toxins such as fumonisins (FB1, FB2, and FB3), moniliformin, beauvericin, fusaric acid, and fusaproliferin, all of which present a high risk to food safety (Desjardins, 2006, Li et al., 2017).

In addition to garlic pathogens, okra is highly susceptible to soil-borne fungal diseases caused by *Sclerotinia sclerotiorum* (Lib.) de Bary (1884) and *Rhizoctonia solani* J.G. Kühn (1858).

Sclerotinia sclerotiorum is a necrotrophic fungal pathogen with a broad host range, including okra, and causes white mold or pod rot disease. This pathogen produces long-lived sclerotia that allow it to survive adverse conditions and infect plants under favourable environmental circumstances. In okra, infection leads to water-soaked lesions, pod rot, and fluffy white mycelium interspersed with black sclerotia, similar to cottony growth (Prova et al., 2017). The pathogen infects more than 400 plant species and thrives in cool, moist conditions, where ascospores released from the apothecia germinate and colonize plant tissues (Bolton et al., 2006).

Rhizoctonia solani is a soilborne necrotrophic fungus that causes root rot and damping in okra, especially in seedlings and post-harvest conditions. Symptoms include brown necrotic lesions at the base of the stem and roots, wilting, reduced growth, and in severe infections, plant death. This pathogen may also cause foliar blight under conducive conditions (Henz et al., 2007, Anees et al., 2016). The pathogen persists in the soil via sclerotia and mycelia and often forms disease complexes with nematodes such as *Meloidogyne incognita*, exacerbating plant damage (Sharma, 2015).

Managing these pathogens is challenging. While chemical fungicides provide initial control, their long-term efficacy is limited by pathogen resistance, environmental hazards, and high application costs (Coşkuntuna and Özer, 2008, Rajendran and Ranganathan, 1996). Biological control agents have emerged as sustainable alternatives. Recent advances have shown promising results using *Trichoderma* and *Bacillus* species as biological control agents specifically for garlic. *Trichoderma harzianum* and *Bacillus subtilis* have significantly reduced the incidence of white rot and basal rot in garlic, and both agents individually reduced disease severity and increasing yields in field trials (Lee et al., 2006). Although *Trichoderma* and *Bacillus* were less effective when combined, they still contributed to increased disease tolerance and higher yields under greenhouse conditions (Poromarto et al., 2022). Furthermore, triple applications of *Trichoderma harzianum*, *T. koningii*, and *T. virens* demonstrated improved control of garlic white rot under low disease pressure, achieving results comparable to chemical fungicides (Elshahawy et al., 2019). Furthermore, integrated approaches that combine these bioagents with chemical treatments further enhance efficacy (Dilbo et al., 2015). Consequently, the development of genetically resistant cultivars has been recognised as the most sustainable strategy for the management of soil-borne diseases (Fang et al., 2019, Gordon, 2017, Wille et al., 2019).

Understanding plant defense mechanisms is essential for improving such strategies. Oxidative enzymes such as guaiacol peroxidase (POX) and polyphenol oxidase (PPO) are widely measured as indicators of plant immune activation (Zafar et al., 2020). These enzymes play crucial roles in strengthening cell walls (Bala et al., 2016), scavenging reactive oxygen species (ROS) (Mayer et

al., 2017), and inhibiting pathogen proliferation (Mohammadi and Kazemi, 2002). Monitoring POX and PPO activities in garlic and okra has proven particularly useful in assessing the effectiveness of biocontrol agents, as increased enzyme activity correlates with enhanced immune responses under conditions of biotic and abiotic stress (Khorrami et al., 2014, Hong et al., 2007). Elevated enzyme activity is typically correlated with enhanced resistance levels and reduced disease severity (Mohammadi and Kazemi, 2002). Therefore, these biochemical markers serve not only as defense effectors but also as valuable diagnostic tools in resistance breeding and evaluation of biological treatments (Khorrami et al., 2014, Zafar et al., 2020).

A further complication in disease management is the simultaneous presence of multiple soil-borne pathogens. It is well documented that simultaneous infections by multiple pathogens are a common phenomenon in agriculture (Abdullah et al., 2017, Tollenaere et al., 2016). Previous research has shown that host plants infected by multiple pathogens experience more severe disease impacts than those affected by a single pathogen (Abdullah et al., 2017, Susi et al., 2015, Wille et al., 2019). Given that *F. proliferatum* and *S. cepivora* were observed to co-occur, this study hypothesizes that their interactions could influence infection dynamics and disease progression. Understanding these interactions is essential for improving resistance screening methodologies and developing effective disease management strategies against multipathogen infestations.

Despite advances in breeding for single-pathogen resistance, such resistances often fail under field conditions where co-infections are common (Tollenaere et al., 2016, Wille et al., 2019). This study addresses the critical gap in understanding the interactions between *F. proliferatum* and *S. cepivora* and expands the investigation to include okra pathosystems involving *S. sclerotiorum* and *R. solani*. It aims to develop more effective, economically viable, and environmentally sustainable disease management strategies through multipathogen resistant cultivars and effective biocontrol integration.

Objectives:

This work aims to (1) accurately identify the pathogenic fungi behind garlic bulb rot and white rot, (2) investigate the dynamics of their co-occurrence and pathogen–pathogen interactions, (3) evaluate the resistance of eleven garlic cultivars to single and simultaneous infections, (4) evaluate the effectiveness of *Trichoderma asperellum* Samuels, Lieckf., & Nirenberg (1999) and *Bacillus amyloliquefaciens* Fukumoto (1943) as biocontrol agents against garlic and okra pathogens, and (5) analyse the activation of POX and PPO enzymes in both host plants to elucidate biochemical responses under biotic stress.

CHAPTER 2: LITERATURE REVIEW

2.1. Garlic (*Allium sativum* L.)

2.1.1. Global production and economic importance

According to FAOSTAT (2023), global garlic production was estimated at approximately 28.68 million tons, grown on an area of 1.69 million hectares, with an average yield of 16.96 tons per hectare. The main garlic producing countries include China, India, Bangladesh, and Egypt, with China and India serving as the dominant contributors, collectively accounting for approximately 85% of total global production.

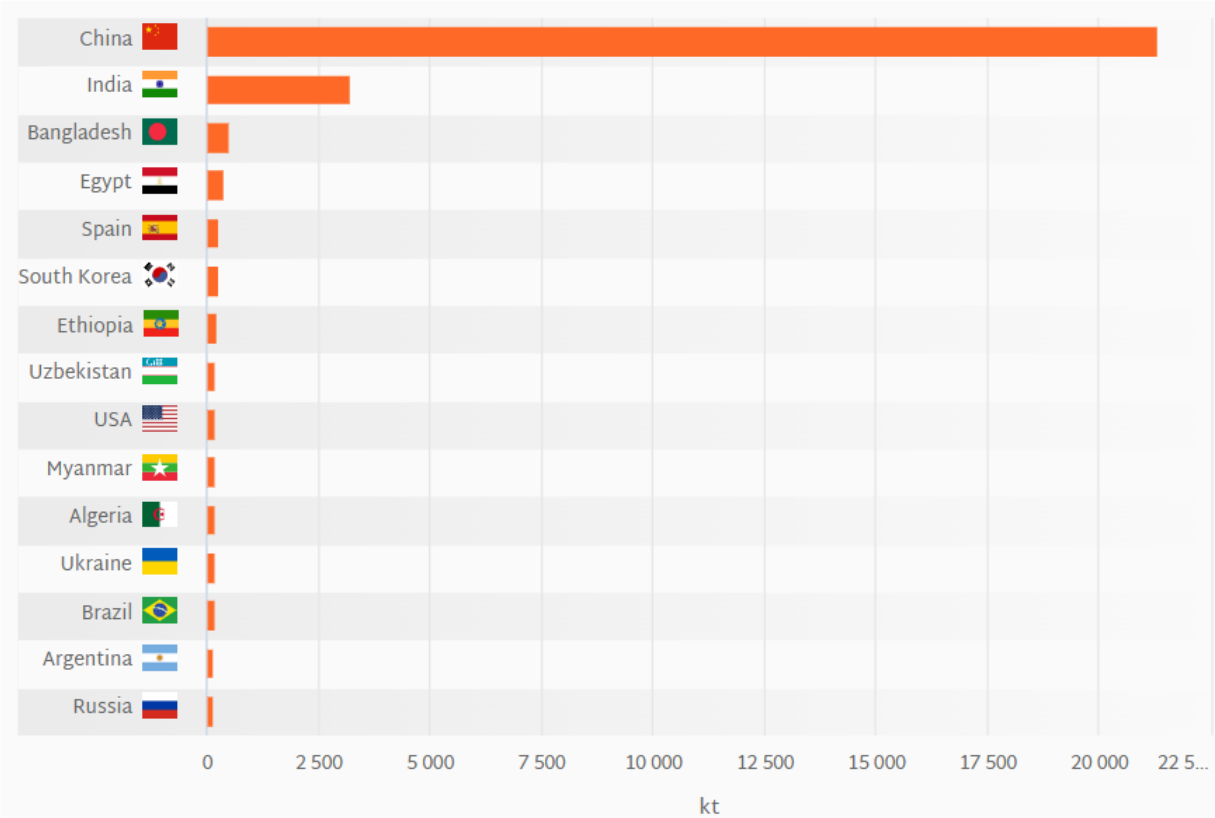

Figure 1: Global garlic production by country in 2023 (kilotons, kt). Image from Helgi Library (2024), data sourced from FAOSTAT (2023).

2.1.2. Benefits and uses

Garlic (*Allium sativum* L.) is a multifunctional crop with applications extending beyond its culinary significance to medicine, agriculture, and biotechnology. The following sections highlight the medicinal, culinary, and plant protection applications of garlic, emphasising its economic importance.

2.1.2.1. Medicinal and health benefits

The medicinal value of garlic has been recognized since ancient civilizations, including Egypt, Greece, Rome, and China, where it was used to treat respiratory, digestive, and circulatory ailments (Kovarovič et al., 2019). Historical accounts indicate that Greek Olympic athletes consumed garlic to improve physical endurance (Afzal et al., 2000). The first major chemical investigation of garlic in the 19th century led to the discovery of allicin as its primary bioactive antimicrobial compound in 1944 (Gruhlke et al., 2015).

Garlic is a rich source of antioxidants, including polyphenols, flavonoids, and sulphur metabolites, which neutralise free radicals and reduce oxidative stress (Benkeblia, 2005, Petropoulos et al., 2020). The high radical-scavenging activity of garlic is linked to its sulphur compounds, particularly diallyl sulphides (Avgeri et al., 2020). These compounds contribute to immune system support and cell protection against oxidative damage (Santhosha et al., 2013).
Garlic has been studied for its potential role in cardiovascular health, and research indicating its ability to regulate blood pressure and improve circulation (Rahman and Lowe, 2006). The presence of bioactive sulphur compounds in garlic has also been associated with the regulation of lipid metabolism, which may contribute to cholesterol reduction (Benkeblia, 2005).

Furthermore, garlic plays a role in metabolic health, and studies suggesting that it has immune-boosting, antidiabetic, and cardioprotective activities (Fong, 2002, Amira and Okubadejo, 2007). The presence of saponins in garlic has also been associated with anti-inflammatory and anticancer properties (Matsuura, 2001). Overall, the therapeutic efficacy of garlic is primarily attributed to its phytochemical profile, which includes organosulfur compounds (alliin, allicin, ajoene, thiosulfinates), polyphenols, flavonoids, vitamins (A, B1, B2, B6, C), and minerals (Ca, Fe, I, K, Mg, Na, Zn) (Kovarovič et al., 2019). Conversion of alliin to allicin upon tissue damage initiates a biochemical cascade, producing reactive bioactive metabolites (Puvača et al., 2014).
Garlic also contains fructans, allinase, arginine, and fibre, which further contribute to its nutritional and therapeutic value (Santhosha et al., 2013). Furthermore, saponins present in garlic have been linked to cytotoxic and antitumor activities, reinforcing the role in disease prevention (Matsuura, 2001).

2.1.2.2. Culinary and functional uses

Garlic is widely cultivated in temperate, subtropical, and tropical regions, making it a significant crop (Fritsch and Friesen, 2002). It is an integral component of traditional and modern cuisines, contributing flavour, aroma, and bioactive compounds that improve food quality and preservation (Amarakoon and Jayasekara, 2017).

Its distinct pungency is attributed to allicin, which is converted enzymatically from alliin after cutting or crushing (Allison et al., 2006, Puvača et al., 2014). Furthermore, garlic's natural antimicrobial properties contribute to its use as a food preservative, extending shelf life and inhibiting spoilage microorganisms.

2.1.2.3. Agricultural and plant protection properties

Garlic has been widely studied for its fungicidal and antibacterial properties, particularly in agriculture and plant disease management.
Organosulfur compounds exhibit strong fungicidal activity, particularly allicin and its derivatives, which inhibit plant pathogenic fungi such as *Fusarium* spp. *Aspergillus* spp., and *Candida* spp. (Gruhlke et al., 2015, Martins et al., 2016). These compounds disrupt fungal cell membranes, interfere with essential metabolic pathways, and have shown synergistic effects with conventional fungicides (Benkeblia, 2005, Ndoye Foe et al., 2016).

Garlic's antibacterial properties also contribute to plant disease control, with allicin and diallyl sulfides demonstrating strong inhibitory effects against phytopathogenic bacteria (Puvača et al., 2014). These compounds have been found to suppress Gram-positive and Gram-negative bacteria, including *Xanthomonas* spp., *Pseudomonas* spp., and *Erwinia* spp. (Rahman and Lowe, 2006, Santhosha et al., 2013). The high reactivity of allicin enables it to disrupt bacterial cell walls and enzymatic functions, making it a promising biocontrol agent in sustainable agriculture.

2.1.3. Major fungal diseases affecting garlic

Garlic is affected by several major fungal diseases that significantly compromise crop productivity and storage quality. Among the most important are white rot (*Sclerotium cepivorum*), purple blotch (*Alternaria porri*), stemphylium blight (*Stemphylium vesicarium*), basal rot (*Fusarium oxysporum* f. sp. *cepae*), and post-harvest pathogens such as *Botrytis allii*, *Penicillium corymbiferum*, and *Aspergillus niger*. These diseases vary in their epidemiology and ecological requirements but collectively represent a major constraint to sustainable garlic production.

An overview of the predominant oomycete and fungal diseases impacting garlic, listing the symptoms and the specific pathogens responsible for each disease is summarized in Table 1.

Table 1. Summary of the most common oomycete and fungal diseases of garlic, their causative organisms, and main symptoms

Disease	**Causative fungi**	**Symptoms**	**References**
White rot	*Stromatinia cepivora* (Berkeley) Whetzel	The initial symptom of the disease is yellowing and dieback of leaf tips. Scales stem plate and roots get destroyed. The bulbs become soft and water soaked. White fluffy or cottony growths of mycelium with abundant black sclerotia resembling mustard grain are seen on the infected bulbs.	(Mishra et al., 2014)
Purple blotch	*Alternaria porri* (Ellis) Ciferri	Small whitish sunken lesions appear on garlic leaves, quickly turning brown and enlarging into zoned, purplish spots with reddish borders and a yellow halo. In moist conditions, the lesion surface is covered with dark purplish-black fungal growth. Lesions may merge, girdle the leaves and stems, causing them to yellow, wilt, collapse, and die within weeks.	(Mishra et al., 2012)
Basal Rot	*Fusarium oxysporum* f. sp. *cepae* (Hansen) Snyder & Hansen	Yellowing, curling, and tip-drying of garlic leaves, stunted growth, pink discoloration and rotting of roots, formation of a root abscission layer, basal plate decay spreading to the entire bulb, white mycelium on bulb surface or basal scales, and latent infections becoming severe during warm, humid storage.	(Le et al., 2021)
Botrytis Neck Rot	*Botrytis allii* Munn	Softening and sunken, cooked-like appearance of garlic neck tissues, brownish to grayish discoloration with a clear margin separating healthy and diseased areas, decay progressing down the neck scales toward the bulb base, dense gray mold forming on rotting scales in humid conditions, black sclerotia developing between scales near the neck, neck tissue drying and collapsing, entire bulbs becoming mummified, and	(Crowe, 2000)

		secondary bacterial invasion causing watery rot.	
Blue mold	*Penicillium hirsutum* Dierckx	Blue mold typically appears during harvesting and storage. Early symptoms include pale yellowish blemishes, watery soft spots, or occasionally purplish-red stains on the bulb scales. As the disease progresses, green to blue-green powdery mold develops on lesion surfaces. Internally, affected fleshy scales may appear water-soaked with a tan to grey discoloration. In advanced stages, the entire bulb may disintegrate into a soft, watery rot.	(Abba, 2019)
Stemphylium blight	*Stemphylium vesicarium* (Wallroth) E.G. Simmons	Small water-soaked or white spots appear on older leaves, often starting at the tips, then elongate into dark brown to purplish lesions with a purple halo and sunken tissue. These spots expand and merge into large necrotic areas, causing leaf blight, drying of foliage, necrosis of all aerial parts, complete desiccation, and impaired bulb development.	(Mishra et al., 2014)
Downy mildew	*Peronospora destructor* (Berkeley) Caspary	Symptoms appear on the surface of leaves or flower stalk as violet growth of fungus, which later becomes pale greenish yellow and finally the leaves or seed stalks collapse.	(Schwartz and Gent, 2008)
Black mold	*Aspergillus niger* van Tieghem	Black powdery masses of spores appear on the exterior of scales. The same black spore masses are also visible on the inner scales.	(Mishra et al., 2014)

2.2. Okra (*Abelmoschus esculentus* L.)

2.2.1. Global production and economic importance

Okra (*Abelmoschus esculentus* (L.) Moench), commonly known as lady finger or gombo, is one of the most widely cultivated and consumed crops of the Malvaceae family (Naveed et al., 2009). The Malvaceae family also includes several other important plants of economic importance, such as cacao, cotton, durian, and ornamental hibiscus (Tong, 2016). In its early classification, okra was included in the Hibiscus genus and was often referred to as *Hibiscus esculentus* in older publications.

Its cultivation is adaptable to a wide range of geographical locations, as it can be grown in regions with varied climatic conditions such as tropical, subtropical, and warm temperate regions (Adiaha, 2017), leading to its widespread cultivation and commercial use in numerous countries (Kumar et al., 2013). Global okra production shows significant growth, increasing from 1.8 million tonnes in 1972 to 11.2 million tonnes in 2022, with India accounting for 61.2% of global total production (FAOSTAT, 2022). India's leading role as the world's largest okra producer has also made it a focal point for extensive research on okra cultivation, pest dynamics, and management strategies. Other countries, such as Nigeria, Mali, Pakistan, Sudan, Côte d'Ivoire, and Iraq, also play a notable role in contributing to the global production of okra (FAOSTAT, 2022).

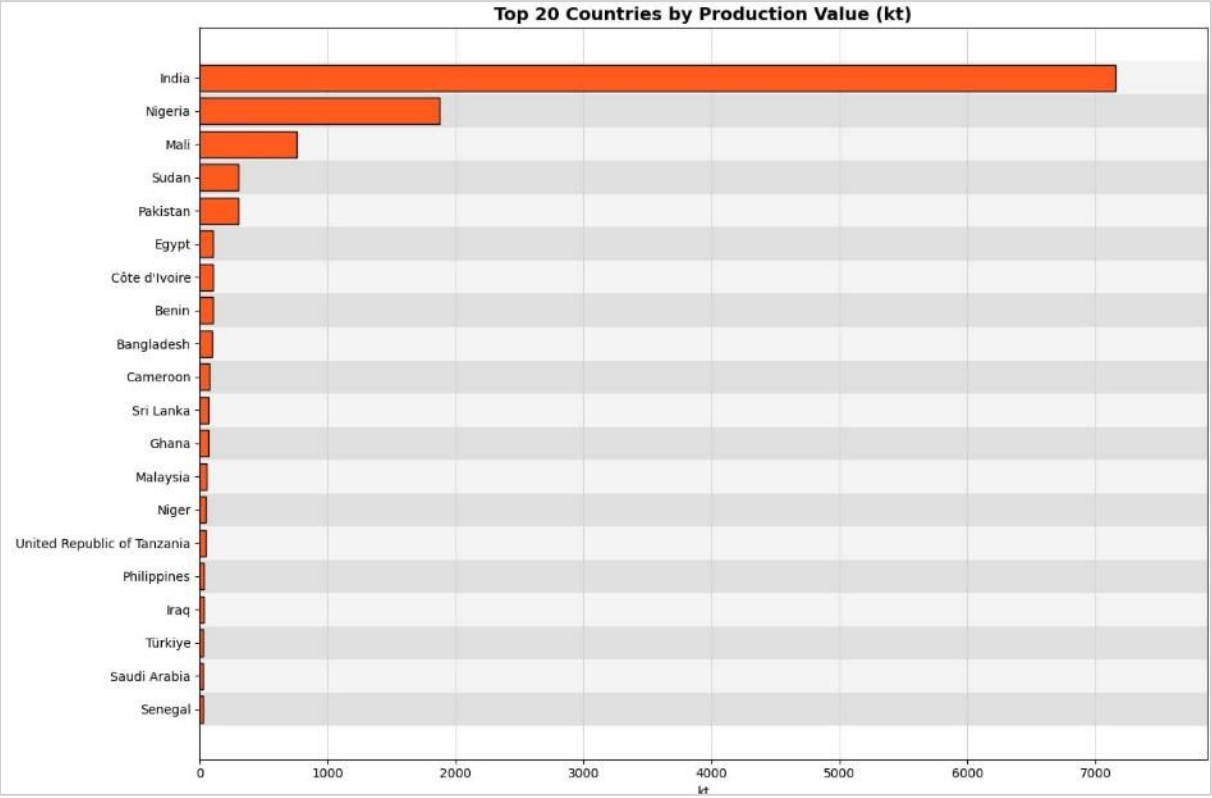

Figure 2: Global garlic production by country in 2022 (kilotons, kt). (FAOSTAT, 2022).

2.2.2. Nutritional and medicinal benefits

Although the crop has multiple uses, its primary cultivation and consumption are focused on the green soft fruits of the plant that are rich in minerals such as iron and irodine and vitamins A, B and C and also possess a significant amount of protein and oil, approximately 20.0% of each (Tindall, 1983, Charrier, 1984, Adebooye and Oputa, 1996). This vegetable is an essential source of viscous fibre and is reported to contain low levels of sodium, saturated fat, and cholesterol (Kendall and Jenkins, 2004, Adebooye and Oputa, 1996). Okra seeds and leaves have been reported to have antidiabetic, antioxidant, and antimicrobial properties. Studies have shown that

okra has various human health benefits, such as blood sugar regulation, inflammation reduction, and even cancer prevention, and it has been traditionally used in herbal medicine (Tantawy et al., 2020, Ardestani et al., 2020). Okra has also found medical application as a plasma replacement or expander of blood volume (Savello et al., 1980, Lengsfeld et al., 2004, Adetuyi et al., 2008, Kumar et al., 2010). It was found that an alcohol extract of leaves can improve renal function, reduce proteinuria, and alleviate renal tubular interstitial diseases by eliminating oxygen free radicals (Liu et al., 2005, Kumar et al., 2009). The oil and protein-rich fruits have been utilized for oil production on a limited scale (Çalışır et al., 2005). Furthermore, the crude fibre in its mature fruit and stems is used to make paper (Kochlar, 1986).

2.2.3. Major fungal diseases affecting okra

Okra is vulnerable to several significant challenges posed by fungal, viral, and bacterial pathogens and arthropod and nematode pests, which can significantly affect its cultivation success (Jiskani, 2006, Gulati, 2004).

Okra production is affected by many fungal and oomycete diseases that adversely affect both the quantity and quality of the crop (Thippeswamy et al., 2007). The main diseases include damping off, powdery mildew, *Cercospora* leaf spot, grey mold, *Alternaria* leaf spot and pod rot, *Phyllosticta* leaf spot, *Fusarium* wilt, *Verticillium* wilt, collar rot, stem canker, and anthracnose. Detailed images of the symptoms of the diseases are available in the Global Database of the European and Mediterranean Plant Protection Organisation (EPPO) Global Database (EPPO (European and Mediterranean Plant Protection Organization), nd), which serves as a valuable resource for researchers and practitioners.

Table 2 provides an overview of the predominant oomycete and fungal diseases impacting okra, listing the symptoms and the specific pathogens responsible for each disease.

Table 2. Summary of the most common oomycete and fungal diseases of okra, their causative organisms, and main symptoms

Disease	**Causative fungi**	**Symptoms**	**References**
Damping-off	*Pythium aphanidermatum* (Edson) Fitzpatrick *Rhizoctonia solani* Kühn *Fusarium solani* (von Martius) Saccardo) *Macrophomina phaseolina* (Tassi) Goidanich *Phytophthora nicotianae* Breda de Haan	Water-soaked lesions at the stem collar region. Browning and shrinkage of the stem tissue, and seedling collapse.	(Jukte et al., 2016).
Powdery mildew	*Golovinomyces cichoracearum* (de Candolle) Heluta	White to grayish-white powdery fungal growth on leaves, stems, and occasionally flowers or fruits. Leaf deformation, curling, yellowing, and stunted plant growth.	(Dahivelkar et al., 2017).
Cercospora leaf spot	*Cercospora malayensis* Stevens & Solheim *C. abelmoschi* (Ellis & Everhart) Deighton	Irregular brown or black spots on mature leaves, developing into reddish-brown with yellow margins, expanding and reducing photosynthesis.	(Bolie et al., 2021, Kumar et al., 2010).
Gray mold	*Botrytis cinerea* Persoon	Grayish, web-like fungal growth on leaves, stems, and fruits. Light brown lesions on thin leaves, concentric brown rings on thicker leaves. Wilting in severe cases.	(Afroz et al., 2019).
Alternaria leaf spot	*Alternaria alternata* (Fries) Keissler *A. chlamydospora* Mouchacca	Small, light brown-concentric dark brown lesions on the leaves. Necrosis, wilting, and plant death under severe infections.	(Cho and Moon, 1980, Werner, 1987, Canihos et al., 1999).

Alternaria pod blight	*Alternaria alternata* (Fries) Keissler	Wet rot on young okra pods, development of lesions, leading to decay.	(Gappa-Adachi, 2018).
Phyllosticta leaf spot	*Phyllosticta hibiscini* Ellis & Everh.	Large leaf lesions with a grayish center, progressing to form shot holes. Presence of black pycnidia on both leaf surfaces.	(Awasthi, 2015).
Fusarium wilt	*Fusarium oxysporum* f. sp. *vasinfectum sensu lato* (Atkinson) Snyder & Hansen	Leaf discoloration and wilting, stunted growth, vascular damage, and stem deterioration, leading to wilting and death.	(Beckman, 1987, Hao et al., 2009).
Verticillium wilt	*Verticillium dahliae* Klebahn *V. tricorpus* Isaac	Initial symptoms include Yellowing followed by wilting and drying, V-shaped chlorosis of leaflets, and yellow-to-red-brown lesions near the leaf tip. Severe infections lead to defoliation, shoot dieback, and plant death.	(Schnathorst and Mathre, 1966, Fradin and Thomma, 2006).
Collar rot	*Macrophomina phaseolina* (Tassi) Goidanich	Damping-off, seedling blight, collar rot, stem rot, and root rot in mature plants. Hollow stem formation, pre-emergence and, post-emergence damping-off.	(Pearson et al., 1984).
Stem canker	*Fusarium chlamydosporum sensu lato* Wollenweber & Reinking	Dark circular to oblong lesions on the stems, floral buds, and pods of young plants. Severe infections lead to seedling death.	(Fugro, 1999).
Anthracnose	*Colletotrichum plurivorum* Damm, Alizadeh & Toy. Sato *C. gloeosporioides* (Penzig) Penzig & Saccardo	Yellow-brown, necrotic, sunken lesions on the leaves.	(Amadi et al., 2014, Shi et al., 2019).
Fruit rot	*Choanephora cucurbitarum* (Berkeley & Ravenel) Thaxter	Brown-black water-soaked lesions on fruits, progressing rapidly and causing fruit decay and drop.	(Balogun and Babatola, 1999, Park et al., 2015, Henz et al., 2007).

	Rhizoctonia solani Kühn *Fusarium solani* (von Martius) Saccardo *Phytophthora palmivora* E.J. Butler *Rhizopus stolonifera* (Ehrenberg) Vuillemin *Fusarium oxysporum* Schlechtendal *Aspergillus flavus* Link		

2.3. Fungal pathogens infecting the studied plant hosts

2.3.1. Studied garlic pathogens (*Stromatinia cepivora* and *Fusarium proliferatum*)

2.3.1.1. Pathogenesis and infection cycle

Stromatinia cepivora (Berk.) Whetzel, the causal agent of white rot, is a necrotrophic soil-borne fungus that infects *Allium* species via sclerotia, its long-lived resting structures. The infection begins when sclerotia in the soil detect root exudates from susceptible *Allium* plants, leading to germination and hyphal invasion; colonisation is followed by tissue degradation, characterised by white mycelial growth and formation of sclerotia around the basal stem and bulb surface (Lourenço Jr et al., 2018).

Sclerotia germination is host-specific and requires the presence of sulphur-containing compounds in *Allium* exudates; these signals induce hyphal emergence, which directly penetrates host epidermal cells through mechanical pressure and enzyme degradation of cell walls (Elshahawy and Saied, 2021). After penetration, mycelium spreads intercellularly and intracellularly, secreting toxins and enzymes that kill host tissue; this necrosis favours the proliferation and sclerotial formation of pathogens to complete the cycle (Osman et al., 2023).

In contrast, *Fusarium proliferatum* is a facultative pathogen with a broad host range and high toxigenic potential. Infection begins by entering the root or wound, commonly during bulb formation or post-harvest stages; microconidia or macroconidia germinate and hyphae colonise the vascular tissue, leading to systemic infection and bulb rot (Palmero et al., 2012). In particular, *F. proliferatum* infection does not require prior tissue senescence; instead, it actively penetrates via the cuticle or wounds, followed by invasion of the xylem, causing water-soaked tan lesions and bulb decay, sometimes with visible mycelia (Salvalaggio and Ridao, 2013).

2.3.1.2. Disease symptoms and impact on garlic crops

Stromatinia cepivora, the causal agent of white rot, typically initiates infection with foliar yellowing and wilting in *Allium* crops. As the disease progresses, plants exhibit water-soaked lesions at the base and eventually decay, with dense white mycelial growth and the formation of small black sclerotia on the affected tissues, particularly bulbs and roots (Ounis et al., 2025, Lourenço Jr et al., 2018). White rot caused by *S. cepivora* can cause up to 100% crop loss under favourable conditions. The severity is often correlated with soil inoculum levels and environmental conditions that favour sclerotial germination. In highly infested soils, total stand loss is frequent, leading to complete yield failure (Workneh et al., 2024, Elshahawy and Saied, 2021).

Fusarium proliferatum, associated with bulb and basal rot in garlic, leads to root and lower stem browning, often followed by plant stunting and premature senescence. In severe cases, bulbs become soft and discolored, with necrotic tissues harboring pathogen conidia and mycelia (Stankovic et al., 2007, Delgado-Ortiz et al., 2016). The impact of these pathogens includes not only direct yield loss but also reduced bulb size, weight, and marketability. Furthermore, bulbs infected with *F. proliferatum* may accumulate mycotoxins such as fumonisins and beauvericin, posing health risks and further lowering their commercial value (Stankovic et al., 2007). Despite the development of chemical and biological management strategies, both pathogens remain formidable due to their persistence in soil and their ability to infect multiple Allium species in diverse growing conditions (Workneh et al., 2024, Elshahawy et al., 2021).

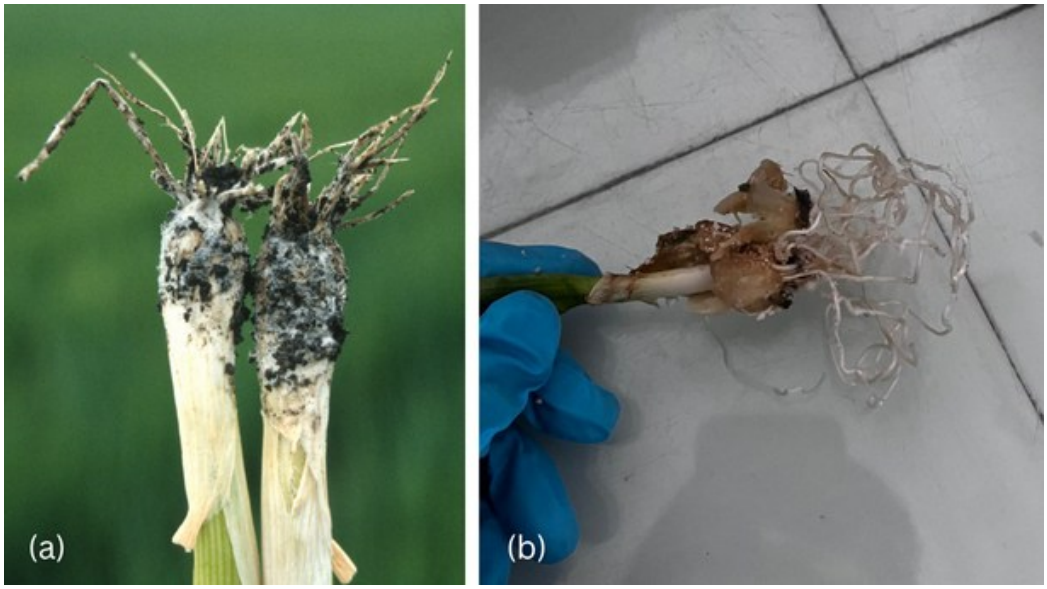

Figure 3: (a) Symptoms of *Stromatinia cepivora* on garlic seedlings showing characteristic white rot with sclerotia formation (a) (source: (PlantwisePlus Knowledge Bank, 2021)), and **(b)** symptoms of *Fusarium proliferatum* on garlic roots exhibiting basal plate rot and tissue degradation (own image).

2.3.1.3. Environmental factors influencing disease severity

The severity of white rot and *Fusarium*-induced diseases in *Allium* crops is closely related to environmental conditions that regulate pathogen activity, host susceptibility, and disease progression. Both *S. cepivora* and *F. proliferatum* are influenced by soil temperature, moisture, and agronomic practices. *Stromatinia cepivora* sclerotia germinates most efficiently at cold soil temperatures ranging from 10 to 20 ° C, which coincides with the early growth stages of garlic crops; This temperature range allows optimal mycelial growth and host colonisation, thus increasing infection risks (Lourenço Jr et al., 2018, Workneh et al., 2024).

Soil moisture is a critical driver of the severity of *S. cepivora* severity; saturated or poorly drained soils favour sclerotial germination and pathogen spread, while dry soils significantly limit disease incidence (Elshahawy et al., 2021). High relative humidity and minimal soil disturbance have also been shown to support the persistence and progression in the field.

The density of sclerotia in the soil is exacerbated by repeated *Allium* cropping; Continuous monoculture or short crop rotations result in accumulation of inoculum and prolonged disease risk, particularly in fields lacking sanitation practices or pathogen-suppressive management (Workneh et al., 2024, Elshahawy et al., 2021).

For *F. proliferatum*, warm temperatures (25–30 °C) and moderate soil moisture facilitate spore germination, colonisation, and disease expression in both garlic crops (Palmero et al., 2012); the fungus is particularly active under abiotic stress conditions such as drought or nutrient imbalance, which compromise host defences and enable aggressive root and bulb invasion (Stankovic et al., 2007).

Fusarium spp. caused diseases are further aggravated by physical damage to roots and bulbs due to poor harvesting practices or insect activity; such wounds offer direct entry points for the fungus, bypassing initial host resistance mechanisms (Delgado-Ortiz et al., 2016, Ounis et al., 2025). The integrated severity of the disease in the presence of both pathogens is influenced by overlapping environmental conditions (Ounis et al., 2025).

2.3.2. Studied okra pathogens (*Sclerotinia sclerotiorum* and *Rhizoctonia solani*)

2.3.2.1. Pathogenesis and infection cycle

Sclerotinia sclerotiorum and *Rhizoctonia solani* are significant necrotrophic fungal pathogens that impact okra cultivation through their distinct infection strategies. *Sclerotinia sclerotiorum* primarily initiates infection by germinating sclerotia under favorable moist conditions, producing mycelia or apothecia that release airborne ascospores capable of infecting host tissues (Derbyshire

and Denton-Giles, 2016). During the infection process, once the spores germinate, *S. sclerotiorum* secretes oxidative compounds like oxalic acid, which can alter the pH of infected tissues, creating a more conducive environment for pathogenicity (Fan et al., 2021). The secretion of cutinolytic enzymes further facilitates tissue softening, allowing rapid penetration and extensive colonisation of okra's stems, leaves, and pods (Ranjan et al., 2018).

The role of oxalic acid in the pathogenesis of *S. sclerotiorum* is crucial, as it helps suppress the production of defensive reactive oxygen species (ROS) by the host while activating pectinolytic enzymes that degrade the walls of plant cell walls, leading to cell necrosis and eventual maceration (Andrade et al., 2018). Research confirms that manipulation of the host's redox environment through the secretion of oxalic acid is vital to overcome host resistance mechanisms, indicating that *S. sclerotiorum* effectively circumvents early immune responses in okra plants (Williams et al., 2011).

On the other hand, *Rhizoctonia solani* employs a different infection strategy characterised by direct contact with its host. This species uses specialized structures known as appressoria to penetrate the host epidermis, allowing it to invade intercellular spaces (Shahoveisi et al., 2022). Upon infection, *R. solani* secretes a range of cell wall degrading enzymes, such as cellulases and hemicellulases, which degrade the host cell walls, resulting in rapid necrosis and the death of okra hypocotyls and roots (Xu et al., 2018b). The pathogen's capacity to persist in the soil as sclerotia or moniloid cells for extended periods greatly enhances its epidemiological success, particularly in warm and moist soil conditions that favour its proliferation (Shahoveisi et al., 2022)

Both pathogens enhance their virulence through the secretion of effector proteins that can manipulate host defences by disrupting salicylic acid-dependent signaling pathways and inhibiting pathogenesis-related protein (PR) expressions, leading to a weakened systemic resistance in okra plants (Fan et al., 2021). This suppression of host defences is a critical factor in the pathogenic success of both fungi, allowing these necrotrophic pathogens to effectively establish and maintain infections.

2.3.2.2. Disease symptoms and impact on okra

Sclerotinia sclerotiorum and *Rhizoctonia solani* severely affect okra, compromising plant health, yield, and post-harvest quality. Their distinct infection strategies and symptomatology contribute to significant economic losses in the cultivation of okra.

Rhizoctonia solani causes damping-off, root rot, and crown rot. Damping leads to the death of seedlings in early growth stages due to basal stem and root decay, resulting in poor crop

establishment (Behiry et al., 2022). Infected plants exhibit stunted growth, wilting, chlorosis, and necrosis of the leaves, symptoms that are often aggravated under conditions of stress from moisture, reflecting the strong interaction with environmental factors (Meena et al., 2024a). Severe infections can result in complete plant mortality, drastically reducing stand density.

On the contrary, *Sclerotinia sclerotiorum* typically manifests as white, cottony mycelium on stems and leaves, leading to Sclerotinia blight characterised by tissue browning, soft rot, and water-soaked lesions on fruits. This results in a cottony rot appearance, as the pathogen decomposes infected tissues, often causing extensive fruit rot and subsequent softening, which reduces marketable yield (Behiry et al., 2022).

The economic impact of these pathogens on okra production is profound. *R. solani* significantly reduces yields by killing seedlings and mature plants, forcing replanting and increasing production costs (Meena et al., 2024a). Similarly, *S. sclerotiorum* infections can cause 10% to 50% post-harvest losses in heavily infested fields, primarily through fruit decay that diminishes texture, flavour, and marketability (Abed and Farhan, 2023).

Beyond direct yield and quality losses, farmers incur additional expenses for pathogen management, including fungicide applications and labour for replanting, further threatening the economic sustainability of okra cultivation in areas where both pathogens coexist (Meena et al., 2024b).

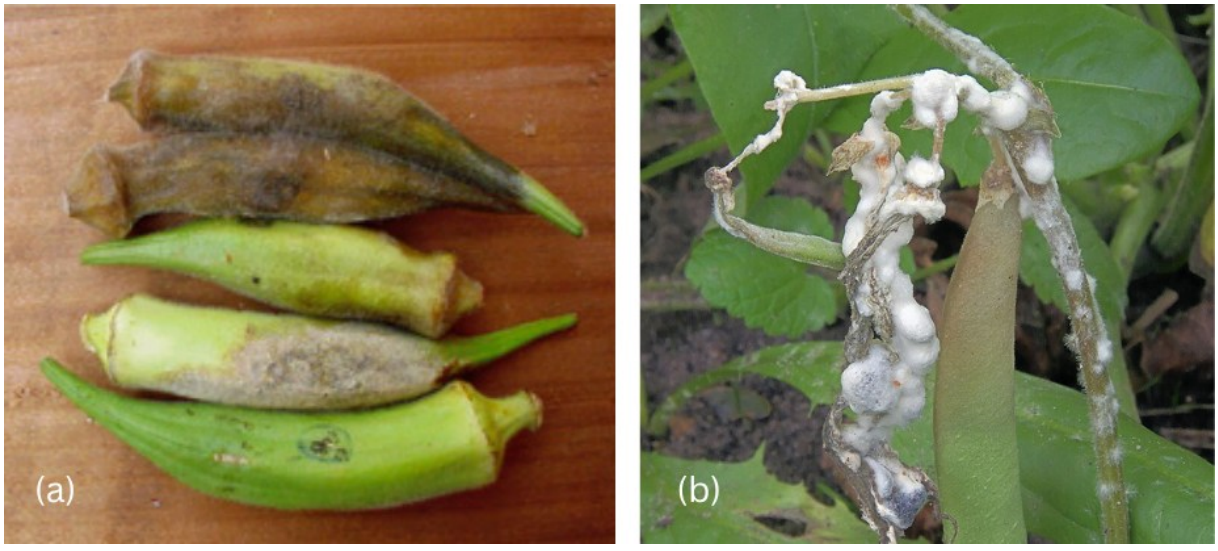

Figure 4. Symptoms of soil-borne fungal pathogens: **(a)** pod rot of okra caused by *Rhizoctonia solani* (source: (Henz et al., 2007)), and **(b)** white mold symptoms caused by *Sclerotinia sclerotiorum* on *Phaseolus vulgaris* (bushbean) used here as a representative image due to the absence of okra-specific symptom documentation (source: (Rasbak, 2009)).

2.3.2.3. Environmental factors influencing disease severity

The impact of *Sclerotinia sclerotiorum* and *Rhizoctonia solani disease* on okra plants is significant, manifesting itself through a variety of debilitating symptoms. *S. sclerotiorum*, known to cause *Sclerotinia* stem rot, typically results in "watery soft rot" in the collar region of the plant. This initial symptom is often followed by wilting and collapse of the plant structure. The characteristic cottony mycelial growth of this pathogen can be observed in affected tissues, which later develop into sclerotia, hard survival structures that allow the fungus to withstand adverse conditions (Xu et al., 2018a, Choi et al., 2017). This symptomology can sometimes be mistaken for bacterial infections due to the water-soaked appearance (Hossain et al., 2023). Environmental factors, particularly cool and humid conditions, play an important role in facilitating the systemic spread of the pathogen from the stem base to other plant parts, contributing to premature defoliation and pod drop, ultimately leading to total plant death when severe (Rana et al., 2021).

In contrast, *R. solani* affects okra seedlings through pre- and post-emergence damping-off syndrome. This results in sunken brown lesions in the hypocotyl, which can girdle the stem base and lead to the collapse of seedlings, significantly impacting early plant establishment (Mu et al., 2025, Chamberlin and Puppala, 2018). Mature plants also suffer from root and crown rot, characterised by stunted growth and yellowing of the foliage, ultimately leading to a decreased pod set (Zhang et al., 2015). Field evidence indicates that *R. solani*-inflicted okra plants frequently exhibit sparse stands and uneven growth, resulting in both aesthetic damage and significant marketable yield reductions (Cao et al., 2018).

The economic implications of infections by both pathogens are especially dire when they cooccur under conducive environmental conditions. This dual infection can worsen the severity of foliar and root symptoms, with potential yield losses reaching 50-70% in susceptible okra cultivars if left unmanaged (Chang et al., 2018). Furthermore, the postharvest quality of okra from infected plants is often compromised, and fruits typically showing reduced shelf life and diminished market value, mainly due to physiological stress and impaired nutrient uptake caused by vascular damage from both fungi (Yang et al., 2024a). Overall, the economic burden and agronomic impact of these diseases underline the critical need for effective management strategies to mitigate their detrimental effects on okra production.

2.4. Importance of resistance screening against fungal diseases

2.4.1. Concept and methodologies of resistance screening

Resistance screening against fungal diseases is an essential component of plant pathology and breeding programmes, focusing primarily on identifying and developing cultivars that show

resilience to fungal pathogens. This process facilitates integrated disease management, helping to improve crop productivity while minimizing losses due to fungal infections, particularly in crops such as garlic and okra, which are susceptible to soil-borne diseases (Mamouei et al., 2018).

Various methodologies, including artificial inoculation and natural infestation, are crucial in the resistance screening process. Artificial inoculation provides a controlled environment with standardised disease pressure, which ensures reliable evaluations of plant responses to pathogens (Lee et al., 2014). Screening can occur under a range of conditions, including fields and controlled environments, each with distinct advantages in managing environmental variables and pathogen specificity (Kelty et al., 2024). In particular, controlled environment systems, such as phytotrons, are effective in studying specific cultivar-pathogen interactions and ensuring uniform inoculum delivery crucial for accurate resistance (Kelty et al., 2024).

In crops such as garlic, resistance screening faces unique challenges primarily due to its vegetative propagation and heterogeneous genetic background. Visual evaluations of disease severity, histopathological evaluations, and physiological trait measurements have been commonly employed to determine resistance (Mamouei et al., 2018, Tebbets et al., 2013). Similarly, okra uses various methods, including seedling assays and quantification of the lesion area, to evaluate responses to pathogens (Niu et al., 2020). The methods used to screen for resistance in these crops highlight the need for adaptability in the face of varying pressures and crop biology.

Recent advances in resistance screening have underscored the integration of biochemical markers and molecular tools to enhance the evaluation process. Biochemical markers, such as guaiacol peroxidase (POX) and polyphenol oxidase (PPO), serve as indicators of oxidative stress responses in plants, helping to assess their resistance capabilities (Liszka et al., 2025). Furthermore, molecular techniques such as PCR-based methods for identifying resistance gene expression offer deeper insight into the mechanisms underlying plant-pathogen interactions, facilitating the identification of cultivars with enhanced resistance traits (Liszka et al., 2025).

Furthermore, with the recognition of multipathogen scenarios, screening methodologies are evolving to simultaneously assess plant responses to multiple pathogens. This approach is particularly relevant in crops such as garlic and okra, where numerous soil-borne pathogens coexist in the rhizosphere, demanding a comprehensive understanding of cultivar resilience under various pathogenic pressures (Kelty et al., 2024).

2.4.2. Resistance mechanisms in Alliums and okra

In Alliums, garlic demonstrates both pre-prepared and induced defence strategies. Structural barriers within garlic, such as thickened epidermal walls and lignified root tissues, form the first

line of defence against pathogen penetration. Upon detection of pathogens, garlic initiates various inducible responses, which encompass the upregulation of pathogenesis-related (PR) proteins and oxidative enzymes, such as peroxidases and polyphenol oxidases. This helps to limit the spread of the pathogen and reinforces cell walls through a process known as lignification (Anisimova et al., 2022, Tini et al., 2024).

In addition, garlic employs a hypersensitive response (HR)-like mechanism when exposed to specific *Fusarium* species, characterised by localized cell death at infection sites to hinder further colonisation. The accumulation of phytoalexins and reactive oxygen species (ROS) contributes to creating an unfavourable environment for pathogens and facilitates the activation of systemic acquired resistance (SAR) pathways.

The activity of antioxidant enzymes has been shown to correlate with enhanced resistance, particularly in scenarios of co-infection, where interactions among multiple pathogens can amplify host damage (Mondani et al., 2022). In the case of okra, resistance mechanisms against *R. solani* and *S. sclerotiorum* include rapid recognition of the pathogen and the consequent activation of downstream signaling pathways mediated by salicylic acid (SA) and jasmonic acid (JA). Okra exhibits structural defences, such as the formation of papillae and callose deposits at infection sites, which contribute to its resistance profile (Filyushin et al., 2023).

Biochemically, okra has an effective antioxidant defence response involving enzyme systems such as peroxidases (POX), polyphenol oxidases (PPO), catalase (CAT), and superoxide dismutase (SOD), which together modulate ROS accumulation and protect host cells from oxidative stress (Ding et al., 2020). In particular, both Alliums and okra exhibit resistance traits that are quantitatively inherited and polygenic, indicating a complex interaction among multiple genes rather than the dependency on single resistance genes. This nuanced genetic framework can complicate breeding strategies, but allows for a more robust and durable resistance profile against various fungal threats (Moharam et al., 2023). Environmental conditions, including temperature, soil moisture and inoculum load, significantly influence resistance expression, pathogen virulence, and overall host susceptibility (De Santis et al., 2021).

In addition, the induced systemic resistance (ISR) facilitated by beneficial microbes such as *Trichoderma asperellum* and *Bacillus amyloliquefaciens* supports the native defenses. These microbial agents enhance resistance by priming defense pathways, increasing enzymatic activity, and promoting physiological adaptations such as improved root architecture and nutrient uptake (Gálvez and Palmero, 2021, Infantino et al., 2023).

2.5. Antagonistic microorganisms used in disease suppression

2.5.1. *Trichoderma asperellum*

Trichoderma asperellum has emerged as a significant biological control agent against various phytopathogenic fungi, using a combination of antagonistic mechanisms. Its mode of action encompasses four synergistic strategies: mycoparasitism, antibiosis, competition for resources, and induction of systemic resistance in plants.

The first mode of action, mycoparasitism, involves the direct predation of *T. asperellum* on pathogenic fungi. This includes the fungus that recognises and coils around the hyphae of its target pathogens, subsequently penetrating and degrading them with the help of various cell wall degrading enzymes such as chitinases and glucanases. For example, chitinases specifically hydrolyze chitin, a crucial component of fungal cell walls, facilitating the collapse and death of pathogens (Zhang et al., 2021). Further supporting this, studies demonstrate that *T. asperellum* can effectively degrade the cell walls of fungi such as *Fusarium oxysporum*, underscoring its capacity for mycoparasitism (Zhang et al., 2021, Ji et al., 2023).

In addition to mycoparasitism, *T. asperellum* synthesises a variety of secondary metabolites with antifungal properties, contributing to its antibiotic activity. These compounds include peptaibols and other bioactive substances that inhibit pathogen growth and spore germination (Hakkar et al., 2014); The action of these metabolites creates a hostile microenvironment for pathogens, facilitating disease suppression (Abd-El-Kareem et al., 2023).

The competition for nutrients and space in the rhizosphere is another crucial aspect of the antagonistic strategies of *T. asperellum.* By rapidly colonising the root zones of plants, *T. asperellum* deprives slower growing pathogens of essential nutrients and physical space necessary for their survival (Estévez-Geffriaud et al., 2020, Ma et al., 2023). This competitive advantage significantly reduces the prevalence of fungal diseases in crops.

Lastly, *T. asperellum* induces systemic resistance in host plants. It activates plant defence pathways, including the jasmonic acid and ethylene signaling pathways. This response results in the up-regulation of various defence-related enzymes and the accumulation of phenolic compounds that improve the plant's resilience against subsequent pathogen attacks (Herrera-Téllez et al., 2019, Zhang et al., 2020). For example, studies have documented the increased expression of defensive enzymes like peroxidases associated with the treatment of *T. asperellum* (Herrera-Téllez et al., 2019, Estévez-Geffriaud et al., 2020).

2.5.2. *Bacillus amyloliquefaciens*

Bacillus amyloliquefaciens, a well-characterised plant-associated bacterium, is widely recognised for its potent biocontrol activity and plant growth promoting capabilities. Its success as a biological control agent lies in its multifaceted antagonistic strategies, which act synergistically to suppress phytopathogens while simultaneously improving host plant health.

A key mechanism of *B. amyloliquefaciens* is antibiosis, primarily mediated by the secretion of bioactive lipopeptides. Notable among these are surfactin and bacillomycin D, which alter the integrity of the fungal cell membrane, causing leakage of cellular contents, lysis, and growth inhibition. These lipopeptides have been extensively documented for their efficacy against major fungal pathogens such as *Fusarium oxysporum* and *Monilinia fructicola* (Vitullo et al., 2012, Liu et al., 2011). Beyond lipopeptides, *B. amyloliquefaciens* emits a range of volatile organic compounds (VOCs), including 2,3-butanediol and acetoin, which exert dual functions: directly inhibiting pathogen growth and indirectly stimulating plant systemic resistance and growth promotion (Yang et al., 2022, Ramírez et al., 2020). These VOCs trigger physiological changes in host plants, such as improved nutrient uptake and enhanced resilience against both biotic and abiotic stresses.

In addition to antibiosis, *B. amyloliquefaciens* uses extracellular hydrolytic enzymes—notably chitinases, β-1,3-glucanases, and proteases—that degrade fungal cell walls, weaken pathogen structures and facilitating nutrient recycling of nutrients in the rhizosphere (Soliman et al., 2022). By breaking down pathogen cell walls, these enzymes also release oligomers that can act as elicitors of plant immune responses. Furthermore, *B. amyloliquefaciens* exhibits remarkable rhizosphere competence, rapidly colonising root surfaces and occupying ecological niches, thus creating a competitive barrier that limits pathogen access to infection sites (Cui et al., 2019). This colonisation is stabilized by biofilm formation, which improves bacterial persistence in the rhizosphere and improves its interaction with plant roots (Xu et al., 2013).

Another crucial aspect of *B. amyloliquefaciens* is its ability to induce systemic resistance (ISR) in plants, strengthening the host's immune system against a wide range of phytopathogens. Through jasmonic acid and ethylene-dependent signaling pathways, *B. amyloliquefaciens* primes the expression of defence-related genes and elevates the activity of key antioxidant enzymes, including guaiacol peroxidase (POX) and polyphenol oxidase (PPO) (Roslan et al., 2020, He et al., 2023). These enzymes play essential roles in lignin deposition, cell wall fortification, and detoxification of reactive oxygen species (ROS), providing plants with enhanced structural and biochemical resistance.

2.6. Oxidative enzyme activity in plant defense mechanisms

2.6.1. Polyphenol oxidase (PPO)

Polyphenol oxidase (PPO) is a key enzyme in plant defence, catalyzing the oxidation of phenolic compounds into quinones, which are toxic to invading pathogens and contribute to the formation of antimicrobial polymers. This enzyme plays a central role during the hypersensitive response (HR) by promoting localised programmed cell death, effectively restricting the spread of the pathogen (Simo et al., 2018, Karsou and Samara, 2021). Elevated PPO activity has been consistently associated with enhanced resistance against various pathogens, particularly necrotrophs (Borges et al., 2022).

2.6.2. Guaiacol peroxidase (POX)

Guaiacol peroxidase (POX) is crucial for the metabolism of hydrogen peroxide (H_2O_2) and the biosynthesis of lignin, strengthening cell walls to form physical barriers against the entry of pathogens. Its activity increases rapidly after pathogen recognition, contributing to structural fortification and oxidative burst during early defence responses (Santos et al., 2023, Bakhshi et al., 2023). This induction has been widely observed during fungal, bacterial, and viral infections, underscoring its integral role in plant immunity (Maia et al., 2024).

2.6.3. Role of PPO and POX in plant defense

Both enzymes are considered early biomarkers of plant defence activation, tightly regulated by signaling molecules such as salicylic acid (SA) and jasmonic acid (JA). Their coordinated induction triggers an oxidative burst, leading to accumulation of reactive oxygen species (ROS) at infection sites, which further stimulates downstream defences, including pathogenesis-related proteins and phytoalexin synthesis (Hahn et al., 2021, Kostelac et al., 2024, Hernández-Ortega et al., 2021).

Importantly, variations in POX and PPO activities between resistant and susceptible cultivars highlight their predictive value in breeding for disease resistance. Cultivars with higher baseline or induced enzyme activities tend to show reduced pathogen susceptibility, making these enzymes reliable biochemical markers for resistance screening (Maia et al., 2024).

In summary, POX and PPO are key components of plant oxidative defence, contributing to ROS signaling, lignin deposition, toxic compound formation, and HR-associated cell death. Their dual roles as defence effectors and regulatory enzymes underscore their importance in shaping inducible resistance and plant resilience under pathogen pressure (Ghiasy-Oskoee and AghaAlikhani, 2025).

2.6.4. Comparative enzymatic defense mechanisms in garlic and okra: Current insights and research gaps

The literature on defence mechanisms against *Stromatinia cepivora* and *Fusarium proliferatum* in garlic and their analogous pathogens, *Sclerotinia sclerotiorum* and *Rhizoctonia solani*, in okra shows notable progress; nonetheless, key knowledge gaps persist. While pathogenesis-related proteins—such as peroxidases, chitinases and glucanases—are known to accumulate following infection, there is insufficient information on how these enzymes are modulated during co-infections or under combined biological and chemical treatments. Most studies examine a single host–pathogen system, leaving open the question of whether similar enzymatic patterns are expressed across different crops and pathogens.

In garlic, infections by *F. proliferatum* substantially elevate total phenolics and antioxidant activity (Sarpkaya, 2025). Although these increases reflect a general stress response, they do not necessarily indicate specific activation of oxidative enzymes. Evidence from related Allium species suggests that white-rot pathogens can trigger the accumulation of peroxidases and polyphenol oxidases. For instance, triple combinations of *Trichoderma* species against onion white rot markedly reduced disease incidence and enhanced peroxidase, polyphenol oxidase and chitinase activities (Elshahawy et al., 2019). Similarly, treatments integrating *Bacillus* spp. and *Trichoderma* spp. elevated POX and PPO activities and lowered disease levels in onion and garlic (Shalaby et al., 2013). These findings imply that biocontrol agents can prime oxidative enzymes in Allium crops, yet direct measurements of POX and PPO in garlic remain limited.

Research on okra provides more direct evidence of oxidative enzyme induction. Applications of chitosan and potassium salts against powdery mildew significantly increased total phenolics, protein content and activities of polyphenol oxidase, peroxidase, chitinase and β-1,3-glucanase (Soliman and El-Mohamedy, 2017). Beneficial fungi show similar effects; seed priming with *Metarhizium anisopliae* increased peroxidase activity by about 10%, catalase by 30%, glutathione S-transferase by 5.62% and ascorbate peroxidase by 5.06%, while reducing disease incidence by 58% (Mimma et al., 2023). Reviews of plant–microbe interactions also note that *Bacillus* species stimulate host peroxidase, polyphenol oxidase and phenylalanine ammonia-lyase as part of induced systemic resistance (Miljaković et al., 2020).

Both garlic and okra employ oxidative enzymes in their inducible defences. POX and PPO contribute to lignin deposition, detoxification of reactive oxygen species and formation of toxic quinones that limit pathogen colonization. However, the magnitude and timing of enzyme responses differ between the two crops. Data from okra show that POX and PPO activities can rise sharply within days of elicitor treatment (Mimma et al., 2023, Soliman and El-Mohamedy, 2017).

In contrast, most garlic studies emphasise general antioxidant capacity rather than specific enzyme assays, and PPO or POX induction appears to depend heavily on the biocontrol treatment and cultivar. Okra also exhibits strong responses to priming with beneficial fungi and plant growth–promoting rhizobacteria, with reductions in disease (Miljaković et al., 2020; Mimma et al., 2023). Comparable multifaceted responses in garlic remain largely speculative and warrant further investigation.

Beyond general assessments of phenolic compounds after *F. proliferatum* infection (Sarpkaya, 2025), few studies quantify POX and PPO activities in garlic, especially under dual inoculation with *S. cepivora* and *F. proliferatum*. Most reports concentrate on a single host species; cross-species analyses are needed to determine whether oxidative defence mechanisms behave similarly in monocots and dicots. For example, *Bacillus* spp.–*Trichoderma* spp. formulations that enhance POX and PPO in onion and garlic (Shalaby et al., 2013) have not been systematically tested in okra. Without such comparisons, it is difficult to generalize the efficacy of biocontrol agents across hosts.

Although plant growth–promoting rhizobacteria such as *Bacillus amyloliquefaciens* are known to induce systemic resistance (Miljaković et al., 2020), reports of decreased POX activity in okra following certain *Bacillus* spp. treatments suggest that host physiology and pathogen pressure modulate this interaction. Peroxidases other than guaiacol peroxidase, notably ascorbate peroxidase, play important roles in managing reactive oxygen species and detoxifying ROS produced during *Fusarium* spp. and plant interactions (Perincherry et al., 2019). Beneficial fungi such as *Metarhizium anisopliae* have been shown to increase ascorbate peroxidase and glutathione S-transferase activities in okra (Mimma et al., 2023), yet their roles in garlic are largely unexamined. Additionally, synergistic treatments combining nanoparticles with salicylic acid have reduced onion white rot while elevating peroxidase and catalase activities (Elenany et al., 2024). Such approaches remain mostly untested in garlic or okra, offering a promising avenue for future research.

Addressing these research gaps—particularly through comparative experiments measuring POX, PPO and related enzymes in both garlic and okra under comparable treatments—would deepen our understanding of the universality and specificity of oxidative defence strategies in these crops.

CHAPTER 3: MATERIALS AND METHODS

3.1. *In vitro* investigation of pathogen-pathogen interactions of *Fusarium proliferatum* and *Stromatinia cepivora* on garlic

3.1.1. Isolation and identification of the phytopathogens

Diseased garlic plants showing fungal infection symptoms consisting of yellowing and wilting were collected from garlic fields located in the Makó region, Csongrád-Csanád County, South-East Hungary (46.2185° N, 20.5299° E). The patchy distribution of symptoms, characterized by areas of yellowing and wilting, was observed from above using drone imaging and is displayed in Figure 5.

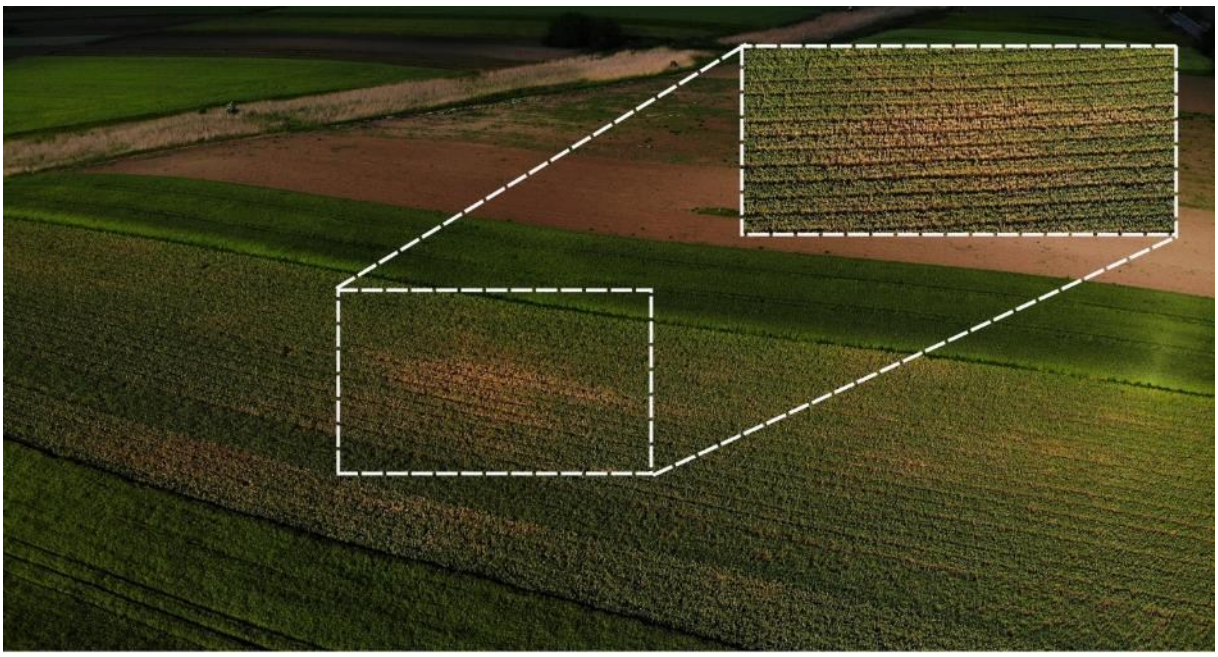

Figure 5: Drone image of a garlic field in Makó, from which symptomatic garlic samples were collected for this study. The visible yellowing spots, indicative of potential fungal infection, are highlighted in the image, with a zoomed-in view of one of the affected areas.

The garlic bulbs were placed in a moist chamber to improve fungal growth for 24 hours. The samples of cloves were cut into small fragments, inoculated under sterile conditions in Petri dishes on PDA medium (Potato Dextrose Agar), and incubated at 25°C for 5 days. The developed fungal cultures were purified using hyphal tip isolation techniques (Brown, 1924). The identification of isolated fungal species was carried out on both morphological characteristics (colony morphology in different media and microscopical morphology). The fungal isolates were further identified using a sequence analysis of the internal transcribed spacer (ITS1-2) region of ribosomal DNA. DNA extraction, amplification, and sequencing were performed according to the SOP-115-11 protocols. The amplified sequences were analysed using the NCBI BLAST algorithm for

comparison. The molecular identification was commissioned by the authors and conducted by the Eurofins BIOMI laboratory. The pure cultures were stored at 5 ° C on PDA slants to maintain viability for further studies.

3.1.2. Selective media screening

To investigate selective media that promote the fungal growth of isolated pathogens, pure fungal colonies were subcultured on potato dextrose agar, Sabouraud Dextrose agar, Czapek-Dox Agar and Malt Extract Agar. All plates were incubated at 25°C and observed regularly for the following 10 days.

3.1.3. *In vitro F. proliferatum* and *S. cepivora* interaction assay

To assess the interaction between the two phytopathogens, a dual culture test was first used. On the selected media suitable for both pathogens (Sabouraud Dextrose Agar), 8mm fungal disks from 8-day-old cultures were placed on opposite sides of the Petri plates. As for the control plates, fungal disks containing the pathogens separately were placed peripherally to ensure consistency. The plates were then incubated at a constant temperature of 25 ° C. To minimise variability across plates, all fungal plugs were taken from the actively growing margins of cultures grown under identical conditions. Three independent experiments were performed, each with 4 replicates per treatment group. The number of replicates was chosen to ensure a sufficient representation of fungal interactions and achieve a robust effect size, as measured by the eta-squared ($\eta 2$) confirming the reliability of the observed differences between treatments. The controlled nature of the *in vitro* environment minimised variability and facilitated precise measurement of fungal growth parameters. Colony growth was monitored daily, and radial growth measurements recorded as means of two perpendicular diameters throughout each fungal colony.

To assess the interaction between the two pathogens, the interaction strength for each pathogen is calculated as follows and is assessed at two time points; the day of contact and the day of full growth of single cultures:

- *Inhibition of growth of F. proliferatum by S. cepivora:*

$$\textbf{\textit{F. proliferatum} growth inhibition (\%)} = (Cf - Df) / Cf \times 100,$$

where Df is the distance the *Fusarium* colonies grow towards the *Stromatinia* colonies and Cf is the mean of the radial growth of the *Fusarium* control plates.

- *Inhibition of S. cepivora growth by F. proliferatum:*

$$\textbf{\textit{S. cepivora} growth inhibition (\%)} = (Cs - Ds) / Cs \times 100,$$

where Ds is the distance the *Stromatinia* colonies grow towards the *Fusarium* colonies, and Cs is the mean of the radial growth of the *Stromatinia* control plates.

3.2. *In planta* screening for resistance against single infections of *F. proliferatum* and *S. cepivora* of garlic cultivars

3.2.1. Plant material preparation

In this study, eleven garlic cultivars were selected for screening to assess their resistance to *S. cepivora* and *F. proliferatum*. The cultivars contained autumn and spring varieties to cover a wide range of genetic diversity. The spring varieties evaluated were ‘Flavor’, ‘Arno’, and 'Makói Tavaszi'. Notably, ‘Makói Tavaszi’ is the only local cultivar examined, distinguishing it from the remaining French varieties, which are cultivated globally. The autumn varieties included 'Thermidrome’, 'Messidor', 'Sabadrome', 'Sabagold', ‘Aulxito’, 'Garcua' and ‘Elephant’. Although commonly referred to as Elephant garlic, this cultivar is not true garlic, but rather belongs to a different species, *Allium ampeloprasum*, closely related to leeks.

3.2.2. *In planta* inoculation of the pathogens

For the *in planta* inoculation of *S. cepivora* and *F. proliferatum* on selected garlic cultivars, the methodology employed was the one suggested by Esler and Coley-Smith (1984). Fungal disks, 8mm in diameter, were cut from 10-day-old cultures of each pathogen, which had been cultivated in selective media. These disks were placed in small wounds on the basal area of the cloves and securely wrapped with parafilm. The samples were incubated at room temperature in humid chambers. Three independent experiments were conducted, each with five replicates per treatment group. Each replicate consisted of 5 cloves, ensuring that variability within replicates was minimised. The number of replicates was chosen to account for the higher biological variability of garlic cloves and achieve a meaningful eta-squared value ($\eta 2$), ensuring robust detection of significant differences in disease incidence between treatment groups. Garlic cloves were randomly assigned to treatment groups. The variation in the size and physiological state was minimised by selecting cloves of similar size and weight. Throughout the evaluation period, the development of mycelia and sclerotia and the progression of necrotic symptoms were documented and analysed over time.

3.2.3. Inspection and analysis

To calculate the percentage of disease incidence for both pathogens, the following formula provided by Manandhar et al. (2016) was used:

Disease incidence (DI (%)) = Number of diseased samples/Total number of samples × 100

The severity of the disease in various garlic cultivars was systematically assessed and classified based on visual evaluations and the severity of symptoms manifested in the cloves of the inoculated replicates. Pathogenicity was classified into the 5 following classes outlined by Mondani et al. (2021):

- **Class 0:** cloves were completely asymptomatic, showing no signs of infection (0%).
- **Class 1:** cloves exhibited small brown spots localized near the basal plate (10%).
- **Class 2:** moderate infection, with brown spots covering half of the basal plate (35%).
- **Class 3:** more extensive infection, with brown spots on the whole perimeter of the basal plate, occasionally accompanied by mycelial growth and/or sclerotia (65%).
- **Class 4:** severe infection, with brown spots on the basal plate extending to the bulb and with prominent visible mycelium and/or sclerotia (90%).

Figure 6: Garlic cloves from the cultivar Topadrome placed in a moist chamber for the *in planta* screening of resistance in garlic cultivars against *F. proliferatum* and *S. cepivora*

3.3. Resistance against simultaneous infections of *F. proliferatum* and *S. cepivora*

To investigate the combined impact of *F. proliferatum* and *S. cepivora* on the various garlic cultivars, a coinoculation approach was undertaken. The methodology used for the dual inoculation mirrored the protocol established for individual pathogen inoculation, adhering to the methodology suggested by Esler and Coley-Smith (1984). However, in this experiment, two fungal disks, each cut from the respective 10-day cultures of *F. proliferatum* and *S. cepivora, were*

concurrently inoculated onto the garlic cloves and secured with parafilm. The samples were incubated at room temperature in humid chambers. Similarly to the single inoculation experiments, three independent experiments were conducted, each with 5 replicates per treatment group. Each replicate consisted of 5 cloves, ensuring that variability within replicates was minimised. The number of replicates was chosen to account for the higher biological variability of garlic cloves and achieve a meaningful eta-squared value (η2), ensuring robust detection of significant differences in disease incidence between treatment groups. The variation in the size and physiological state was minimised by selecting cloves of similar size and weight. The growth of mycelia and sclerotia and the occurrence of necrosis were documented over time.

The classification system suggested by Mondani et al. (2021) used to assess the individual pathogenicity of *F. proliferatum* and *S. cepivora* was also applied in this test, along with the percentage of disease incidence formula provided by Manandhar et al. (2016).

3.4. *In vitro* study of the antagonistic activity of *Trichoderma asperellum* and *Bacillus amyloliquefaciens* against garlic pathogens *Fusarium proliferatum* and *Stromatinia cepivora*

3.4.1. Isolation and identification of *T. asperellum* and use of commercial *B. amyloliquefaciens*

During the initial inoculation of the sampled symptomatic garlic cloves in PDA media, characteristic green mycelial growth indicative of *Trichoderma* spp. was observed. Subsequently, pure cultures were prepared after ensuring the isolation of *Trichoderma* species. The identification of the isolate as *Trichoderma asperellum* was carried out by examining the morphological characteristics and conidial formations of the fungal colonies under microscopic analysis. To preserve the isolates for further studies, pure cultures of the antagonist were stored at 5°C on PDA slants.

The isolation of *Bacillus amyloliquefaciens* was performed using a commercialised Serenade® ASO biopesticide (Bayer), which contains 1×10^9 CFU/ml of the *B. amyloliquefaciens* QST 713 strain (Figure 7), which was cultured in sterile conditions. A measured amount of the product was suspended in sterile distilled water and subjected to serial dilution to obtain well-isolated colonies. A loopful of the diluted suspension was streaked onto NA plates and incubated at 25 ° C for 24 to 48 hours to facilitate bacterial growth. Following incubation, morphologically distinct colonies of *B. amyloliquefaciens* were selected and further streaked onto fresh NA plates to obtain pure cultures.

Figure 7: Commercial formulation of *Bacillus amyloliquefaciens* used in the study. The Serenade® ASO biopesticide (Bayer) contains contains 1×10^9 CFU/mL of *B. amyloliquefaciens* QST 713 strain.

3.4.2. Dual culture assays

The dual culture method was used to evaluate the antagonistic activity of *T. asperellum* and *B. amyloliquefaciens* against isolated garlic pathogens. Each pathogen was cultured in its optimal growth media, with *S. cepivora* grown on Sabouraud Dextrose Agar (SDA) and *F. proliferatum* on Potato Dextrose Agar (PDA). In each Petri plate, an 8 mm disk of *T. asperellum* and a 13 mm disk of *B. amyloliquefaciens*, both taken from pure cultures, were placed on opposite sides of the dish to allow direct interaction and observation of inhibition effects. As for the control plates, fungal disks containing only pathogens were placed peripherally to ensure consistency. The plates were then incubated at a constant temperature of 25°C. To minimise variability across plates, all fungal plugs were taken from the actively growing margins of cultures grown under identical conditions. The controlled nature of the *in vitro* environment minimised variability and facilitated precise measurement of fungal growth parameters. Colony growth was monitored daily, and radial growth measurements recorded as means of two perpendicular diameters throughout each fungal colony.

3.4.3. Inspection and analysis

The inhibitory impact of *T. asperellum* and *B.amyloliquefaciens* on plant pathogenic fungi was quantified using the equation provided by Hernandez Castillo et al. (2011), which is as follows:

$$\textbf{Inhibition (\%)} = [(D1-D2) / D1] \times 100,$$

where **D1** is the growth of the pathogen in the absence of the antagonist and **D2** is the growth of the pathogen in the presence of the antagonist.

The extent of antagonistic activity of *T. asperellum* and *B. amyloliquefaciens* was assessed following the classification system proposed by Bell et al. (1982). This methodology categorises interactions into five levels:

- **Class 1:** Complete overgrowth of the pathogen by the antagonist (100% coverage).
- **Class 2:** The antagonist overgrown at least 3/4th of pathogen surface (75% coverage).
- **Class 3:** The antagonist colonizes half of the pathogen's growth area (50% coverage).
- **Class 4:** The pathogen and the antagonist locked at the point of contact.
- **Class 5:** Dominance of the pathogen, overgrowing the antagonistic agent.

3.5. In *planta* study of the effectiveness of *Trichoderma asperellum* and *Bacillus amyloliquefaciens* against garlic pathogens *Fusarium proliferatum* and *Stromatinia cepivora* under controlled phytotron conditions

3.5.1. Preparation of *T. asperellum* and *B. amyloliquefaciens* suspensions and application

The antagonists were prepared from pure cultures previously isolated and identified (see section 3.3). *Trichoderma asperellum* was cultured on Potato Dextrose Agar (PDA) for 10 days at 25°C, while *B. amyloliquefaciens* was grown on Nutrient Agar (NA) at the same temperature for 2 days.

To prepare the suspensions, 20 mL of sterile distilled water was added to the surface of the cultures, and the colonies were gently scraped using a sterile glass rod to dislodge conidia (for *T. asperellum*) or cells (for *B. amyloliquefaciens*). The concentrated suspension was then diluted with sterile water to reach the target concentrations of 1×10^7 conidia/mL for *T. asperellum* and 1×10^8 CFU/mL for *B. amyloliquefaciens*, based on direct counts using a Neubauer chamber.

Immediately after planting, cloves in the antagonist-treated groups were drenched with 50 mL of freshly prepared suspension. For combination treatments, 25 mL of each suspension was applied sequentially to ensure even colonization. Untreated control plants received an equal volume of sterile distilled water to maintain uniform soil moisture levels across treatments.

3.5.2. Experimental setup

The experiment was conducted in a controlled phytotron environment maintained at a temperature of 22°C and a relative humidity of 70%, conditions suitable for both garlic growth and pathogen development, under a 12h light/ 12h dark photoperiod. Healthy, uniform-sized garlic cloves were selected and surface-sterilized by immersion in 1% sodium hypochlorite for 2 minutes, followed by rinsing three times with sterile distilled water. The cloves were then planted in individual pots

filled with sterile perlite, ensuring well-aerated and pathogen-free substrate conditions. To ensure adequate nutrient availability throughout the growth period, a balanced liquid nutrient solution was added to the perlite at planting.

For the pathogen inoculation, 1 cm agar plugs taken from actively growing 8-day-old cultures of *F. proliferatum* (on PDA) and *S. cepivora* (on SDA) were placed directly beneath each clove, with the mycelial surface facing the basal plate of the garlic clove to ensure direct contact upon root emergence. Each clove was then planted in individual pots filled with perlite. Perlite was selected as the planting media due to its inert nature, providing a sterile, well-aerated, and well-drained substrate, minimizing interactions from external microbiota.

To ensure direct contact between the pathogens and the cloves, a 1 cm agar plug excised from the actively growing edge of 8-day-old fungal cultures was placed directly beneath the basal plate of each clove at a depth of 1 cm, with the mycelial surface of the plug facing the clove base. This positioning ensured immediate pathogen contact with emerging roots, simulating natural soilborne infection.

The experiment consisted of five treatment groups:

- Cloves inoculated with *F. proliferatum* (untreated control).
- Cloves inoculated with *S. cepivora* (untreated control).
- Cloves inoculated with *F. proliferatum* and treated with antagonists.
- Cloves inoculated with *S. cepivora* and treated with antagonists.
- Healthy (uninoculated) cloves (absolute control).

Each treatment was applied to 5 replicate plants, and the experiment was conducted twice as two independent experimental repetitions, resulting in a total of 50 experimental units/treatment group.

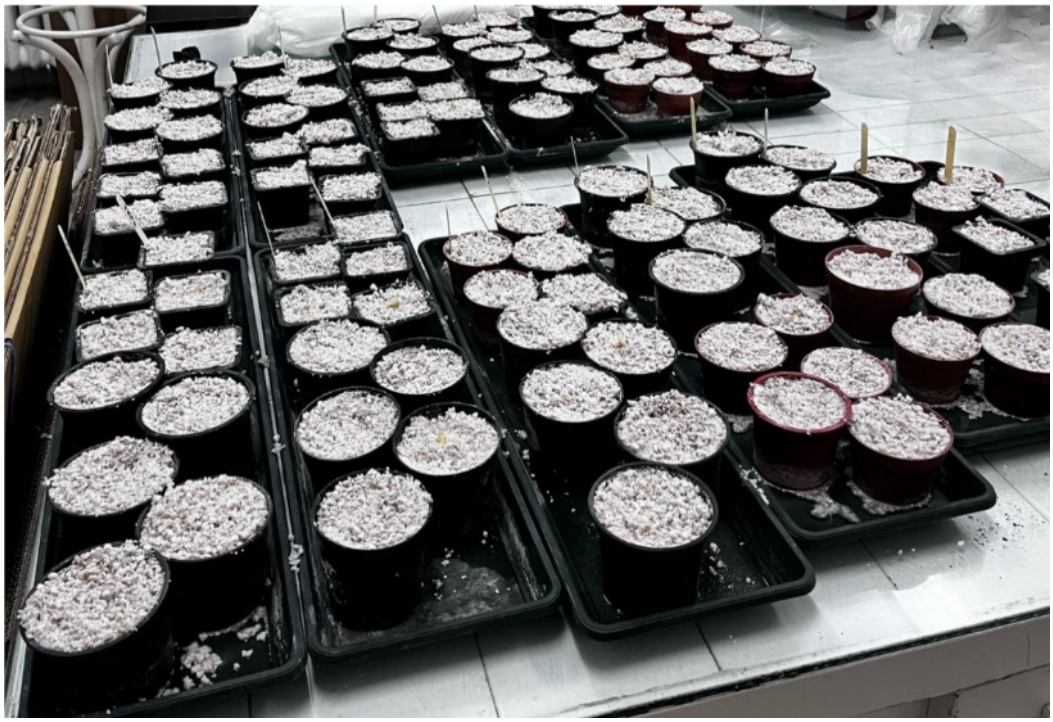

Figure 8: Experimental setup of garlic plants grown in perlite-filled pots for the *in planta* evaluation of biocontrol efficacy of *Trichoderma asperellum and Bacillus amyloliquefaciens* against *Fusarium proliferatum* and *Stromatinia cepivora* under controlled phytotron conditions.

3.5.3. Plant height measurements and inspection for symptoms

Plant growth and health were monitored for 22 days. Plant height was recorded at weekly intervals, measured from the base of the stem to the tip of the tallest leaf. Monitoring plant height served as an indirect indicator of both pathogen damage and potential biocontrol efficacy.

Disease symptoms were visually inspected throughout the trial, with a specific focus on stunting, foliar wilting, and chlorosis.

3.6. Enzymatic analysis of oxidative responses in garlic and okra seedlings under pathogen and biocontrol treatments

3.6.1. Garlic and okra plant material preparation

This study evaluated the oxidative enzyme responses of garlic and okra seedlings to pathogen infection and biocontrol treatments. Garlic cloves (cv. Makoi) and okra seeds were surface sterilised using 1% sodium hypochlorite for 2 minutes and thoroughly rinsed with sterile distilled water. Germination was carried out in humid chambers at 24 ° C under ambient light conditions (Figure 9). The garlic seedlings were grown for 10 days and okra seedlings for 4 days, until adequate development of the shoot and root allowed for experimental treatments.

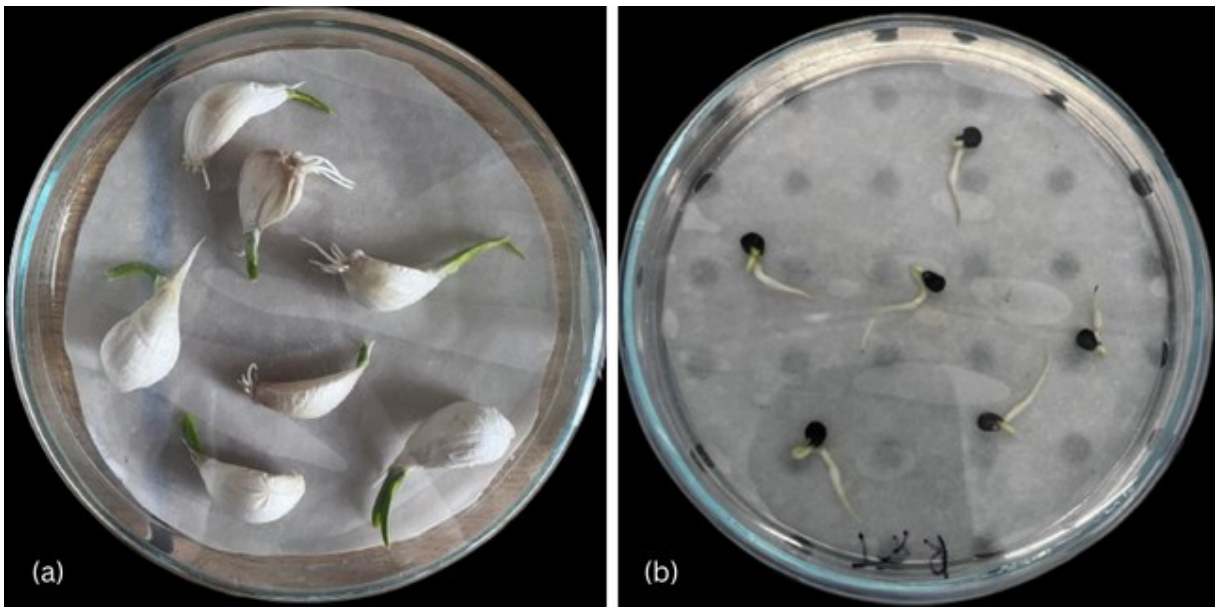

Figure 9: Germination of garlic and okra seeds for enzyme activity experiments. (a) Garlic cloves and (b) okra seeds germinated under humid chamber conditions on sterile filter paper at room temperature (24 °C) prior to inoculation with pathogens and biocontrol agents.

3.6.2. Pathogen and biocontrol inoculation

The pathogens included *Fusarium proliferatum* and *Stromatinia cepivora* for garlic, and *Rhizoctonia solani* and *Sclerotinia sclerotiorum* for okra. Mycelial disks (1cm for garlic and 0.7 cm for okra) were cut from the edge of actively growing fungal cultures and placed directly on the basal part of the seedlings, targeting the root–hypocotyl zone.

The biocontrol agents included *Trichoderma asperellum* and *Bacillus amyloliquefaciens*. *T. asperellum* was cultured on PDA for 7 days; Conidial suspensions were prepared in sterile distilled water with 0.01% Tween 20 and adjusted to 1×10^7 conidia/mL using a hemocytometer. *B. amyloliquefaciens* was grown on Nutrient agar (NA) for 24 hours. Bacterial suspensions were prepared in sterile distilled water and standardised to 1×10^8 CFU/mL. A 100 µL aliquot of each suspension was applied in the root zone for each seedling.

The control groups were not inoculated and remained healthy throughout the experiment. All treatments were performed in three replicates.

3.6.3. Enzyme extraction

Forty-eight hours after the okra inoculation and five days after inoculation for garlic—corresponding to the onset of visible symptoms, 500 mg of fresh seedling tissue was collected per treatment for enzymatic analysis. The tissue was placed in a pre-chilled mortar and thoroughly ground using a pestle under continuous addition of liquid nitrogen to ensure rapid freezing and prevent enzymatic degradation. The resulting fine powder was immediately transferred to a 2 mL

volume of ice-cold Tris extraction buffer. The buffer consisted of 0.05 M Tris-HCl (pH 7.8), 1 mM EDTA-Na_2, and 7.5% (v/v) polyvinylpyrrolidone (PVP K25), formulated to stabilize proteins and inhibit phenolic oxidation during extraction. The homogenate was then centrifuged at 12,000 × g for 15 minutes at 4 ° C. The resulting clear supernatant was carefully collected and kept on ice for immediate use in the guaiacol peroxidase (POX) and polyphenol oxidase (PPO) activity assays.

Figure 10: Preservation of supernatants and assay buffer for guaiacol peroxidase (POX) activity determination, showing microcentrifuge tubes containing clarified extracts from seedling tissues and the POX assay buffer (50 mM Tris-HCl, pH 7.0, 0.2 mM EDTA, 2% PVPP, 10% glycerol) maintained on ice to ensure enzymatic integrity and substrate stability prior to spectrophotometric analysis.

3.6.3.1. Guaiacol peroxidase (POX)

POX activity was quantified by guaiacol oxidation following the method of Chance and Maehly (1955) with minor modifications, with absorbance measured at 470 nm. The reaction mixture included:

- 2.2 mL of 0.1 M sodium phosphate buffer (pH 6.0).
- 100 µL of 50 mM guaiacol
- 100 µL of 32.5 mM hydrogen peroxide.

- 50 µL of enzyme extract.

Results were expressed as $\Delta A \cdot min^{-1} \cdot g^{-1}$ FW using a conversion factor of 11.05.

3.6.3.2. Polyphenol oxidase (PPO)

PPO activity was assessed via catechol oxidation following the method of Kar and Mishra (1976) with minor modifications, with absorbance measured at 400 nm. The assay mixture consisted of:

- 1.6 mL of 0.1 M sodium phosphate buffer (pH 6.0).
- 200 µL of 0.2 M catechol.
- 200 µL of enzyme extract.

Activity was calculated using a conversion factor of 63.16 and expressed in $\Delta A \cdot min^{-1} \cdot g^{-1}$ FW.

3.6.4. Enzyme activity assays

Enzyme activity was measured spectrophotometrically at 0 seconds, 30 seconds, and 1 minute after mixing. The values at 1 minute were used for graph presentation, while all timepoints were included in statistical analysis. All treatments were conducted with three independent biological replicates.

3.7. Statistical analysis

Statistical analyses were performed using IBM SPSS Statistics (version 27.0) and Python (version 3.11.6). Both platforms were employed for assumption testing, model fitting, effect size estimation, and data visualization.

Prior to hypothesis testing, datasets were examined for conformity with parametric assumptions. Normality of residuals was assessed with the Shapiro–Wilk test, and homogeneity of variances was verified using Levene's test. When assumptions were met, data were analyzed by one-way or two-way analysis of variance (ANOVA) to evaluate differences among treatments. In factorial designs, both main effects and interaction terms were considered. Post hoc pairwise comparisons were carried out with Tukey's Honestly Significant Difference (HSD) test where appropriate.

For datasets that did not satisfy parametric assumptions, non-parametric procedures were applied. The Kruskal–Wallis H test was used as a rank-based analogue to ANOVA, and significant outcomes were followed by Dunn's post hoc test with Bonferroni-adjusted p-values to control the familywise error rate.

In all cases, effect sizes were calculated to complement significance testing. For ANOVA, eta squared (η^2) values were reported to indicate the proportion of variance explained by each factor, whereas for non-parametric analyses, η^2 was derived from the H statistic.

CHAPTER 4: RESULTS

4.1. *In vitro* investigation of pathogen-pathogen interactions of *Fusarium proliferatum* and *Stromatinia cepivora* on garlic

4.1.1. Isolation and identification of the phytopathogens

Inoculation of symptomatic parts from garlic tissues into growth media, followed by purification protocols, facilitated the isolation of two distinct fungal pathogens.

Macroscopic identification was conducted on colony morphological characteristics. On PDA, the *F. proliferatum* colonies exhibited distinct aerial white mycelia with a dark violet pigmentation on PDA, while *S. cepivora* was identified by the abundant development of black microsclerotia within the colonies, a specific trait of the pathogen.

Microscopical examination of *F. proliferatum* revealed distinct characteristics that confirm its identification (Figure 11). Under the microscope, thin, thin-walled macroconidia were observed, which were relatively straight and predominantly 3- to 5-septate. Apical cells were curved and the basal cells appeared poorly developed. These macroconidia were found to form in pale orange sporodochia, although these structures were observed infrequently. Microconidia were abundant, forming moderate-length chains produced by both monophialides and polyphialides. They were mainly club-shaped with a flattened base. Importantly, no chlamydospores were detected, which is characteristic of this species and further corroborates its identification. Our observations align with descriptions of the morphology of *F. proliferatum,* as detailed by Leslie and Summerell (2006).

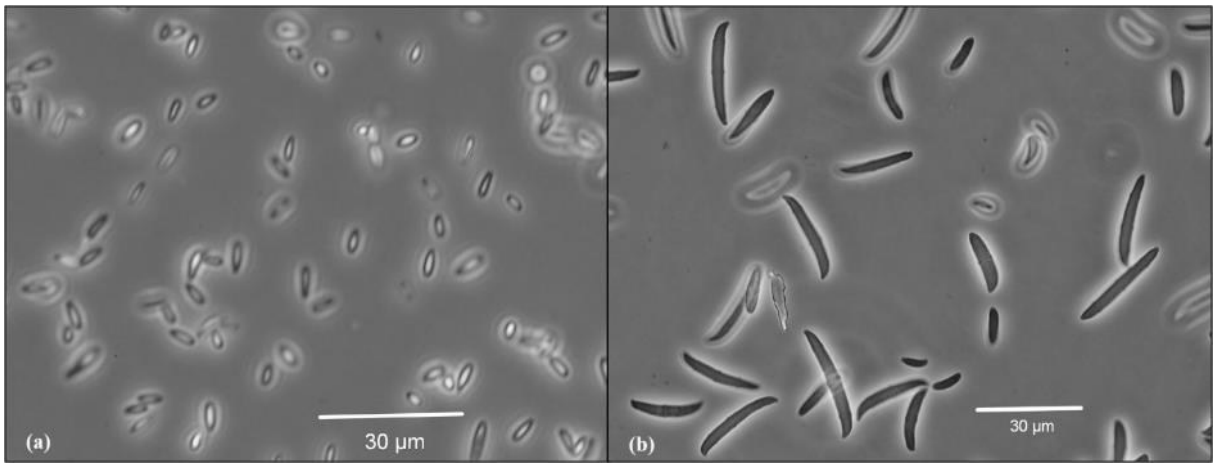

Figure 11: Microconidia **(a)** and macroconidia **(b)** of the *Fusarium* strain isolated from garlic.

ITS sequencing complemented these findings and provided additional confirmation. ITS sequences were compared against the NCBI database using the BLAST algorithm. *Stromatinia cepivora* was identified with 100% similarity according to the ITS1-2 region (Accession No. KP257580.1) and did not show nucleotide polymorphisms. The second isolate was identified as

part of the *Fusarium fujikuroi* species complex (FFSC) with 100% similarity. However, *F. proliferatum, a* known member of the FFSC, has previously been identified as the primary causal agent of dry rot in garlic (Gálvez and Palmero, 2022). Given this established role, the morphological observations, and the genetic similarity observed, the isolate is conclusively identified as *F. proliferatum*. These observations, which include macroscopic, microscopic and molecular analyses, confirm the identity of the isolates. Phylogenetic trees, based on the results of the BLAST analyses, were constructed to validate these identifications and are shown in Figure 12 and Figure 13.

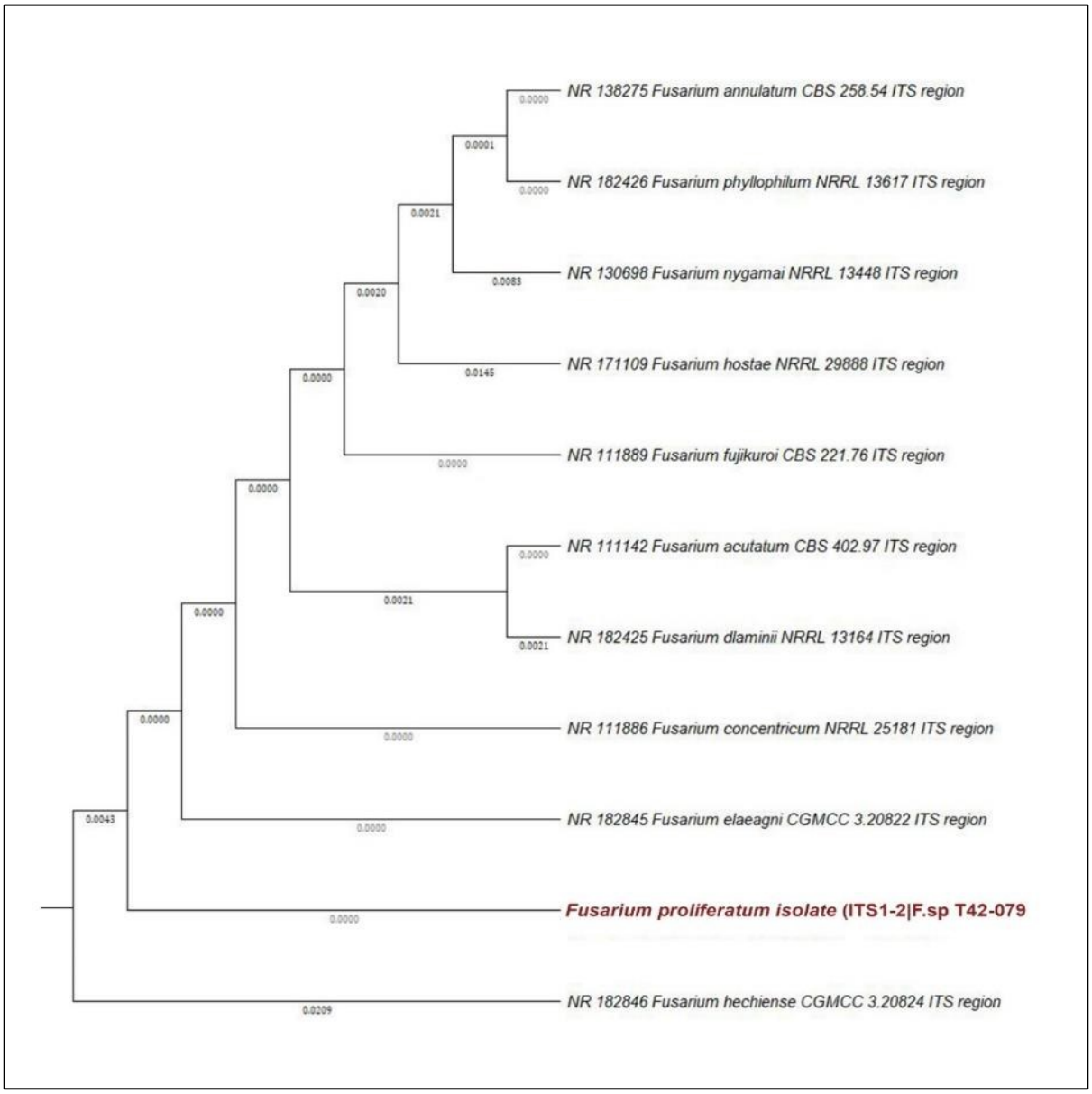

Figure 12: Phylogenetic tree constructed using the Maximum Likelihood (ML) method based on the ITS region sequences of *Fusarium* spp. The tree was generated with MEGA software (version 12.0.14), and the branch labels represent genetic distances (substitutions per site) between sequences. The isolate "*Fusarium proliferatum* isolate (ITS1-2|F.sp T42-079)" is

highlighted in red and shows its evolutionary relationship with closely related *Fusarium* species. The sequences are labeled with GenBank accession numbers and species names.

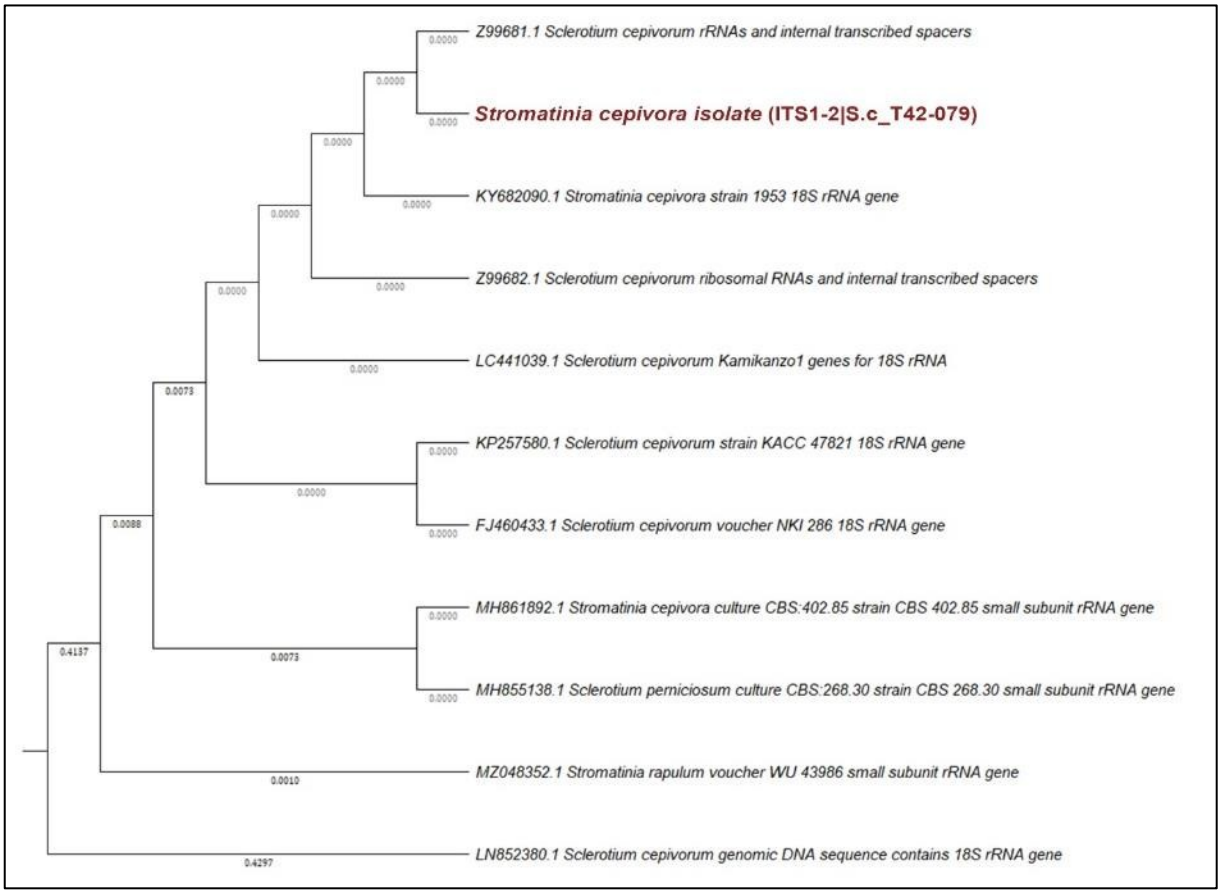

Figure 13: Phylogenetic tree constructed using the Maximum Likelihood (ML) method based on the ITS region sequences of *Stromatinia* spp. (*Sclerotium* spp.). The tree was generated with MEGA software (version 12.0.14), and the branch labels represent genetic distances (substitutions per site) between sequences. The isolate "*Stromatinia cepivora* isolate (ITS1-2|S.c T42-079)" is highlighted in red and shows its evolutionary relationship with closely related *Stromatinia* species. The sequences are labeled with GenBank accession numbers and species names.

4.1.2. Selective media analysis

Figure 14 shows the growth phenotypes and colony morphology of *F. proliferatum* and *S. cepivora* in different media. All four media employed successfully supported the growth of *F. proliferatum.* Malt Extract Agar (MEA) promoted the formation of white mycelia with progressively intensifying dark red pigmentation. On Sabouraud Dextrose Agar (SDA), the fungus developed aerial white colonies accompanied by yellow to light brown pigmentation. Potato Dextrose Agar (PDA) supported the growth of white mycelia with dark violet pigmentation. On the contrary,

Czapek-Dox Agar (CDA) was conducive to the growth of cotton-like white mycelia exhibiting white pigmentation.

On the contrary, for *S. cepivora*, only malt extract agar (MEA) and Sabouraud Dextrose agar (SDA) proved to be effective in promoting prolific fungal growth, showing yellowish and white pigmentations, respectively. Furthermore, both mediums facilitated the development of abundant black sclerotia on the surface of cultures.

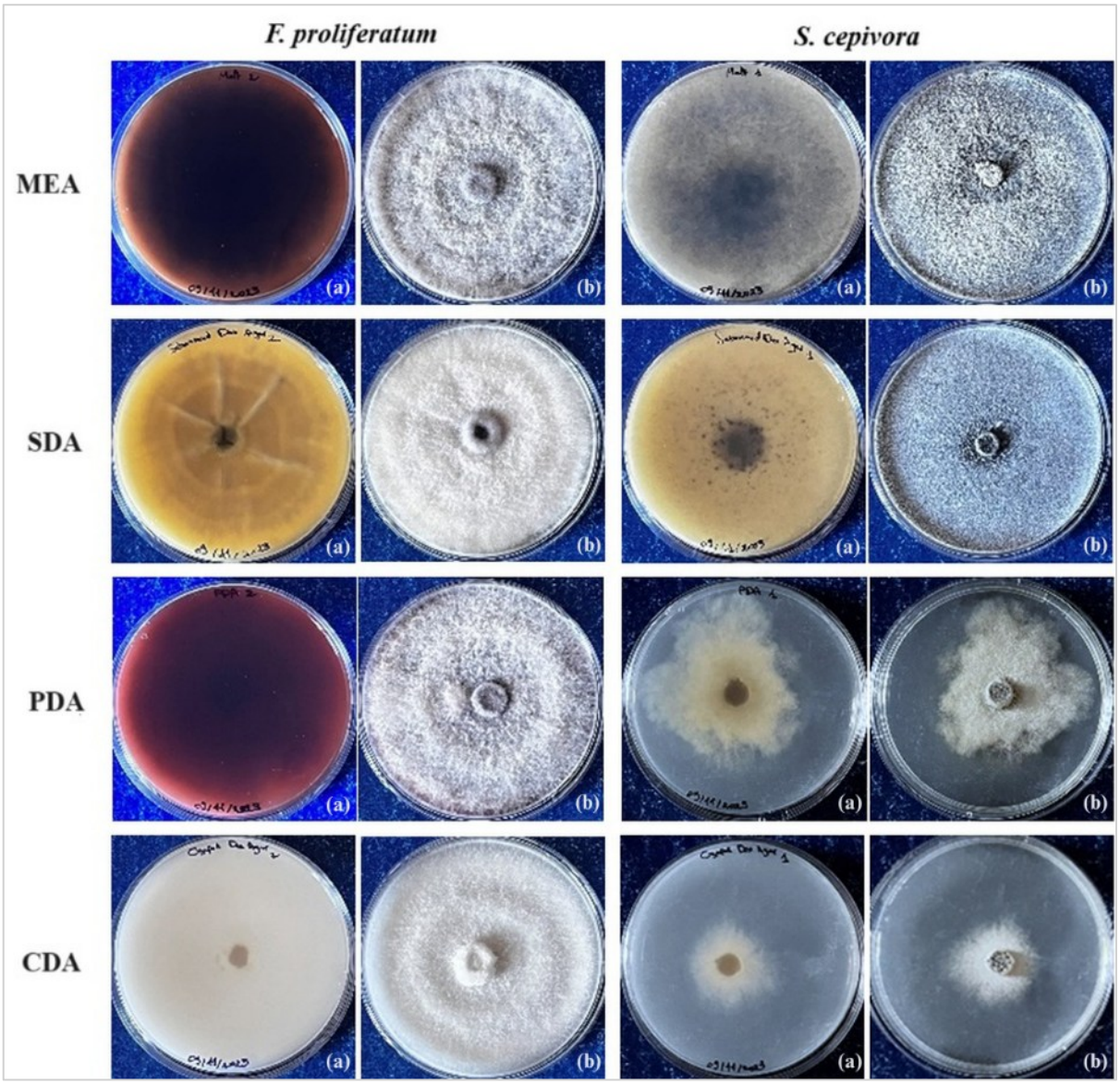

Figure 14: Growth phenotypes and colony morphology of *Fusarium proliferatum* and *Stromatinia cepivora* on different media: Malt Extract Agar (MEA); Sabouraud Dextrose Agar (SDA); Potato Dextrose Agar (PDA); Czapek-Dox Agar (CDA). For each media, (**a**) presents the reverse side of the Petri dish and (**b**) presents the upper side.

4.1.3. *In vitro F. proliferatum* and *S. cepivora* interaction assay

The interactions between *F. proliferatum* and *S. cepivora* were observed and quantified daily through a dual culture assay. The experiment was carried out on Sabouraud Dextrose Agar (SDA), which prompted the growth of both pathogens. Figure 15 illustrates visual observations of dual cultured dishes of S. *cepivora* and *F. proliferatum*. Both fungi have kept on their side of the dish, neither overgrowing the other. This further illustrates the hypothesis that these two fungi have a certain type of co-existence, which is likely a competitive one. Figure 15 also highlights a clear area of contact between the two fungi, where there is a significantly pronounced darkening of the colonies *of S. cepivora*.

Daily radial growth measurements were recorded throughout the experiment and are presented in Figure 16 over a period of 14 days with a clear section of the two studied time points, providing a detailed visualisation of the growth dynamics over time. Table 3 shows the radial growth pattern of each pathogen under both co-cultured and control conditions, as well as the percentage of growth inhibition presented.

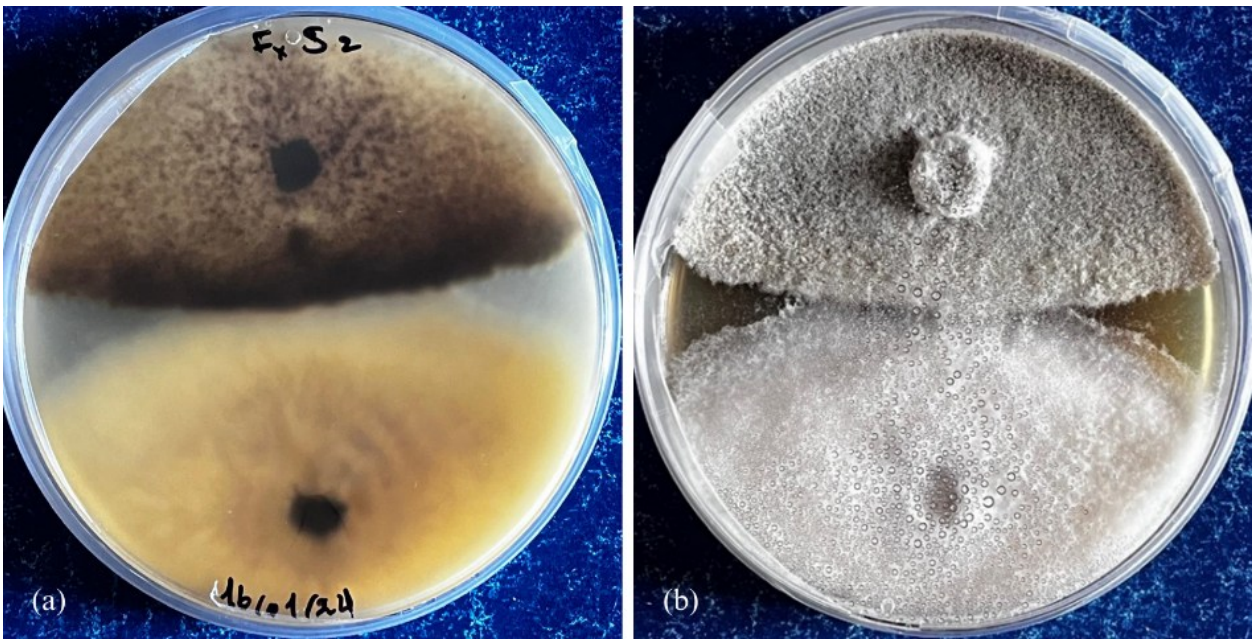

Figure 15: Pathogen–pathogen interaction observed in co-culture of *S. cepivora* and *F. proliferatum* on SDA media. Section **(a)** shows the reverse side of the Petri dish, and section **(b)** shows the front side (images taken by the authors).

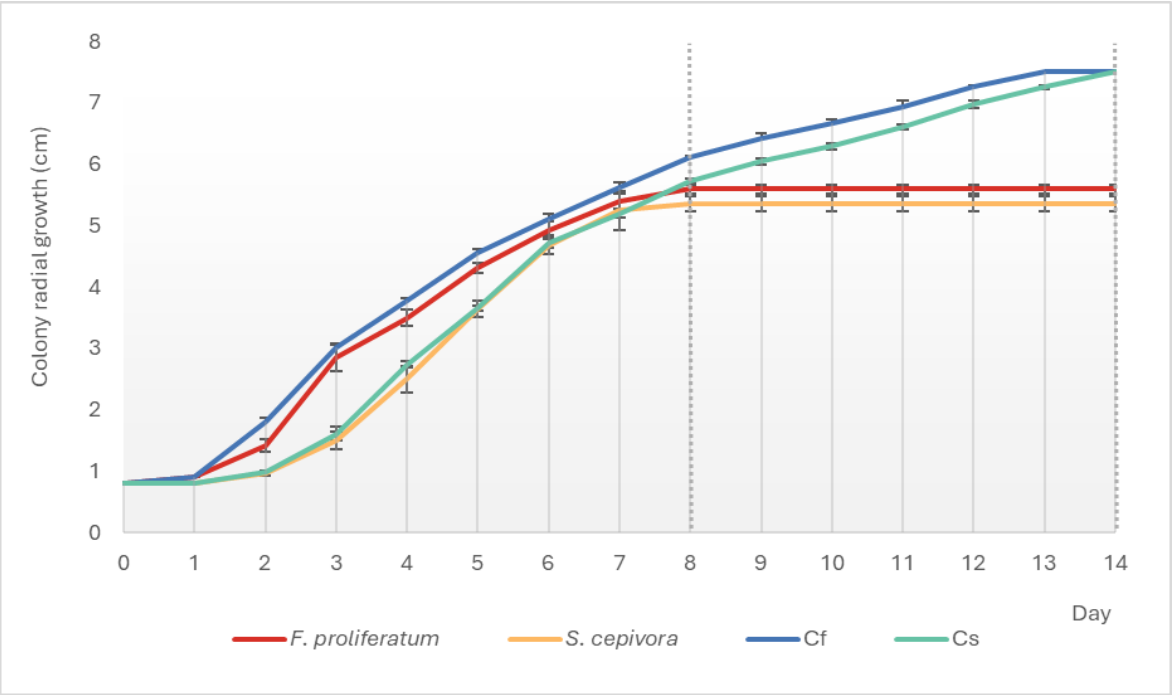

Figure 16: Daily radial growth of *F. proliferatum* and *S. cepivora* in dual inoculation compared to control colonies over a 14-day period. Cf represents the radial growth of the *F. proliferatum* control plates. Cs represents the radial growth of the *S. cepivora* control plates. Vertical dashed lines indicate key time points: Day 8, when growth ceased in dual cultures, and Day 14, when single cultures reached full radial growth. Error bars represent SD values.

Table 3: Radial growth and growth inhibition measurements of *Fusarium proliferatum* and *Stromatinia cepivora* under dual culture conditions on Days 8 and 14. Data are presented as mean ± SE from four replicates of three independent experiments. Statistical significance was determined using one-way ANOVA, with effect sizes reported as eta-squared (η^2).

Time-point		Radial growth (cm)				Growth inhibition (%)			
		F. proliferatum	***S. cepivora***	***p*-value**	**η2**	***F. proliferatum***	***S. cepivora***	***p*-value**	**η2**
Day 8	Dual	5.60 ± 0.02	5.35 ± 0.03	<0.001	0.57	8.27% ± 0.35	6.40% ± 0.63	0.01	0.23
	Control	6.10 ± 0.02	5.71 ± 0.02						
Day 14	Dual	5.60 ± 0.02	5.35 ± 0.03	<0.001	0.57	25.39% ± 0.29	28.61% ± 0.47	<0.001	0.60
	Control	7.5 ± 0.00	7.5 ± 0.00						

Values are means of four replicates from three independent experiments.
Percentage of inhibition is measured based on the mean growth of control dishes.
Data are shown in "mean ± standard error" form.

Both fungi exhibited growth patterns comparable to their respective controls until approaching the proximity zone of interaction (Figure 15). In dual cultures, fungal growth slowed earlier on the mycelial front directed toward the opposing pathogen due to competition in the proximity zone, while the mycelial front expanding away from the interaction continued to grow. On the contrary, single cultures grew uninhibited, resulting in slightly greater radial growth at the same time point (Day 8), when dual cultures had already stopped growth at the point of contact between the colonies on the interacting front. *F. proliferatum* exhibited a growth reduction to 5.60 cm from 6.10 cm observed under control conditions. Similarly, *S. cepivora* showed reduced growth, measuring 5.35 cm in the presence of *F. proliferatum* compared to its control growth of 5.72 cm. The percentage growth inhibition recorded for *F. proliferatum* and *S. cepivora* was 8.27% and 6.40%, respectively. The results of one-way ANOVA at the first time point (Day 8), summarised in Table 3, confirmed significant differences in the radial growth patterns between *F. proliferatum* and *S. cepivora* under dual culture conditions, the results being statistically significant at $p < 0.001$. The size of the effect size ($\eta^2 = 0.57$) indicates a large effect, which means that a substantial proportion of the variance in radial growth can be attributed to the fungal species at this time point. For growth inhibition, ANOVA revealed a statistically significant difference at $p = 0.01$, with an effect size ($\eta^2 = 0.23$) representing a moderate effect, suggesting that the competitive interaction had a noticeable impact on inhibition rates by Day 8.

On day 14, the inhibition zone between the colonies remained stable on dual culture plates, and no further growth observed along the interacting fronts. The noninteracting fronts of both fungi had already reached their respective maximum radial extents on Day 8, indicating that resource competition and mutual inhibition had effectively halted growth. The darkening of the colonies of *S. cepivora* in closest proximity to *F. proliferatum* became relatively more pronounced, suggesting an intensified response to the interaction. In control plates, *F. proliferatum* and *S. cepivora* continued to grow, reaching full radial growth of 7.5 cm on day 13 and Day 14, respectively. Growth inhibition at the second studied time point (day 14) reached 25.39% for *F. proliferatum* and 28.61% for *S. cepivora*, highlighting the extent of the competitive interaction. On day 14, one-way ANOVA confirmed continued significant differences in radial growth patterns between *F. proliferatum* and *S. cepivora* under dual culture conditions ($p < 0.001$), with a large effect size ($\eta^2 = 0.57$) observed at this time point. For growth inhibition, the results were highly significant ($p < 0.001$), with an effect size ($\eta^2 = 0.60$) indicating a large effect, reflecting that the difference in growth between control and dual culture conditions had become more pronounced on day 14.

The box plot visualised in Figure 17 illustrates the percentage of pathogen growth inhibition under dual culture conditions at the two critical time points and further confirms the trends observed in Figure 16. The inclusion of jitter points in this visualisation provides additional insight into the distribution of individual data points across replicates.

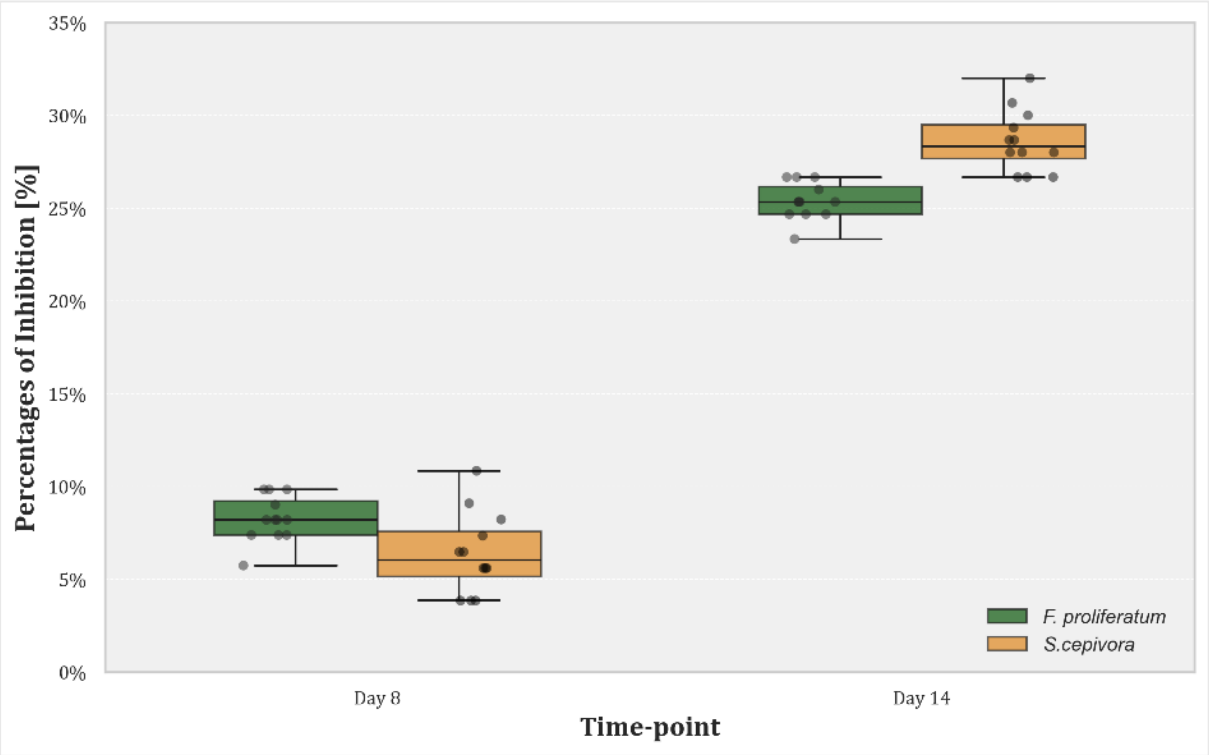

Figure 17: Box plot illustrating the percentage of growth inhibition of *F. proliferatum* and *S. cepivora* in dual culture conditions at two time points: Day 8 and Day 14. Day 8 represents the time when dual culture colonies ceased growth due to competitive interactions, while Day 14 corresponds to the point where single cultures reached full radial growth.

On day 8, growth inhibition is relatively low for both fungi, reflecting the initial effects of competitive co-existence in dual cultures. The difference between dual cultures and single cultures in terms of growth is moderate, with inhibition rates remaining consistent between replicates. On day 14, inhibition rates increased significantly for both fungi, with *S. cepivora* showing slightly higher inhibition percentages than *F. proliferatum*. At this stage, single cultures have reached full radial growth, while dual cultures exhibit sustained growth inhibition. The visualised data highlight that the difference between the growth of dual culture and single culture increases with time, demonstrating the cumulative impact of prolonged interaction.

4.1.4. Resistance against single infections of *F. proliferatum* and *S. cepivora*

The pathogenic impact of *F. proliferatum* and *S. cepivora* after the *in planta* inoculation of pathogen fungal disks on the basal plates of the garlic cultivars was individually assessed.

Evaluation of disease incidence was systematically expressed as the percentage of infected samples relative to the total number of samples per cultivar, and the severity of symptoms was classified according to the observed symptoms, which ranges from Class 0 (asymptomatic) to Class 4 (severe infection).

Figure 18 shows the disease symptoms of *Fusarium* bulb rot and white rot due to individual and co-inoculations with *F. proliferatum* and *S. cepivora* in the eleven tested garlic cultivars tested.

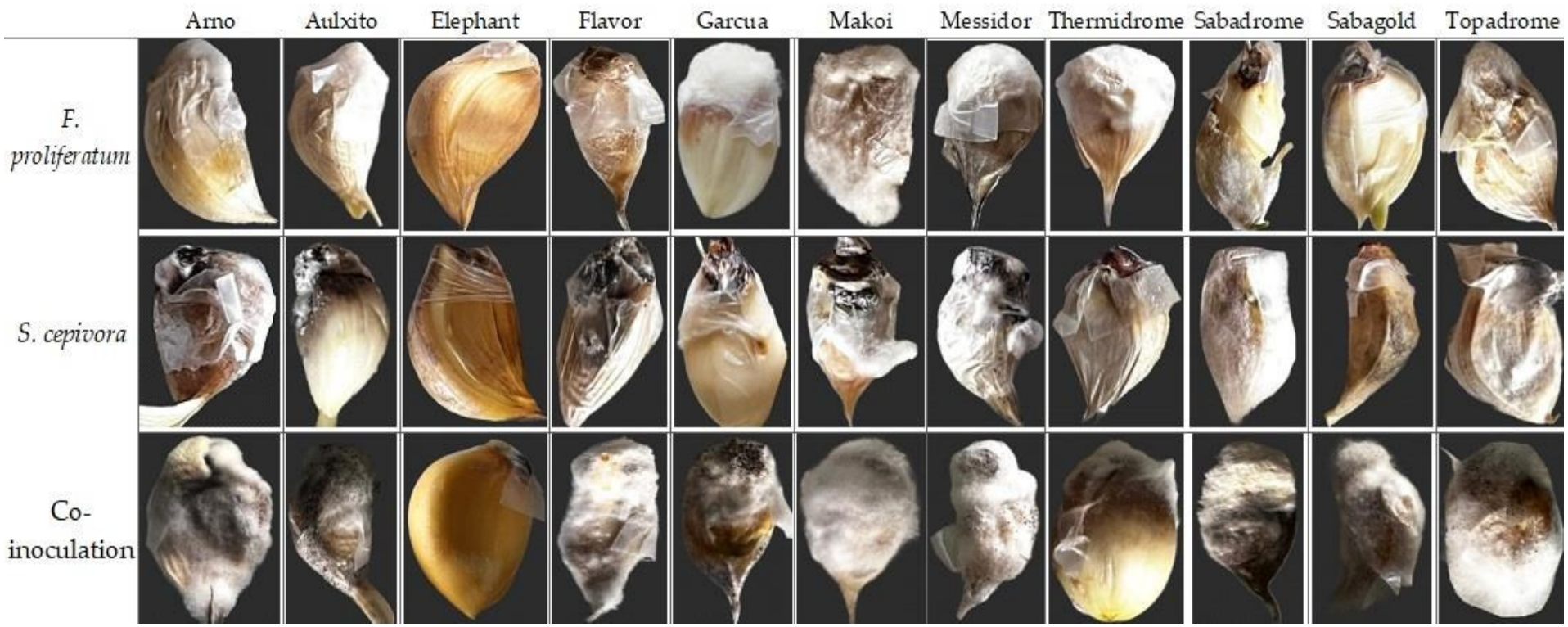

Figure 18: Disease symptoms of *Fusarium* bulb rot and white rot due to individual and co-inoculations with *F. proliferatum* and *S. cepivora* on the eleven tested garlic cultivars (images taken by the authors).

The results summarised in Table 4 show the class and percentage of disease incidence for each cultivar under single and dual inoculation conditions. Figure 19 provides a visualisation of disease incidences across garlic cultivars in these inoculation trials. The results of the one-way ANOVA confirmed that the differences in disease incidence were statistically significant ($p < 0.001$) for single inoculations of *F. proliferatum* and *S. cepivora* in garlic cultivars. The size of the effect size ($\eta 2 = 0.48$) indicates a moderate to large effect, suggesting that fungal species and their interactions with different garlic cultivars accounted for a substantial part of the variance in disease incidence in single inoculations.

Table 4: Disease incidence and severity classification of garlic cultivars due to single and dual inoculation with *F. proliferatum* and *S. cepivora*. Statistical analysis was performed, and p-values and effect sizes (eta-squared η2) are included.

Experiment	***F. proliferatum***		***S. cepivora***		**Dual inoculation**	
Cultivars	**Class**	**DI (%)**	**Class**	**DI (%)**	**Class**	**DI (%)**
Sabagold	3	82.67% ± 0.04 c	1	85.33% ± 0.04 c	4	97.33% ± 0.01 b
Garcua	4	96.00% ± 0.02 d	2	84.00% ± 0.04 c	4	97.33% ± 0.01 b
Thermidrome	4	93.33% ± 0.02 d	2	96.00% ± 0.02 c	4	97.33% ± 0.01 b
Flavor	1	89.33% ± 0.03 d	4	65.33% ± 0.05 b	4	98.67% ± 0.01 b
Messidor	3	68.00% ± 0.05 c	4	85.33% ± 0.04 c	4	97.33% ± 0.01 b
Topadrome	4	93.33% ± 0.02 d	3	97.33% ± 0.01 c	4	98.67% ± 0.01 b
Arno	3	92.00% ± 0.03 d	4	90.67% ± 0.03 c	4	96.00% ± 0.02 b
Makói	4	29.33% ± 0.05 b	4	98.67% ±0.01 c	4	97.33% ± 0.01 b
Aulxito	4	93.33% ± 0.02 d	4	93.33% ±0.02 c	4	98.67% ± 0.01 b
Elephant	0	0.00% ± 0.00 a	0	0.00% ± 0.00 a	0	0.00% ± 0.00 a
Sabadrome	4	89.33% ± 0.36 d	4	97.33% ± 0.01 c	4	97.33% ± 0.01 b
SE Total		**0.015**		**0.014**		**0.011**
***p*-value**		**< 0.001**		**< 0.001**		**< 0.001**
Effect size (η2)		**0.48**		**0.48**		**0.78**
Values are means of three experiments, with five replicates per experiment and five garlic cloves per replicate. **Data are shown in "mean ± standard error" form.** **Values marked with the same letter are not scientifically different at $p < 0.05$**						

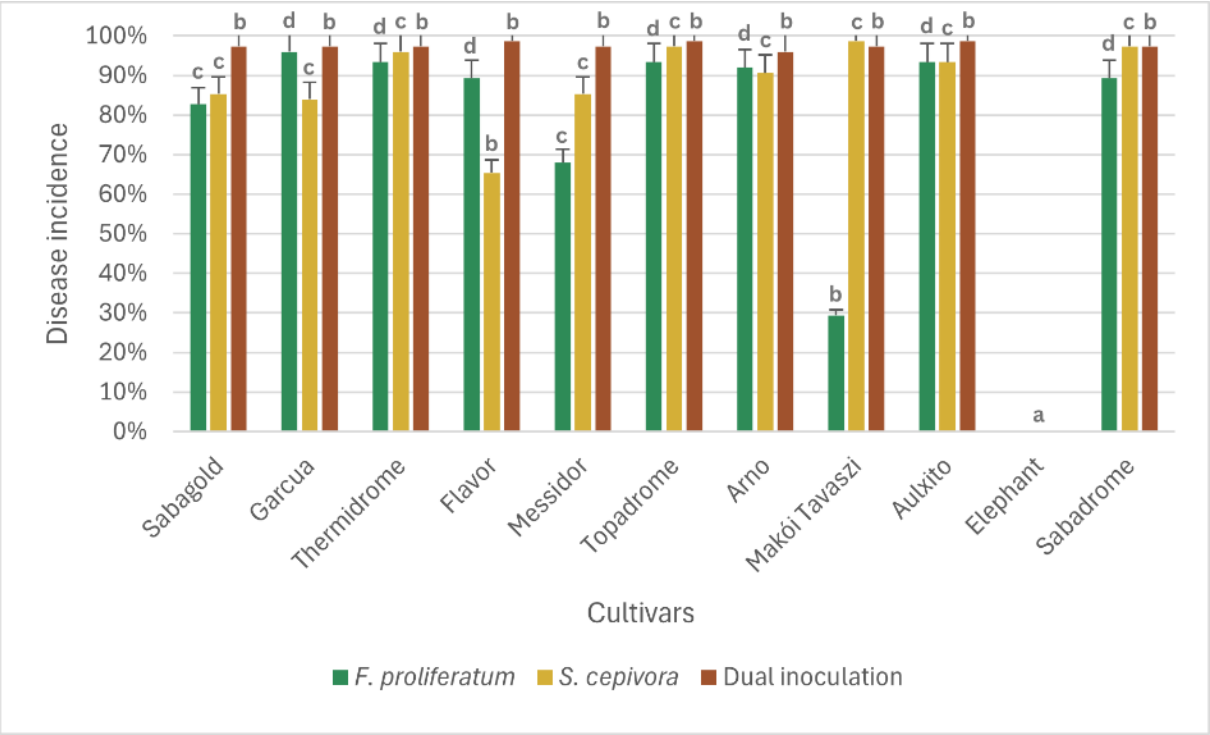

Figure 19: Bar chart presenting disease incidences of garlic cultivars due to single and dual inoculation with *F. proliferatum* and *S. cepivora*. The data were analyzed using Tukey's post-hoc test, and significant differences between groups are indicated, with values marked with the same letter not being scientifically different. Error bars represent SD values.

Initial symptoms were first observed at 5 days post-inoculation. *F. proliferatum* showed severe infection (Class 4) in cultivars 'Garcua' (96.00%), 'Thermidrome' (93.33%), 'Topadrome' (93.33%), 'Aulxito' (93.33%), and 'Makoi Tavaszi' (29.33%). This severity was characterized by rotting of the basal plate, extensive brown spotting that extended from the basal plate to the clove, and a prominent presence of mycelium and sclerotia covering the entire clove. 'Messidor' (68.00%), 'Arno' (92.00%), and 'Sabagold' (82.67%) demonstrated Class 3 severity. Brown spots and discoloration covering half of the basal plate characterized this classification. 'Flavor' (89.33%) displayed mild infection marked by isolated brown spots on all samples and was categorized under Class 1, indicative of slight infection. Exceptionally, 'Elephant' was completely symptomless, with a disease incidence of 0%, indicating the highest level of resistance among all tested cultivars.

In terms of *S. cepivora*, severe infections (Class 4) were observed in 'Flavor' (65.33%), 'Messidor' (85.33%), 'Arno' (90.67%), and 'Sabadrome' (97.33%), with symptoms including extensive browning, rotting, and mycelial growth that enveloped more than half of each clove. Similarly, 'Makoi Tavaszi' and 'Aulxito', recording 98.67% and 93.33% disease incidences, respectively, were classified under the most severe category. 'Topadrome' (97.33%) showed severity of Class

3, showing an extensive infection characterized by localized mycelium formation and browning of the basal plate. ‘Garcua’ (84.00%) and ‘Thermidrome’ (96.00%) exhibited moderate infection. ’Elephant’ remained intact against *S. cepivora*, showing no infection symptoms.

4.1.5. Resistance against simultaneous infections of *F. proliferatum* and *S. cepivora*

The pathogenic effects of *F. proliferatum* and *S. cepivora* on various garlic cultivars were evaluated using a dual inoculation approach under *in planta* conditions. This methodology mirrored the protocol established for individual pathogens but involved the simultaneous application of fungal discs from both pathogens on the basal plates of garlic cloves. The incidence was quantified as the percentage of infected samples relative to the total number of samples per cultivar, and the severity was categorized on a scale from Class 0 (asymptomatic) to 4 (severe infection). The results summarised in Table 4 show the class and percentage of disease incidence for each cultivar under single and dual inoculation conditions, while Figure 19 provides a visualisation of disease incidences across garlic cultivars. For dual inoculations, one-way analysis of variance also revealed statistically significant differences ($p < 0.001$) with a larger effect size ($\eta 2 = 0.78$). This large effect reflects the stronger and more pronounced interaction between the two fungi, as the dual inoculation resulted in more severe symptoms and a higher incidence of the disease compared to single inoculations.

Advanced infection symptoms, including browning at the base and formation of the mycelium, appeared as early as 2 days after inoculation, indicating a rapid onset of pathogenic activity. These symptoms were followed by the appearance of sclerotia after 4 days. Co-inoculation led to severe infections (Class 4) in all cultivars except ’Elephant’, which remained asymptomatic with a disease incidence of 0%, demonstrating its strong resistance. The remaining ten garlic cultivars recorded disease incidences greater than 96.00%, highlighting their high susceptibility to the combined pathogenic effects of *F. proliferatum* and *S. cepivora*. As illustrated in Figure 18 (Section 4.1.4), the severity of Class 4 observed in these susceptible cultivars was characterised by extensive rotting at the basal plate, pronounced browning that extended from the basal plate to the cloves, and significant development of mycelium and sclerotia enveloping the cloves (Figure 18). In particular, these symptoms manifested much more rapidly than in individual inoculations of the pathogens.

4.2. *In vitro* study of the effectiveness of *Trichoderma asperellum* and *Bacillus amyloliquefaciens* against garlic pathogens *Fusarium proliferatum* and *Stromatinia cepivora*

4.2.1. Isolation and identification of *Trichoderma* spp. and *Bacillus amyloliquefaciens*

The isolation procedures successfully yielded pure antagonistic cultures suitable for subsequent assays. Inoculation segments of diseased garlic cloves on PDA resulted in concurrent growth of *Trichoderma* spp. alongside pathogenic fungi, including *Fusarium* and *Stromatinia* species. Characteristic green-pigmented colonies indicative of *Trichoderma* was observed (Figure 20). To obtain pure cultures, repeated subcultures were performed, enabling the successful isolation of *Trichoderma* colonies free from pathogenic contaminants. Microscopic analysis of the purified isolate revealed densely branched conidiophores and ellipsoidal conidia arranged in characteristic whorls, confirming its morphological identity as *T. asperellum*.

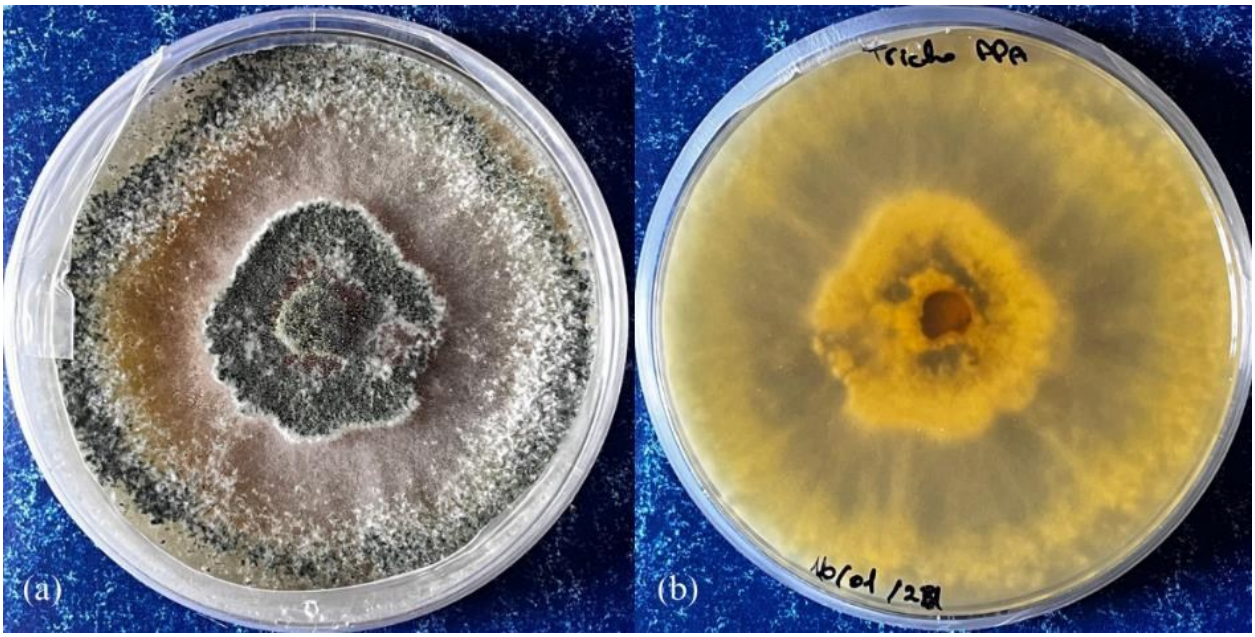

Figure 20: *Trichoderma asperellum* culture isolated from infected garlic cloves on PDA media. **(a)** Obverse view of the Petri dish; **(b)** Reverse view of the same plate.

For *B. amyloliquefaciens*, streaking of serially diluted suspensions of the Serenade® ASO biopesticide onto Nutrient Agar (NA) facilitated the development of discrete, creamy-white, circular colonies with irregular margins (Figure 21). After 24–48 hours of incubation at 25°C, representative colonies exhibiting typical *Bacillus* morphology were selected and successfully subcultured.

Figure 21: *Bacillus amyloliquefaciens* isolate cultured on Nutrient Agar (NA) media. **(a)** Obverse view of the Petri dish showing well-isolated, opaque, creamy-white colonies; **(b)** Reverse view of the same plate.

4.2.2. Dual culture assays

To assess the antagonistic potential of *T. asperellum* and *B. amyloliquefaciens* against *F. proliferatum* and *S. cepivora* on garlic, a series of dual culture assays were conducted under controlled *in vitro* conditions. Antagonist and pathogen isolates were co-inoculated on nutrient-appropriate media (SDA for *B. amyloliquefaciens* and PDA for *F. proliferatum* respectively) and fungal growth was monitored over time and evaluated based on radial expansion and percentage inhibition relative to untreated controls. Statistical analyses, including two-way ANOVA, were performed to assess the influence of treatment and incubation period on mycelial development.

4.2.2.1. Antagonistic interaction of *Trichoderma asperellum* against *Fusarium proliferatum* in dual culture assays

Figure 22 presents the dual culture interaction between *F. proliferatum* and *Trichoderma asperellum* on PDA media, showing the obverse (a) and reverse (b) views of the Petri dish.

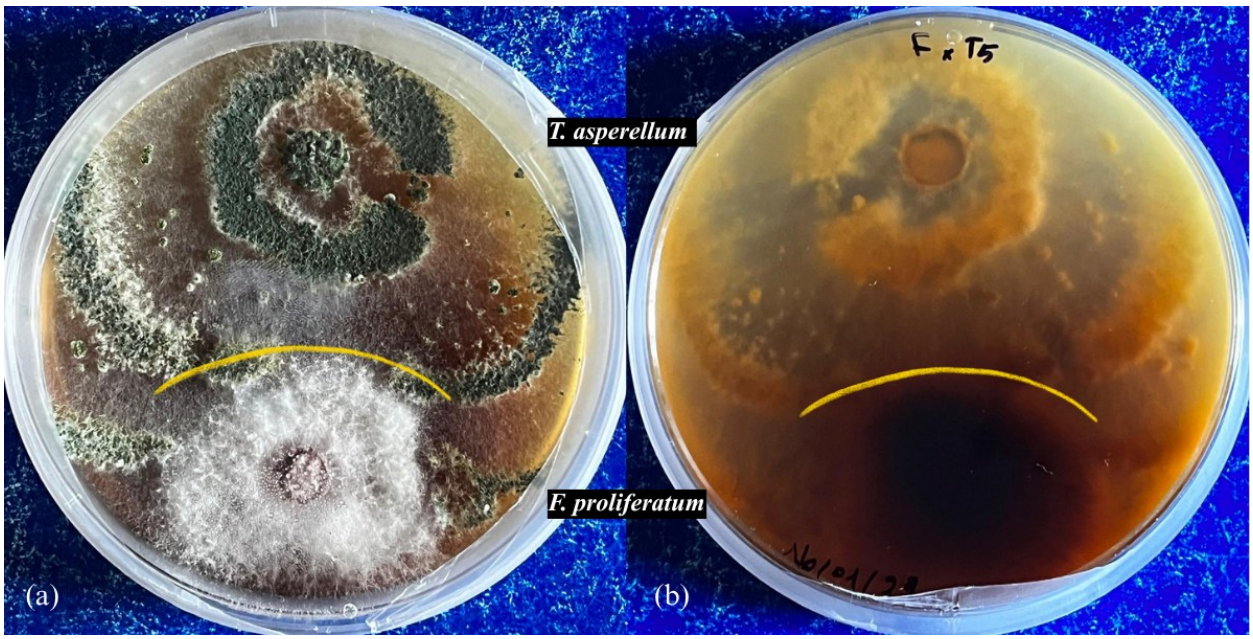

Figure 22: Dual culture of *Fusarium proliferatum* and *Trichoderma asperellum* on PDA media. **(a)** Obverse view of the Petri dish; **(b)** Reverse view.

In the obverse view (Figure 22a), *F. proliferatum* is represented by a cottony colony with a pinkish central pigmentation and a relatively diffuse hyphal front. In contrast, *T. asperellum* displays dense, green sporulating mycelium with a sharply demarcated margin. A visible interaction zone is present where the two colonies confront each other. *T. asperellum* appears to have advanced beyond its original growth front, partially overlapping the *F. proliferatum* colony. At the interface, *F. proliferatum* exhibits a marked darkening of the hyphal front, forming a melanised reaction zone—indicative of cellular stress likely due to the presence of antifungal metabolites or oxidative insult. The overgrowth pattern and boundary suppression suggest a combination of competitive exclusion and possible mycoparasitic activity of *T. asperellum*.

In the reverse view (Figure 22b), the pigmentation changes are more pronounced. The central area of the *F. proliferatum* colony retains its natural colouration, but the zone of interaction displays a dark brown to black band corresponding to the area of hyphal inhibition and confrontation. This pigmentation is consistent with the accumulation of melanin, often associated with defensive responses against antagonistic organisms. In particular, the *T. asperellum* colony does not show discolouration on the reverse side, maintaining a homogeneous appearance.

These morphological and pigmentation features provide strong visual evidence of antagonism, consistent with the biocontrol action of *T. asperellum* involving antibiosis, competitive colonisation, and local suppression of pathogen growth.

Figure 23 provides the quantitative assessment of this antagonistic interaction. (a) The percentage of inhibition of *F. proliferatum* growth by *T. asperellum* over a 14-day incubation period, while (b) shows the radial growth trajectories of *F. proliferatum* under control and dual culture conditions.

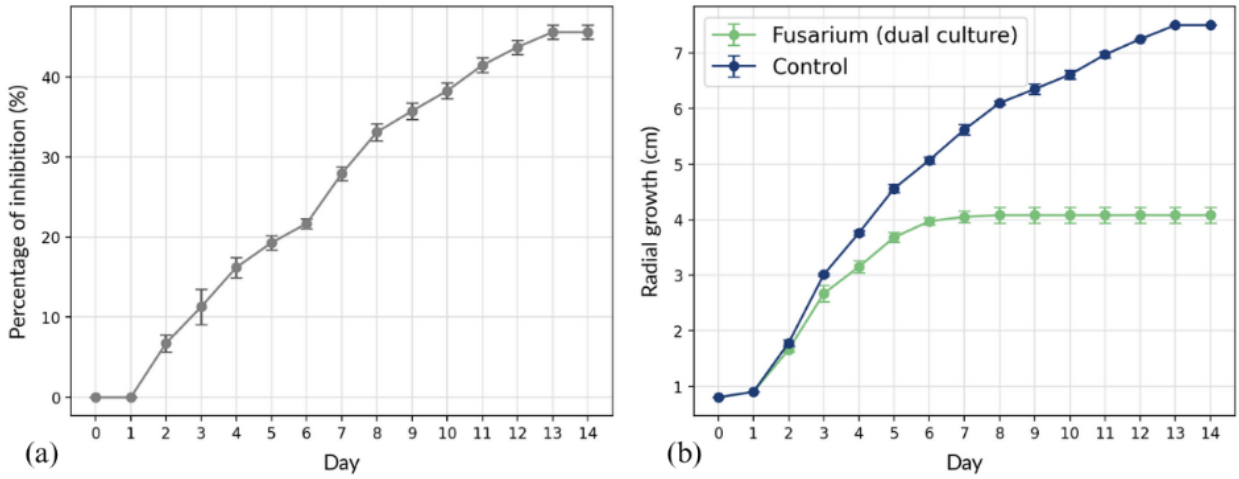

Figure 23: Dual culture assay of *Fusarium proliferatum* with *Trichoderma asperellum* on PDA media. **(a)** Percentage of inhibition of *F. proliferatum* over 14 days; **(b)** Radial growth of *F. proliferatum* in control and dual culture conditions.

A two-way ANOVA was performed to analyse the effects of treatment (control versus dual culture) and time (day 0-14) on radial colony growth. Assumptions of normality and homogeneity of the variances were confirmed by Shapiro-Wilk and Levene's tests ($p > 0.05$), validating the use of a parametric model. The analysis revealed a highly significant effect of time on fungal growth ($F(14, 120) = 3775.9$, $p < 1.8 \times 10^{-151}$), accounting for 73.5% of the total variance ($\eta^2 = 0.735$). Treatment also had a strong main effect ($F(1, 120) = 1.20 \times 10^4$, $p < 3.9 \times 10^{-122}$, $\eta^2 = 0.167$), indicating that the presence of *T. asperellum* significantly reduced the growth of *F. proliferatum*. Furthermore, a significant Treatment × Day interaction ($F(14, 120) = 496.8$, $p < 4.8 \times 10^{-99}$, $\eta^2 = 0.097$) showed that the inhibitory effect was dynamic, intensifying over the incubation period. Residual variance remained below 2%, confirming the robustness and precision.

Inhibition remained undetectable during the initial two days, corresponding to the lag phase before the colonies interacted or secreted sufficient bioactive compounds. However, from Day 3 onward, a sharp rise in inhibition (%±SE) was observed: 6.66% on Day 3, increasing to 16. by Day 4, and reaching 28.80% by Day 7. The inhibition curve continued to climb gradually, plateauing at 45.60% by Day 13, with negligible change on Day 14, indicating a sustained and consistent antagonistic effect.

Similarly, the radial growth curve (Figure 23b) shows that *F. proliferatum* under control condition expanded steadily, achieving a final mean diameter of approximately 7.5 cm on day 14. On the contrary, when co-cultured with *T. asperellum*, fungal growth slowed markedly after day 4 and stabilized around 4.1 cm, with minimal additional expansion thereafter.

These combined visual and quantitative results confirm the strong biocontrol potential of *T. asperellum* against *F. proliferatum*. The progressive inhibition pattern and morphological changes observed are consistent with known antagonistic mechanisms of *T. asperellum*, including the production of antifungal secondary metabolites, rapid competitive colonisation, and potential mycoparasitic activity at the hyphal interface.

4.2.2.2. Antagonistic interaction of *Bacillus amyloliquefaciens* against *Fusarium proliferatum* in dual culture assays

Figure 24 presents the dual culture interaction between *F. proliferatum* and *Bacillus amyloliquefaciens* on PDA media, showing the obverse (a) and reverse (b) views of the Petri dish.

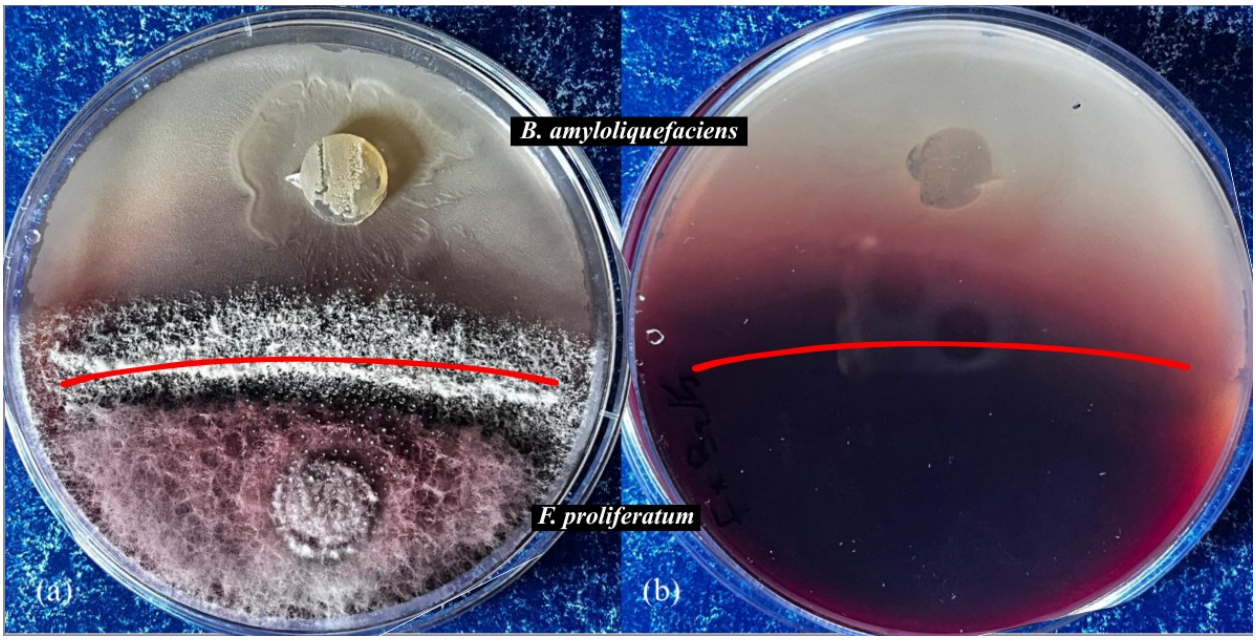

Figure 24: Dual culture of *Fusarium proliferatum* and *Bacillus amyloliquefaciens* on PDA media. **(a)** Obverse view of the Petri dish; **(b)** Reverse view.

In the obverse view (Figure 24a), *F. proliferatum* occupies approximately half of the plate, forming a dense cottony colony with the characteristic pink to violet pigmentation of this species. In contrast to this, the bacterial colony of *B. amyloliquefaciens* appears as a small, translucent mucoid growth with a smooth boundary. A distinct and uncolonized inhibition zone separates the two organisms, indicating that fungal progression was stopped before direct contact. The hyphal

margin of *F. proliferatum* facing the bacterium is compressed and irregular, suggesting localised suppression of hyphal extension likely caused by volatile or diffusible inhibitory compounds.

The reverse view (Figure 24b) accentuates this interaction. A clear boundary divides the plate into two chromatic zones: the fungal side displays a reddish pigmentation associated with the secondary metabolites of *F. proliferatum,* while the region adjacent to *B. amyloliquefaciens* remains pale and unpigmented. In particular, the fungal mycelium does not spread to the bacterial half of the dish. This pattern indicates inhibition via antibiosis rather than spatial competition, since no direct overgrowth or contact is observed. These morphological observations are consistent with known modes of action for the *B. amyloliquefaciens* strain QST 713, which produces a broad spectrum of antimicrobial lipopeptides (eg, iturins, fengycins) capable of suppressing filamentous fungi through membrane disruption and metabolic inhibition.

Figure 25 presents the quantitative analysis of this antagonistic interaction. Panel (a) displays the percentage inhibition of *F. proliferatum* over a 10-day period; panel (b) illustrates the radial growth of the fungal colony under control and dual culture conditions.

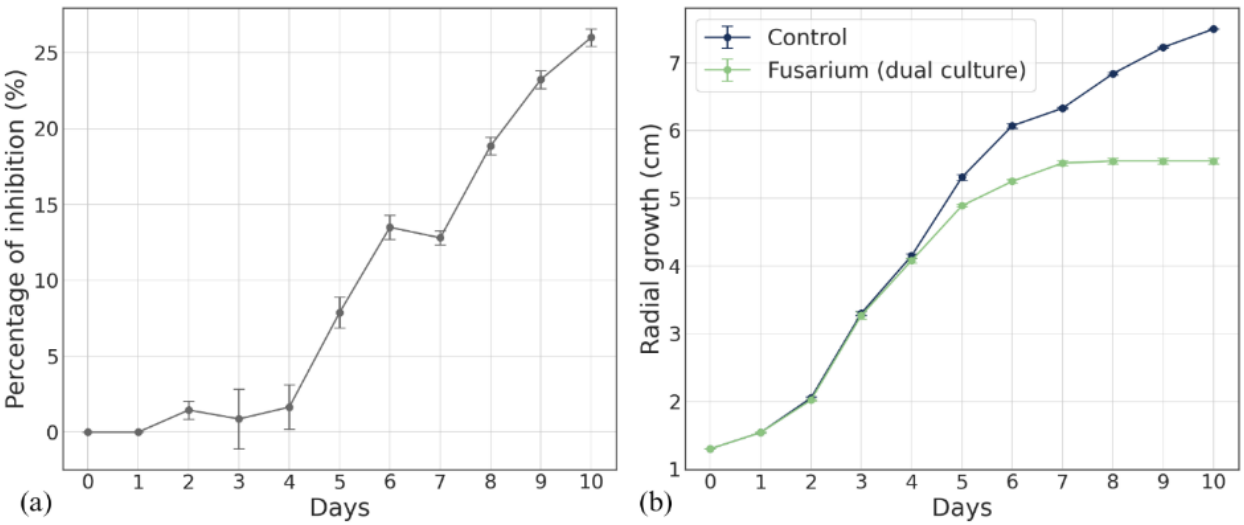

Figure 25: Dual culture assay of *Fusarium proliferatum* with *Bacillus amyloliquefaciens* on PDA media. **(a)** Percentage of inhibition of *F. proliferatum* over 14 days; **(b)** Radial growth of *F. proliferatum* in control and dual culture conditions.

Since residuals were not normally distributed (Shapiro–Wilk test, $p < 0.05$) and variance homogeneity was not met (Levene's test, $p < 0.05$), a nonparametric analysis was applied. A Kruskal–Wallis test was conducted to evaluate the effects of treatment (Fusarium + *Bacillus amyloliquefaciens* vs. control) and time (Days 0–10) on fungal growth. The global test indicated a significant overall treatment effect ($H = 4.32$, $p = 0.038$, $\eta^2 = 0.031$). When analyzed by day, no significant differences were observed during the early stages (Days 0–4). However, from Day 5

onward, growth differences became highly significant ($H \approx 6.9–7.9$, $p < 0.01$), confirming that *Bacillus* treatment exerted a strong inhibitory effect on *Fusarium* expansion at later stages. These results demonstrate a time-dependent suppression pattern consistent with the biocontrol activity of *Bacillus*.The inhibition curve (Figure 25a) did not show suppression during the first two days. A mild, variable inhibition was observed on Day 3 (mean = 0.87%, SE = 1.96), followed by a more consistent rise from Day 5 onward. By Day 6, inhibition reached 13.49% and peaked at 26.06% on Day 10. The steady increase in inhibition, along with the narrowing of standard error bars, reflects a stable and reproducible effect in all replicates.

In the control plates (Figure 25b), *F. proliferatum* expanded linearly, reaching a final radius of ~7.5 cm by Day 10. In the dual-culture treatment, initial fungal growth was comparable to the control until Day 4. Subsequently, the radial expansion decelerated markedly, stabilising at 5.6 cm by Day 9. This divergence of growth trajectories (Figure 25b) clearly visualises the inhibitory impact of *B. amyloliquefaciens*.

Although the maximum inhibition achieved by *B. amyloliquefaciens* was lower than that observed with *T. asperellum*, the effect was consistent and biologically relevant. The absence of physical contact and the presence of a persistent inhibition zone support antibiosis as the primary mechanism. These results align with established findings on QST 713-mediated biocontrol, strengthening its potential to suppress *F. proliferatum* growth through extracellular metabolites.

4.2.2.3. Antagonistic interaction of *Trichoderma asperellum* against *Stromatinia cepivora* in dual culture assays

Figure 26 presents the dual culture interaction between *Stromatinia cepivora* and *Trichoderma asperellum* in SDA media, showing the antagonistic activity of the fungal isolate. Panel (a) displays the obverse view of the Petri dish, while panel (b) shows the reverse.

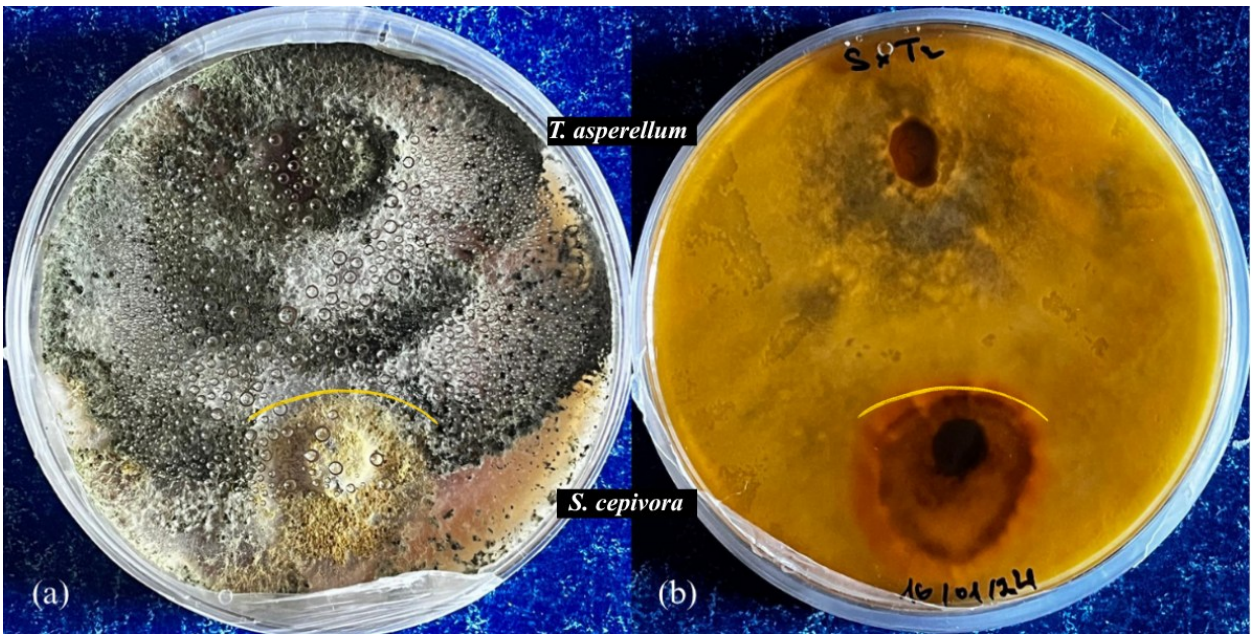

Figure 26: Dual culture of *Stromatinia cepivora* and *Trichoderma asperellum* on SDA media. **(a)** Obverse view of the Petri dish; **(b)** Reverse view.

In the obverse view (Figure 26a), *S. cepivora* appears as a compact colony with very limited radial development, characterized by a dense, dark central zone. Its margin is irregular and notably compressed on the side facing *T. asperellum*. The *T. asperellum* colony, in contrast, displays rapid outward expansion, profuse sporulation, and the development of a pronounced inhibition arc clearly encircling the pathogen colony. This spatial arrangement and morphology strongly indicate early and sustained antagonistic activity exerted by *T. asperellum*.

The reverse view (Figure 26b) reinforces these observations. A distinct reddish-brown pigmentation encircles the *S. cepivora* colony, especially pronounced on the side toward *T. asperellum*. This pigmentation suggests oxidative stress or secondary metabolite accumulation in the pathogen in response to antagonism. The wide halo and absence of any fungal regrowth in this area imply the secretion of potent diffusible metabolites by *T. asperellum*. The antagonist's ability to arrest growth and completely surround and overgrow the pathogen colony demonstrates a high level of competitive exclusion and supports a mycoparasitic mode of action.

These phenotypic observations are consistent with the quantitative data that follow, confirming the significant and progressive suppression of *S. cepivora* by *T. asperellum in vitro*.

Figure 27 presents the inhibitory effect of *Trichoderma asperellum* on *Stromatinia cepivora* over a 14-day dual culture assay. Panel (a) shows the percentage of inhibition, while panel (b) displays radial growth under control and dual culture conditions.

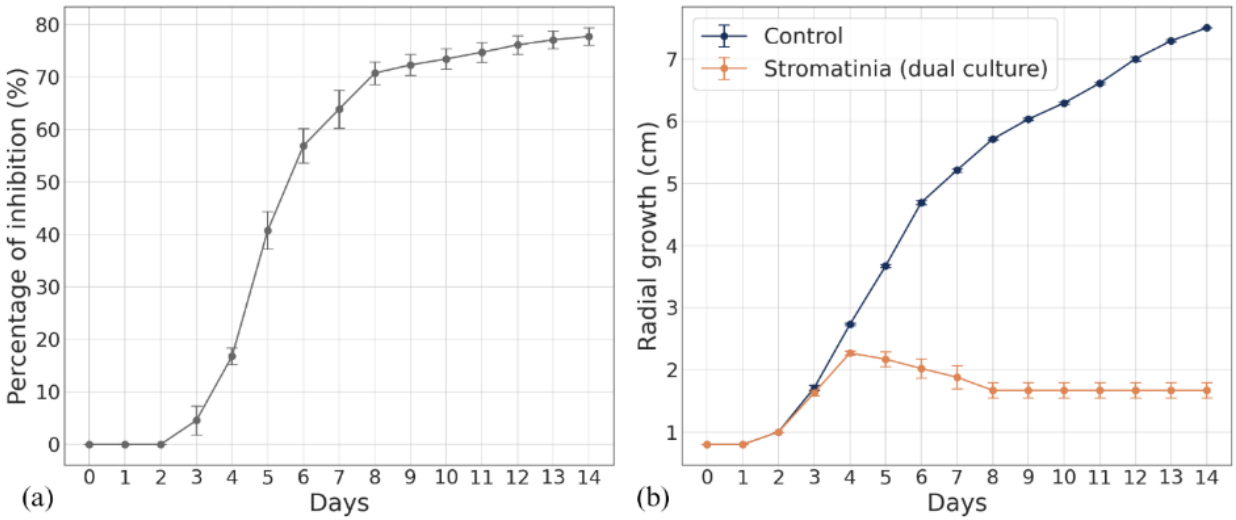

Figure 27: Dual culture assay of *Stromatinia cepivora* with *Trichoderma asperellum* on SDA media. **(a)** Percentage of inhibition of *S. cepivora* over 14 days; **(b)** Radial growth of *S. cepivora* in control and dual culture conditions.

A two-way ANOVA was performed to assess the effects of treatment (control vs. dual culture) and incubation time (Day 0–14) on *S. cepivora* colony growth. Both main effects were highly significant. The treatment factor alone accounted for nearly all of the variance in colony radius ($F_{1,104} = 9572$, $p < 10^{-115}$, $\eta^2 = 0.99$), demonstrating the exceptional inhibitory potential of *T. asperellum*. The effect of time was also highly pronounced ($p < 0.001$, $\eta^2 > 0.98$), reflecting the rapid baseline expansion of the fungus. The interaction between time and treatment was statistically robust ($F_{14,104} = 413$, $p < 10^{-93}$, $\eta^2 = 0.98$), confirming that the extent of inhibition was dynamic and intensified as the colonies interacted. Residual error was <1% of total variance, indicating excellent consistency among replicates and a near-complete model fit (adjusted $R^2 \approx 0.99$).

The inhibition percentage curve (Figure 27a) showed that during the first three days there was no measurable antagonism (0%). From Day 4 onward, the inhibition values rose sharply: reaching 16.82% on Day 4 and continuing to increase rapidly to 58.3% by Day 6. The curve stabilized thereafter, plateauing at 77.4% by Day 14. The narrowing error margins in the later days underscore the reproducibility and uniformity of the inhibitory effect.

Radial growth measurements (Figure 27b) closely mirrored this trend. *S. cepivora* in the control group exhibited regular expansion, reaching approximately 7.5 cm by Day 14. In contrast, growth in the dual culture treatment followed the control trajectory until Day 4, after which radial expansion declined markedly. From Day 5, a severe reduction in growth was observed, and by Day 8 the pathogen colony size stabilized at around 1.7 cm in radius. This decline corresponded

with visible overgrowth by *T. asperellum*, suggesting that inhibition progressed beyond metabolic interference to physical suppression and mycelial colonization.

Taken together, the visual, statistical, and kinetic evidence confirms that *T. asperellum* exerts a potent, time-dependent antagonistic effect against *S. cepivora*. The sharp transition in growth behavior of the pathogen, followed by its full encirclement and overgrowth, highlights the biocontrol potential of *T. asperellum*. Its ability to maintain consistent inhibitory pressure over time reinforces its suitability for practical application in the management of *S. cepivora*.

4.2.2.4. Antagonistic interaction of *Bacillus amyloliquefaciens* against *Stromatinia cepivora* in dual culture assays

Figure 28 presents the dual culture interaction between *Stromatinia cepivora* and *Bacillus amyloliquefaciens* on SDA media, showing the antagonistic activity of the fungal isolate. Panel (a) displays the obverse view of the Petri dish, while panel (b) shows the reverse.

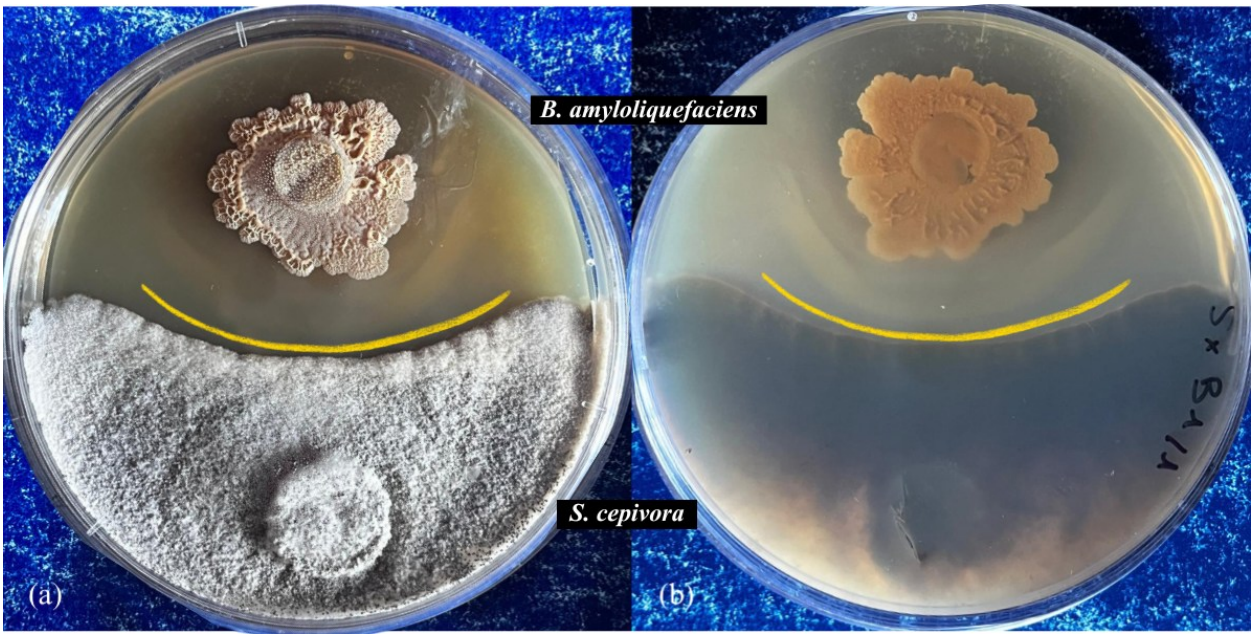

Figure 28: Dual culture of *Stromatinia cepivora* and *Bacillus amyloliquefaciens* on SDA media. **(a)** Obverse view of the Petri dish; **(b)** Reverse view.

In the obverse view (Figure 28a), *S. cepivora* occupies roughly half of the Petri dish, forming a dense, white mycelial colony with a compact, cottony morphology. Opposing it, *B. amyloliquefaciens* exhibits its characteristic convoluted, lobate colony structure with a central domed elevation indicative of biofilm-like growth. A distinct and stable inhibition zone is observed between the two organisms, marked by the absence of fungal growth along the axis of bacterial expansion. The fungal colony margin adjacent to the bacterial zone is smoothed and retracted—a

hallmark of growth arrest due to antagonistic pressure, likely through the diffusion of inhibitory bacterial metabolites.

The reverse view (Figure 28b) further confirms this inhibitory interaction. A conspicuous black pigmentation is visible around the advancing front of *S. cepivora*, restricted to the margin facing *B. amyloliquefaciens*. This melanization is likely a stress-induced response triggered by exposure to antifungal compounds (melanin biosynthesis in fungi is a common defense against oxidative or toxic stress). The absence of any visible bacterial infiltration into the fungal zone supports a non-contact inhibitory mechanism—suggestive of antibiosis rather than direct competition.

Figure 29 presents the temporal development of inhibition in the dual culture of *Stromatinia cepivora* with *Bacillus amyloliquefaciens*. Panel (a) shows the percentage of inhibition over the 10-day assay period, while panel (b) depicts the radial growth trajectories of *S. cepivora* under control and treated conditions.

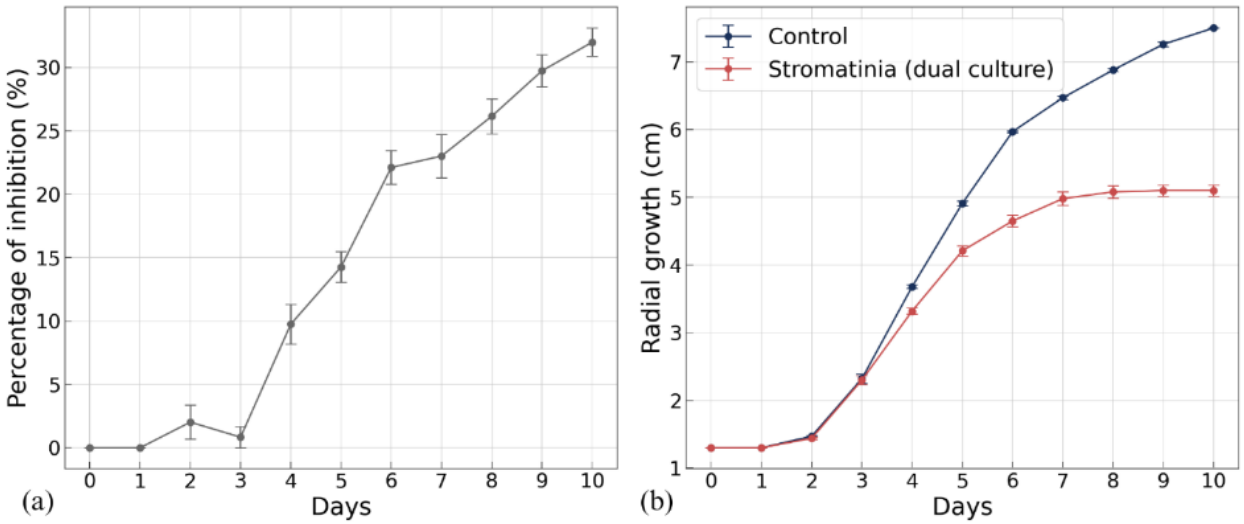

Figure 29: Dual culture assay of *Stromatinia cepivora* with *Bacillus amyloliquefaciens* on SDA media. **(a)** Percentage of inhibition of *S. cepivora* over 10 days; **(b)** Radial growth of *S. cepivora* in control and dual culture conditions.

A two-way ANOVA was performed with Treatment (control vs. dual culture) and Day (0–10) as fixed factors. All sources of variation were statistically significant. The presence of *B. amyloliquefaciens* had a strong main effect on fungal growth ($F_{1,88} = 1.70 \times 10^3$, $p = 2.2 \times 10^{-59}$), explaining ~95% of the variance ($\eta^2 = 0.95$). Temporal variation also contributed substantially ($F_{10,88} = 3.06 \times 10^3$, $p < 10^{-107}$, $\eta^2 = 0.997$), reflecting the inherent expansion of fungal colonies over time. The Day × Treatment interaction was significant as well ($F_{10,88} = 153$, $p = 3.3 \times 10^{-51}$, $\eta^2 = 0.95$). These results indicate that the inhibitory effect of *B. amyloliquefaciens* was not constant

but dynamically intensified over time. Residual error was <1% of total variance (adjusted $R^2 \approx 0.99$).

As shown in Figure 29a, inhibition remained undetectable during the first two days. On Day 2, the inhibition curve rose slightly to ~2.0%, possibly due to early volatile interactions or nutrient competition. A temporary drop on Day 3 (to 0.83%) suggested a brief adjustment phase. From Day 4 onward, inhibition increased consistently: reaching 9.75% on Day 4, 14.1% by Day 5, and 22.5% ± 1.08 SE by Day 6. Inhibition then progressed steadily to 26.0% by Day 10, marking the peak of sustained antagonistic activity.

The radial growth plot (Figure 29b) corroborates these observations. Control colonies of *S. cepivora* exhibited continuous expansion, reaching ~7.5 cm in radius by the end of the assay. In contrast, growth in dual culture began to diverge noticeably after Day 4. Beyond this point, fungal development was markedly slower, plateauing at a mean radius of ~5.6 cmfrom Day 9 onward.

These findings, both visual and quantitative, confirm that *B. amyloliquefaciens* exerts a progressive and measurable inhibitory effect on *S. cepivora*. The formation of a persistent inhibition zone, accompanied by stress-induced pigmentation and reduced radial growth of the pathogen, is characteristic of antibiosis mediated by bioactive bacterial metabolites. The consistent inhibition observed across replicates—evidenced by narrowing SE margins—reinforces the reliability of the QST 713 strain as a potential biocontrol agent against *S. cepivora in vitro*.

4.3. *In planta* study of the effectiveness of *Trichoderma asperellum* and *Bacillus amyloliquefaciens* against garlic pathogens *Fusarium proliferatum* and *Stromatinia cepivora* under controlled phytotron conditions

Under standardised phytotron conditions, the effectiveness of *T. asperellum* and *B. amyloliquefaciens* against *F. proliferatum* and *S. cepivora* infections was evaluated in garlic plants grown in sterile perlite (Figure 30). Pathogen inoculation was performed at planting and antagonist treatments were applied individually or in combination. Plant height and visible symptoms were monitored over 22 days as indicators of disease impact and biocontrol performance.

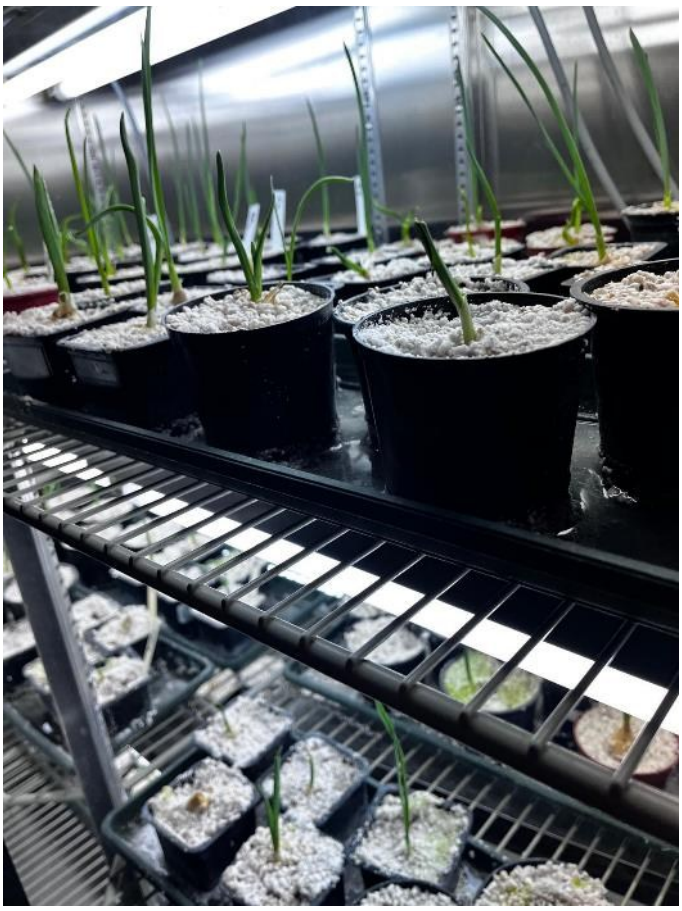

Figure 30: Garlic plants grown in perlite pots under controlled phytotron conditions for *in planta* pathogen and biocontrol interaction experiments.

Garlic seedling height was significantly affected by the type of pathogen inoculation and biocontrol treatment, with clear differences emerging over the three-week period. The initial two-way ANOVA indicated a deviation from normality (Shapiro–Wilk W = 0.961, $p<0.001$), which was resolved by a log(transformation of the data (W = 0.985, $p = 0.057$). Levene's test confirmed homogeneity of variances ($F_{8,243} = 1.31$, $p = 0.24$), validating the assumptions for parametric analysis.

The main effect of treatment was highly significant ($F_{8,243} = 20.27$, $p = 2.2 \times 10^{-23}$), with a large effect size (partial $\eta^2 = 0.40$), indicating that the applied treatment accounted for about 40% of the variance in seedling height. Week (time) was also a significant factor ($F_{2,243} = 20.40$, $p = 6.5 \times 10^{-9}$, $\eta^2 = 0.14$), while the Treatment × Week interaction was not significant ($p = 0.60$). This suggests that treatment effects remained consistent across the three weeks. Tukey's HSD post hoc tests were conducted to determine pairwise differences between treatment means within each week; results are summarized in Table 5.

Table 5: Mean height (±SE) of garlic plants under different treatments across three weeks (phytotron experiment with significance groupings and ANOVA summary). Within each week, values followed by the same letter are not significantly different according to Tukey's HSD test (α = 0.05); values with different letters are significantly different.

Treatment	Week 1 (cm)	Week 2 (cm)	Week 2 (cm)
C (control)	3.58 ± 0.42 a	11.26 ± 0.44 a	17.93 ± 1.01 a
F (*Fusarium* only)	1.07 ± 0.38 b	3.32 ± 0.75 c	5.05 ± 1.19 d
TF (*T. asperellum* + *Fusarium*)	5.4 ± 1.01 a	8.15 ± 1.98 b	10.3 ± 2.45 b
BF (*B.* amyloliquefaciens + *Fusarium*)	1.58 ± 0.38 a	5.7 ± 1.09 b	8.12 ± 1.7 c
TBF (*T. asperellum* + *B.* + *Fusarium*)	1.0 ± 0.31 b	5.75 ± 2.09 b	8.5 ± 2.92 b
S (*Stromatinia* only)	0.0 ± 0.0 b	0.0 ± 0.0 c	0.0 ± 0.0 e
TS (*T. asperellum* + *Stromatinia*)	1.9 ± 0.64 b	3.65 ± 1.18 c	5.45 ± 2.25 d
BS (*B. amyloliquefaciens* + *Stromatinia)*	1.19 ± 0.59 a	3.3 ± 1.36 c	4.58 ± 1.94 d
TBS (*T. asperellum* + *B.* + *Stromatinia*)	2.7 ± 0.65 b	5.1 ± 1.03 b	6.43 ± 1.57 c
F	8,68	1,8E-08	0,46
p	6,39	2,1E-06	0,39
Eta_sq	7,01	5,4E-07	0,41
Values are means of three experiments, with five replicates per experiment and five garlic cloves per replicate. Data are presented as "mean ± standard error." Values sharing the same letter within a column are not significantly different at $p < 0.05$.			

The control group 'C', consisting of uninoculated seedlings, exhibited the greatest plant height throughout the experiment. Mean heights increased steadily from 3.58 cm in Week 1 to 11.26cm in Week 2 and 17.93cm in Week 3. These plants consistently formed a distinct statistical group "a" in post hoc comparisons, reflecting normal growth in the absence of biotic stress. Leaves were fully expanded, uniformly green, and upright, with no signs of chlorosis, deformation, or collapse, indicating optimal plant health (Figure 31).

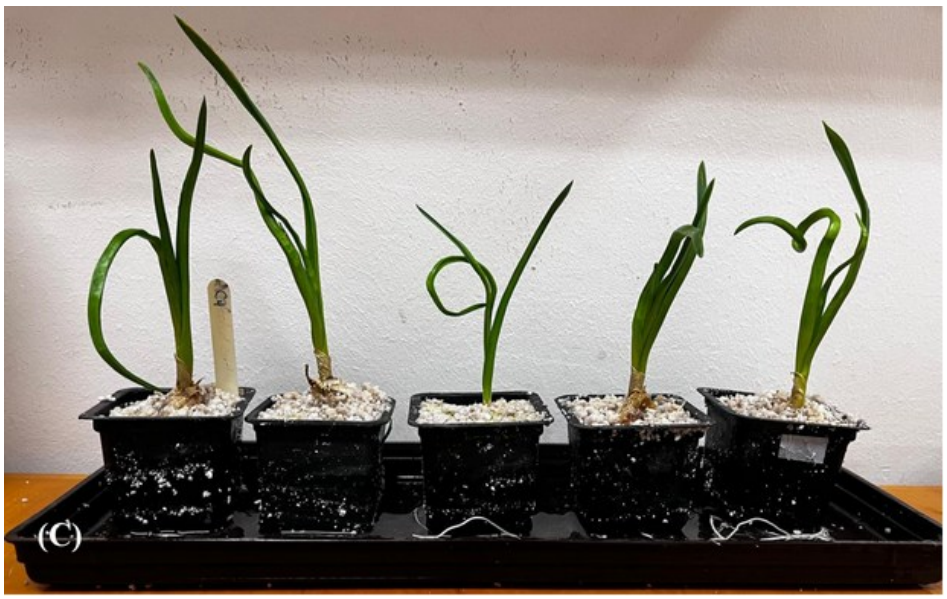

Figure 31: Garlic plants presenting the non-inoculated control group.

By contrast, seedlings inoculated with *F. proliferatum* (treatment 'F') exhibited pronounced stunting, with mean height only 1.07 cm in Week 1 and reaching just 5.05 cm by Week 3. This severe growth reduction reflects the pathogen's ability to colonize root vascular tissue, disrupt nutrient transport, and impair shoot elongation. Statistically, the 'F' treatment consistently ranked in the lowest-performing groups across all weeks. Visibly, *Fusarium*-infected plants showed severe leaf curling, wilting, and chlorosis, with some individuals exhibiting tissue collapse and deformation.

Application of *T. asperellum* in conjunction with *F. proliferatum* (treatment 'TF') significantly mitigated the pathogen's effects. 'TF'-treated plants attained mean heights of 5.40 cm, 8.15 cm, and 10.30 cm in Weeks 1, 2, and 3, respectively. These values were consistently higher than those of the F-only group and, in Week 1, were statistically indistinguishable from the control. The partial restoration of height is likely due to *Trichoderma*'s biocontrol action. Morphologically, most 'TF' plants had erect, healthy green shoots; only occasional individuals showed mild twisting or residual curling, suggesting that *T. asperellum* provided substantial but not complete protection from *Fusarium*-induced stress. In the 'BF' treatment (*B. amyloliquefaciens* + *Fusarium*), seedlings showed moderate recovery relative to the F-only group. Mean heights reached 1.58 cm in Week 1, 5.70 cm in Week 2, and 8.12 cm in Week 3. While not as effective as *Trichoderma*, *Bacillus* still conferred a significant benefit. The improvement may be attributed to *Bacillus* producing antifungal lipopeptides and possibly promoting plant growth. Phenotypically, BF plants were

generally upright and green with only minimal leaf curling or distortion, indicating partial recovery with some residual stress symptoms.

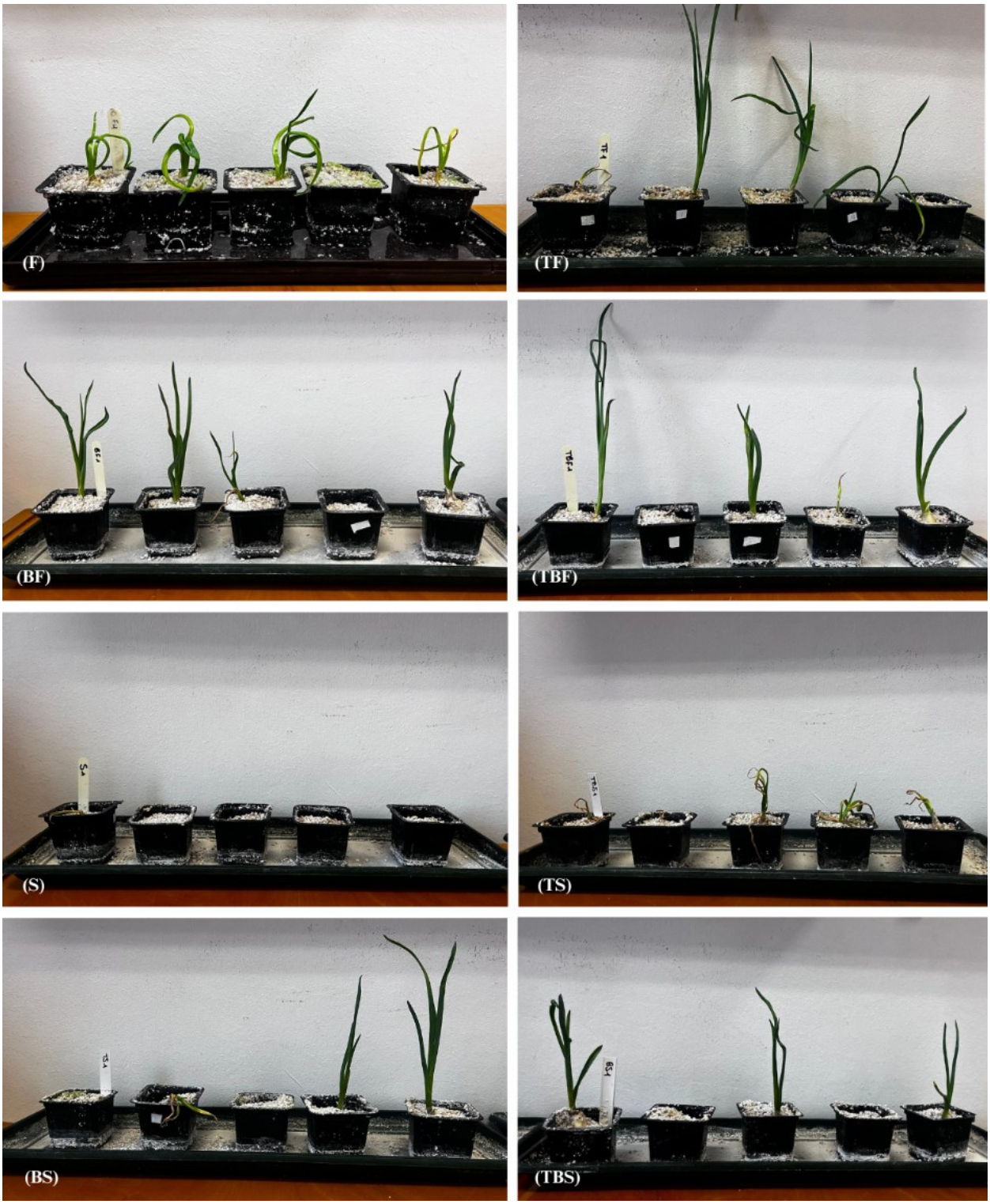

Figure 32: Overview of garlic plants inoculated with *F. proliferatum* and/or *S. cepivora* under different biocontrol treatments with *T. asperellum* and *B. amyloliquefaciens*.

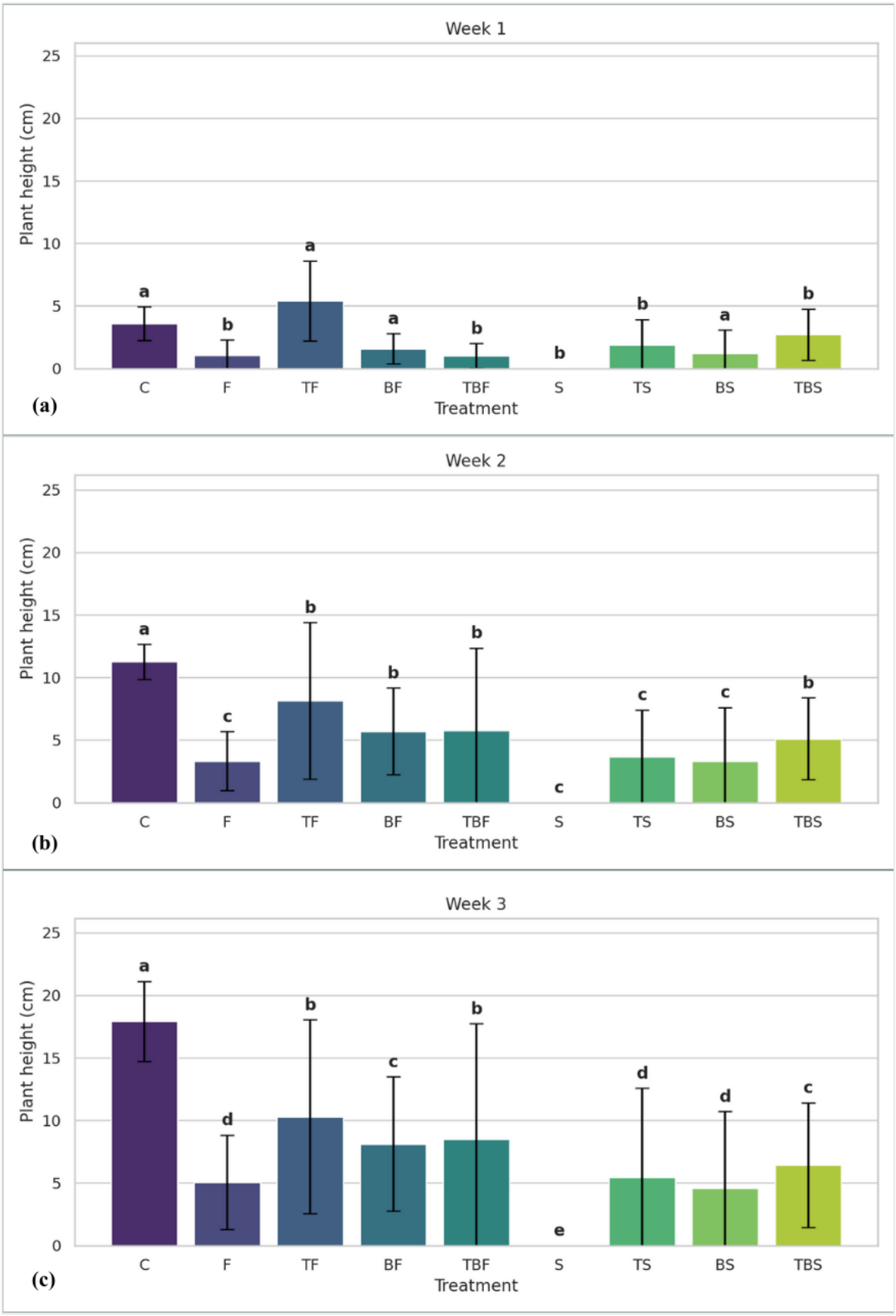

Figure 33: Mean plant height of garlic plants under different treatments across three consecutive weeks under phytotron conditions: **(a)** Week 1, **(b)** Week 2, and **(c)** Week 3. Error bars represent standard deviation of the mean (±SD). Treatments sharing the same letter within each panel are not significantly different based on Tukey's HSD test ($\alpha = 0.05$).

The combined treatment TBF (*T. asperellum* + *B. amyloliquefaciens* + *Fusarium*) produced further enhancement in plant growth. 'TBF'-treated seedlings attained 1.22 cm in Week 1, 6.01 cm in Week 2, and 8.35 cm in Week 3. Although performance did not significantly exceed the 'TF' treatment, the 'TBF' plants consistently belonged to statistical groups. Visually, several 'TBF' plants showed vigorous, well-formed green shoots, while some still showed leaf curling or wilting. This variability suggests partial synergistic effects between *T. asperellum* and *B. amyloliquefaciens*, with some variation in how individual plants benefited from dual colonisation.

Seedlings inoculated with *S. cepivora* (treatment 'S') showed complete inhibition of shoot emergence throughout the 22-day experiment. The mean height remained 0 cm at all time points, underscoring the aggressive necrotrophic behavior. No shoots emerged in any replicate; pots remained barren, indicating immediate seedling mortality or failure of emergence due to severe basal rot. The absence of any green tissue highlights the rapid and lethal impact of *S. cepivora* under these conditions.

When *T. asperellum* was applied alongside *S. cepivora* (treatment 'TS'), a modest improvement in plant growth was observed compared to S alone. Some seedlings managed to emerge, with heights increasing from 1.98 cm in Week 1 to 5.57 cm in Week 3. Although significantly higher than in the *Stromatinia*-only group, growth remained severely suppressed relative to healthy control or *Fusarium* inoculations. Morphologically, the few 'TS' seedlings that emerged had twisted, chlorotic and wilted leaves, with some collapse in structure. These symptoms suggest that *T. asperellum* only partially countered *Stromatinia*'s pathogenic effects.

Similarly, application of *B. amyloliquefaciens* in the presence of *Stromatinia* (treatment 'BS') yielded limited recovery. Heights progressed from 1.43 cm in Week 1 to 4.68 cm in Week 3. Only one or two seedlings per replicate emerged, and those that did showed pronounced wilting, chlorosis, and premature senescence. Most 'BS' pots had no surviving shoots, indicating that *Bacillus* alone was largely ineffective against *Stromatinia*'s suppression of emergence.

In the 'TBS' treatment (combined *T. asperellum* + *B. amyloliquefaciens* against *Stromatinia*), the highest plant heights were achieved between the *Stromatinia*-infected groups. The seedlings reached 2.64 cm in Week 1, 5.01 cm in Week 2, and 6.83 cm in Week 3. These values were significantly higher than those in the 'S', 'TS', or 'BS' treatments. Visually, most TBS plants successfully emerged with upright green shoots, although some curling and minor twisting were still observed. The improved consistency in emergence and the reduced severity of symptoms indicate a meaningful synergistic effect that partially suppressed *Stromatinia*'s impact.

In summary, both *F. proliferatum* and *S. cepivora* severely impeded the growth of garlic seedlings, and *S. cepivora* causing complete failure of emergence. Among the biocontrol interventions, *T. asperellum* consistently provided the greatest growth restoration, both alone and in combination with *B. amyloliquefaciens*, particularly in *Fusarium*-infected plants. In the case of *Stromatinia,* the biocontrol treatments were overall less effective, but the dual treatment 'TBS' offered significant improvement compared to single agent treatments or pathogen-only controls. In particular, the absence of a significant Treatment × Week interaction in the ANOVA indicates that these effects were stable over time. Together, these findings support the integration of strategies based on *T. asperellum, particularly* in combination with *B. amyloliquefaciens*—for mitigating early-stage losses due to soilborne fungal pathogens in garlic.

4.4. Enzymatic defense responses in garlic under pathogen infections and biocontrol treatments

To investigate the impact of pathogen infection and the application of biocontrol on oxidative defense mechanisms in garlic (*Allium sativum*), we measured the activity of two key enzymes: guaiacol peroxidase (POX) and polyphenol oxidase (PPO). Garlic plants were inoculated with *F. proliferatum* 'F' or *S. cepivora* 'S' (single pathogens), as well as combinations of both pathogens 'FS' and co-inoculations with the biocontrol agents *T. asperellum* 'T' and *B. amyloliquefaciens* 'B'. The objective was to determine how the presence and biocontrol interactions influence the activity of oxidative enzymes in plants, and whether distinct patterns emerge for different enzymes and microbial pairings. Enzyme activities were recorded at 0, 30 seconds, and 1 minute after extraction, with the final values (at 1 minute) visualised in bar graphs (Figure 34). A complete statistical analysis (incorporating all time points) was performed to assess the significance and specificity of the enzymatic responses elicited by each treatment.

Enzyme activity analysis revealed significant treatment-dependent variation in garlic's oxidative defense responses, as indicated by both POX and PPO activity profiles. Because the data did not meet normal distribution assumptions (Shapiro–Wilk $p < 0.001$ for both enzymes), non-parametric tests were used. Kruskal–Wallis H tests showed highly significant treatment effects for POX ($H = 42.85$, $df = 7$, $p < 0.001$) and PPO ($H = 43.12$, $df = 7$, $p < 0.001$), each with large effect sizes ($\eta^2 \approx 0.51$ for both). This suggests that the treatments accounted for over 50% of the variance in enzyme activity.

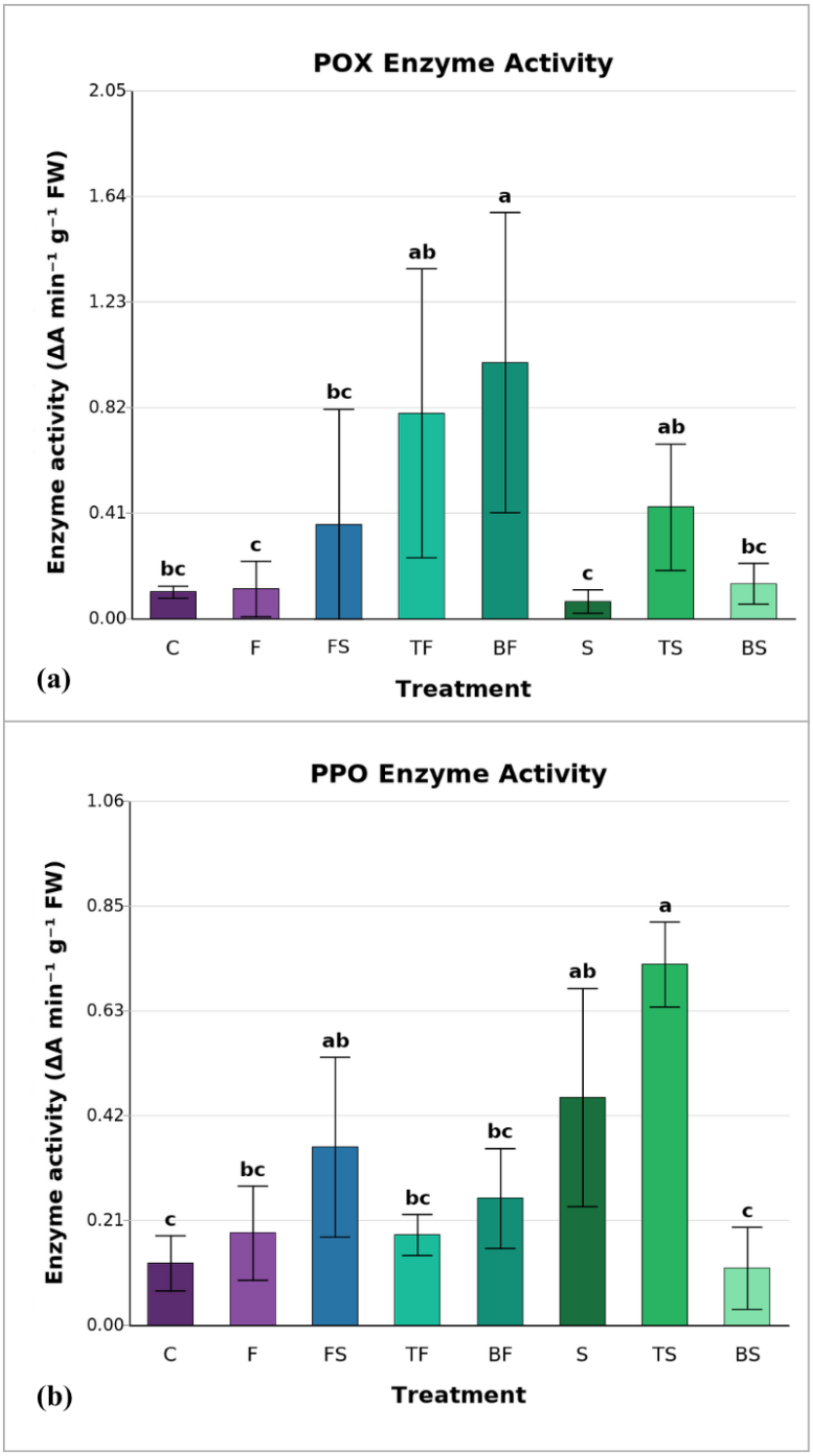

Figure 34: Effects of pathogen and biocontrol treatments on enzyme activity in garlic. **(a)** Guaiacol peroxidase (POX) activity; **(b)** polyphenol oxidase (PPO) activity), measured 1 minute after inoculation. Bars represent mean enzyme activity (units), and error bars indicate standard deviation (SD). Different letters above bars denote statistically significant differences among treatments based on Dunn's post-hoc test with Bonferroni correction ($p < 0.05$).

For POX, the highest activity was recorded in the treatment in which *B. amyloliquefaciens* was co-inoculated with *Fusarium* (BF), reaching 0.0847 $\Delta A \cdot min^{-1} \cdot g^{-1}$ FW. This was followed by the

combination of *T. asperellum* with *Fusarium* (TF; 0.0743) and *T. asperellum* with *S. cepivora* (TS; 0.0693). These three treatments formed the highest statistical group in post hoc comparisons, indicating a clear enhancement of POX activity under dual inoculations that include a biocontrol agent and a pathogen. Intermediate levels of POX activity were found in the dual-pathogen treatment (FS, 0.0647), in the combination of *B. amyloliquefaciens* + *S. cepivora* (BS; 0.0627), and in the control (0.0617). The lowest POX activities were observed in single-pathogen inoculations with *S. cepivora* (S; 0.0583) and *F. proliferatum* (F; 0.0563), which clustered in the lowest significance group. These patterns suggest that POX induction in garlic is most effectively triggered by biocontrol–pathogen co-inoculations, particularly those involving *B. amyloliquefaciens* or *T. asperellum* in the presence of *F. proliferatum*.

The PPO activity exhibited a different response pattern. The highest PPO activity was observed in the TS treatment (*T. asperellum* + *S. cepivora*; 0.0893), closely followed by the single *S. cepivora* inoculation (S; 0.0847) and the FS dual pathogen inoculation (FS;0.0793); these formed the upper statistical group. Moderate PPO activity was measured in *F. proliferatum* alone (F; 0.0747), in TF (0.0697), and in BF (0.0647). The lowest levels of PPO occurred in the control (0.0597) and in the BS treatment (0.0547). In particular, the presence of *B. amyloliquefaciens* appeared to reduce the activity of PPO when combined with *S. cepivora* (BS treatment), indicating a potential suppressive effect of *Bacillus* on this specific defence pathway.

The divergent trends between POX and PPO underscore the enzyme-specific nature of the garlic oxidative defence system. While POX activity was predominantly enhanced by treatments involving *F. proliferatum* together with a biocontrol agent, PPO activity was more responsive to treatments related to *S. cepivora,* particularly when paired with *T. asperellum*. The large effects sizes observed for both enzymes reinforce the biological significance of these findings, indicating that the garlic oxidative defence network is differentially activated depending on the invading pathogens and the presence of biocontrol microbes. These results provide valuable information on the nuanced interactions between garlic and microbial agents, and offer a basis for optimizing biocontrol strategies to generate targeted host defense responses.

4.5. Enzymatic defense responses in okra under pathogen infections and biocontrol treatments

To examine how fungal pathogens and biocontrol agents affect the activity of oxidative enzymes in okra, guaiacol peroxidase (POX) and polyphenol oxidase (PPO) activities after inoculation with *Sclerotinia sclerotiorum* (Sc) and *Rhizoctonia solani* (R) were measured. Treatments included individual pathogen infections and their combination, as well as co-inoculations with *T. asperellum*

(T) and *B. amyloliquefaciens* (B). Enzyme activity was measured at 0, 30, and 60 seconds after extraction, expressed as $\Delta A \cdot min^{-1} \cdot g^{-1}$ fresh weight (FW). The data presented here focus on 1-minute measurements, while the statistical analysis incorporated all time points to account for temporal trends.

Figure 35 provides a comparative visualization of guaiacol peroxidase (POX) and polyphenol oxidase (PPO) activities across individual and dual inoculations of the two pathogens and applications of the biocontrol agents, summarizing the differential enzyme responses observed among the tested conditions.

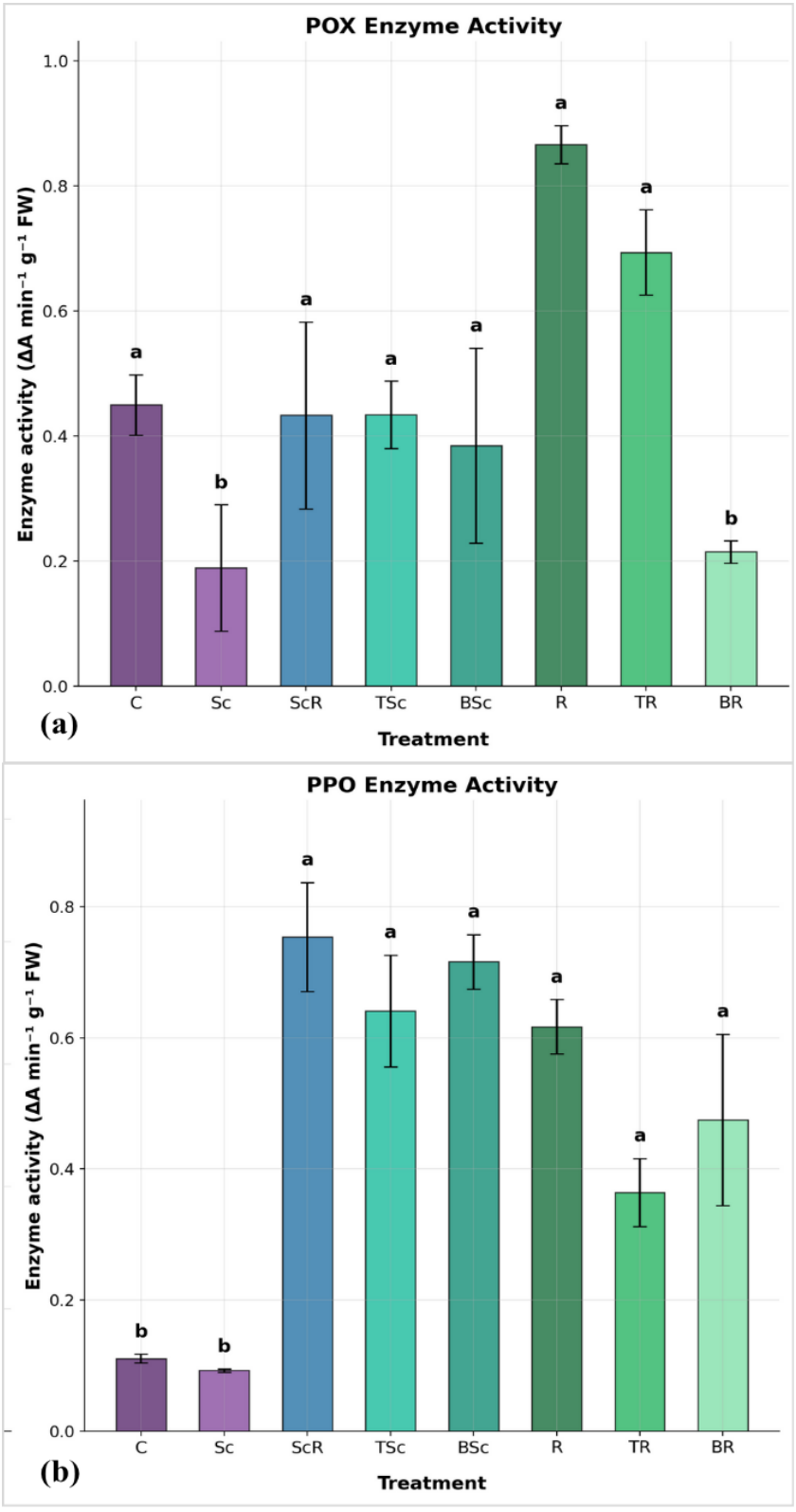

Figure 35: Effects of pathogen and biocontrol treatments on enzyme activity in okra. **(a)** Guaiacol peroxidase (POX) activity; **(b)** polyphenol oxidase (PPO) activity), measured 1 minute after inoculation. Bars represent mean enzyme activity (units), and error bars indicate standard deviation (SD). Different letters above bars denote statistically significant differences among treatments based on Dunn's post-hoc test with Bonferroni correction ($p < 0.05$).

Non-parametric Kruskal–Wallis tests were used due to non-normal residuals. For POX activity, a significant treatment effect was observed ($H = 15.76$, $df = 7$, $p = 0.027$) with a large effect size ($\eta^2 = 0.547$), indicating that nearly 55% of the total variance in POX activity was attributable to treatment differences. Post hoc Dunn's tests grouped treatments R, TR, ScR, TSc, BSc, and C into a high-activity cluster ("a"), whereas BR and Sc treatments formed a significantly lower group ("b"). These groupings highlight the substantial influence of microbial interactions on POX dynamics in okra.

POX activity was highest in plants infected with *R. solani* alone (0.867 $\Delta A \cdot min^{-1} \cdot g^{-1}$ FW), followed by the R + *T. asperellum* treatment (TR, 0.694). The combined pathogen treatment (ScR) and the *T. asperellum* + Sc treatment (TSc) showed intermediate POX levels (0.433and 0.434, respectively), similar to the *B. amyloliquefaciens* + Sc treatment (BSc, 0.385) and the control (0.450). The lowest POX values were recorded in the R + *B. amyloliquefaciens* treatment (BR, 0.215) and in the single *S. sclerotiorum* treatment (Sc, 0.189). This pattern suggests that *R. solani* is a particularly potent inducer of peroxidase activity in okra—likely triggering lignification and cell wall reinforcement as primary defense mechanisms. Notably, the combination of *R* with *Bacillus* (BR) strongly repressed POX activity, suggesting a possible antagonistic interaction between *B. amyloliquefaciens* and the host's peroxidase activation pathways. The moderate POX level in control plants likely reflects constitutive peroxidase activity in unstressed okra tissue.

By contrast, PPO activity followed a different trend. The highest PPO activity was observed in the Sc + R dual-pathogen treatment (ScR, 0.754), followed by TSc (0.716), BSc (0.678), and R alone (0.634). Intermediate values were recorded for TR (0.456) and BR (0.445), while the lowest PPO activities were seen in the single *S. sclerotiorum* treatment (Sc, only 0.093) and in the control (0.123). This pattern suggests that PPO responds most strongly to complex or dual microbial challenges, especially those involving *S. sclerotiorum*. The extremely low PPO activity under *S. sclerotiorum* alone may indicate active suppression of host oxidative pathways by this pathogen, consistent with its aggressive necrotrophic strategy. Co-inoculation with biocontrol agents, particularly *T. asperellum*, was effective in restoring or enhancing PPO activity, supporting a priming effect on okra defenses.

In summary, POX and PPO in okra showed distinct activation profiles. POX was most directly activated by *R. solani*, whereas robust PPO induction required either dual-pathogen stress or enhancement by a biocontrol agent. These divergent enzyme responses reflect the compartmentalized nature of okra's oxidative defense: POX is likely associated with structural defenses (e.g., strengthening cell walls), while PPO is linked to phenolic oxidation and the

production of antimicrobial compounds. Among the biocontrol strategies, *T. asperellum* had a more consistently positive influence on both enzymes, whereas *B. amyloliquefaciens* had variable effects depending on the pathogen context. Overall, these results underscore that different microbial challenges modulate okra's oxidative enzymes in distinct ways, highlighting the importance of strategic biocontrol pairings in shaping host defense outcomes. This enzyme-specific reactivity provides a biochemical foundation for optimizing disease management in okra through targeted biocontrol deployment.

CHAPTER 5: DISCUSSION

5.1. Dynamics of the interaction of *S. cepivora* and *F. proliferatum*

The interaction assay of *F. proliferatum* and *S. cepivora* revealed notable dynamics within the dual cultures of the pathogens. Abdullah et al. (2017) highlighted various types of pathogen–pathogen interactions, including competition, cooperation, coexistence, and mutualism. They described that in co-infected plants, pathogens may engage in competition by forming physical barriers or secreting toxins to exclude each other, cooperation by exchanging nutrients or signals that mutually enhance virulence, or stable coexistence through niche specialization within the host. In our study, the findings from the dual culture assay provide compelling evidence of competitive coexistence between *F. proliferatum* and *S. cepivora,* as observed at both Day 8 and Day 14. On Day 8, the fungi exhibited mutual growth limitation, with radial expansion ceasing at the interaction fronts. This early stabilization of the inhibition zone indicates that both fungi quickly claimed the available substrate and likely released inhibitory metabolites, creating a standoff where neither could advance further. Such an outcome aligns with the competition interaction mode noted by Abdullah et al. (2017), where each pathogen restricts the other's access to resources. The interaction at this stage reflects a balance where neither fungus could overcome the inhibitory effects exerted by the other, resulting in restricted growth along the shared boundary. By Day 14, single cultures of the pathogens reached full radial growth. The continued stability of the inhibition zone, with no further growth along the interacting fronts, demonstrates the persistence of competitive coexistence. The establishment of a stable inhibition zone demonstrates that both pathogens can coexist within the same environment without one completely outcompeting the other. This interaction is indicative of mutual growth limitation, where resource competition and proximity-driven interactions prevent further radial expansion along the interacting fronts.

The measurements at two distinct time points, Day 8 and Day 14, allowed us to capture both the early establishment of the inhibition zone and the cumulative effects of competitive coexistence over time. Day 8 represents the point when fungal growth in dual cultures ceased due to mutual limitation, providing insight into the onset of competitive interactions. In contrast, Day 14 reflects the sustained interaction dynamics and the long-term stabilization of the competitive equilibrium, emphasizing the persistence and extent of growth inhibition. These two time points offer a comprehensive view of how competitive coexistence evolves temporally in dual culture conditions. This temporal observation suggests that initial competitive interactions (nutrient capture, toxin production) quickly set the outcome, and no delayed antagonistic mechanisms (such as secondary metabolite secretion at later stages) arose to tip the balance in favor of either fungus.

Yuan and Chen (2021) described co-culture as an emerging and potential way to investigate microbial interaction under laboratory conditions, using a double-sided Petri dish to explore the interactions between *Monascus* spp. and *Aspergillus niger*. They found that the interaction between these fungi did not show antagonism, but rather a symbiotic relationship, where each fungus influenced the production of secondary metabolites in the other. This finding supports our observations, where both fungi coexisted without one outcompeting the other. Yuan and Chen (2021) also noted that the colour of the *Monascus* spp. colony that contacted *A. niger* became redder due to the increased pigment production triggered by the presence of *A. niger*, reflecting a metabolic response, similar to our observation where the area of *S. cepivora* in contact with *F. proliferatum* became significantly darker, likely due to the abundance of sclerotia production. The competitive stress from *F. proliferatum* presumably stimulated *S. cepivora* to generate more sclerotia (hence a darker appearance) as a defense mechanism. This parallels observations in other fungi where competition or oxidative stress induces sclerotial formation (Lin et al., 2023, Georgiou et al., 2006). Thus, the color changes in both studies indicate physiological responses: enhanced pigment synthesis in *Monascus* spp. and enhanced sclerotial melanization in *S. cepivora*, each fungus biochemically reacting to the presence of a competitor.

5.2. *In vitro* resistance screening against *S. cepivora* and *F. proliferatum* via single inoculation

Resistance screening against *S. cepivora* showed significant variability in incidence and severity between garlic cultivars. Most tested garlic cultivars were susceptible to white rot to varying degrees, with only a few exhibiting any level of resistance. The standout case was ‘Elephant’, which remained entirely symptomless, whereas cultivars like ’Messidor’ and ’Arno’ suffered severe rot. A few cultivars fell in between: for example, ’Sabagold’ and ’Thermidrome’ developed only minor lesions (indicating partial resistance), and interestingly ’Flavor’ had many infected cloves (moderate incidence) but each infected clove rotted extensively, suggesting it resists initial infection to some extent but cannot halt the disease once established. Akter et al. (2021) similarly tested eight garlic varieties and found significant variability in disease incidence and severity caused by *S. cepivora*, which is consistent with our findings in which ‘Elephant’ showed complete resistance, while the other cultivars showed different levels of susceptibility. Coley-Smith and Entwistle (1988) found no resistance among five garlic cultivars under field conditions. Similarly, Adams and Papavizas (1971) found that resistance to *S. cepivora* was rare in the *Allium* genus, consistent with the high susceptibility seen in our study in most garlic cultivars. However, in a study conducted by Delgadillo-Sánchez et al. (2001), lower susceptibility was observed in white

cultivars such as ‘Perla’ and ’Blanco de Cortazar’, which is similar to ’Elephant’ and ‘Sabagold’ in our study, although other white cultivars showed a high susceptibility.

Esler and Coley-Smith (1984) suggested that resistance in *Allium* species could result from the inability to stimulate sclerotial germination.This hypothesis provides a plausible explanation for the robust resistance of ‘Elephant’, whereby its root exudates or tissue chemistry may fail to trigger *S. cepivora* sclerotia to germinate, thereby effectively preventing the initiation of infection. The exceptional performance of ‘Elephant’ observed in our study could thus be attributed to such non-stimulatory properties or other unique genetic traits that impede the early stages of the infection process. Further investigation is warranted—for instance, by determining whether compounds exuded by ‘Elephant’ cloves lack the sulfur volatiles typically associated with the attraction and germination of *S. cepivora*. This requires performing more detailed biochemical analyses and genetic studies to identify these traits and to investigate the genetic basis of resistance in ’Elephant’ to identify its resistance genes.

The differential response of garlic cultivars to *F. proliferatum* infection underscores the complex relationship between disease incidence and symptom severity. For example, although ‘Makoi’ displayed a low infection rate, the few affected cloves exhibited extreme symptom intensity. This suggests a form of resistance that effectively limits initial infection but offers little containment once the pathogen becomes established, highlighting the need to evaluate both incidence and severity when assessing cultivar resistance.. These observations align with the findings of Jannatun et al. (2020), who highlighted significant differences in disease incidence between eight garlic varieties infected with *F. proliferatum*. BARI Rashun-4 exhibited the highest disease incidence at 25%, while the local Indian variety had the lowest at 3.80%. These findings underscore the variability in how *F. proliferatum* affects different garlic cultivars, suggesting that certain varieties such as BARI Rashun-3 and BARI Rashun-4 are more susceptible to high disease incidence (Jannatun et al., 2020).

The severity of the disease varied significantly; All cultivars exhibited the most severe class of symptoms, except ‘Flavor’, which displayed only slight infection symptoms, suggesting potential partial resistance despite its high incidence rates. This suggests that cultivars such as ’Flavor’ may possess tolerance mechanisms that suppress symptom progression, limiting the pathogen’s ability to cause severe damage despite its high infection rate. Specifically, ‘Elephant’ once again exhibited complete resistance, showing no symptoms of infection and a 0% incidence of the disease, reflecting its reaction against *S. cepivora*. This echoes the findings of Jannatun et al. (2020), who screened eight garlic varieties for resistance to *F. proliferatum*, finding significant variation in susceptibility.

Filyushin et al. (2021) investigated the genetic response of garlic cultivars to *F. proliferatum* by identifying and analysing class I chitinase genes (AsCHI1–7). Resistant cultivars, including 'Sarmat','Kuntsevsky', and 'Ershui', exhibited higher expression of AsCHI2, AsCHI3, and AsCHI7, particularly in roots and cloves, compared to susceptible cultivars such as 'Strelets' and 'Sofievsky'. This study suggests that chitinase genes could be strategically leveraged in breeding programmes to enhance resistance to *F. proliferatum* (Filyushin et al., 2021). This is particularly relevant to our findings, where the cultivars 'Flavor' and 'Elephant' demonstrated partial and complete resistance, respectively, to *Fusarium* bulb rot. The resistance observed in 'Elephant' can be attributed to genetic factors unique to its classification within *Allium ampeloprasum*, which could potentially be identified and used in breeding programs to enhance resistance in commercially important garlic cultivars. By exploring these genetic traits, breeding programmes could develop new varieties with enhanced resistance to both white rot and *Fusarium* bulb rot. This approach holds promise for significantly reducing the occurrence and impact of these diseases, aligning with sustainable agriculture goals by minimising dependency on chemical controls. Furthermore, the use of 'Elephant' as a genetic resource opens new possibilities for durable species-crossing resistance mechanisms that could strengthen the resistance of garlic plants against a wide range of pathogens.

5.3. *In vitro* resistance screening against the dual inoculation of *F. proliferatum* and *S. cepivora* on garlic cultivars

Despite the competitive coexistence of the fungi observed *in vitro,* dual inoculation on garlic cultivars resulted in a significantly increased disease severity compared to individual inoculations. All tested cultivars, except for 'Elephant', exhibited disease incidences greater than 96.00%, with symptoms such as rotting and mycelial formation appearing three days earlier than in single infections, developing into much more severe symptoms that envelope the whole clove. This confirms that while pathogens exhibit competitive co-existence *in vitro*, their combined presence *in planta* can lead to synergistic effects that exacerbate disease symptoms. The competitive coexistence observed in the dual culture assay, where mutual inhibition limited radial growth, reflects the ability of pathogens to compete for limited resources in an *in vitro* controlled environment. However, *in planta,* pathogens interact differently due to host factors such as the availability of various nutrients, structural barriers, and host metabolic responses. These conditions enable a synergistic relationship where the activity of one pathogen facilitates the colonisation or pathogenicity of the other. This shift is evident in the earlier onset of symptoms and the significantly more severe manifestations under dual inoculations compared to single inoculations.

Fang et al. (2021) examined the effects of co-infection by *Fusarium oxysporum* f. sp. *medicaginis* and *Rhizoctonia solani* on various varieties of alfalfa. Their findings showed that co-infection led to significantly increased disease severity and reductions in plant growth and biomass allocation compared to single infections. This mirrors our results in garlic, where co-inoculation resulted in more severe disease symptoms and reduced plant health. Importantly, Fang et al. (2021) found that no single alfalfa variety was resistant to both pathogens under co-infection, highlighting the complexity of breeding for disease resistance in the presence of multiple pathogens, proving the importance of the 'Elephant' the discovery of cultivar and its resistance to both single and dual fungal infections in garlic. Lamichhane and Venturi (2015) and Abdullah et al. (2017) noted that pathogen–pathogen interactions can lead to more severe disease symptoms than those caused by single infections and can significantly alter host responses. Similarly, Susi et al. (2015) observed that co-infection with two strains of the fungal pathogen *Podosphaera plantaginis* in *Plantago lanceolata* significantly increased disease prevalence, as compared to infections involving only a single strain. These observations are particularly relevant to our garlic study, where co-inoculation with *F. proliferatum* and *S. cepivora* resulted in significantly increased disease severity in garlic cultivars. The observed transition from competitive co-existence *in vitro* to synergistic pathogenicity *in planta* is consistent with the dynamic nature of fungal interactions and confirms the validity of the experimental findings. In the study by Marchetto and Power (2018), the effects of co-infection timing on barley infected with barley yellow dwarf virus and barley stripe mosaic virus were examined, finding that simultaneous co-infections were significantly more damaging to the host than sequential co-infections, leading to greater reductions in seed production. This partially mirrors our findings in garlic, where despite the fact that sequential infections were not studied, the simultaneous co-inoculation with *F. proliferatum* and *S. cepivora* significantly increased disease severity on garlic compared to single infections.

The notable resistance of cv. 'Elephant', even under co-infection conditions, distinguished it from other cultivars, which demonstrated significant susceptibility under similar conditions. This robust resistance is presumably underpinned by complex defence mechanisms, potentially facilitated by specific genetic traits that manifest structural or biochemical barriers to pathogenic infection. These observations corroborate the observations of Tollenaere et al. (2016), which underscore the significance of genetic diversity within plant populations in imparting resistance to a multitude of pathogens. The steadfast resistance shown in our study by the 'Elephant' cultivar to single and concurrent infections in controlled environments requires further validation within field settings and a comprehensive analysis of its genetic framework. Studying the genetic foundations of the resistance exhibited by 'Elephant' would represent a significant advancement in the development

of Allium disease management strategies. Through detailed genetic characterisation, breeders can cultivate new garlic varieties endowed with similar resilient traits, thus increasing crop resilience against diverse and combined pathogen threats and promoting sustainable agricultural methodologies.

5.4. Comparative antagonistic efficacy of *Trichoderma asperellum* and *Bacillus amyloliquefaciens* against *Fusarium proliferatum* and *Stromatinia cepivora in vitro* and *in planta* in garlic

The antagonistic potential of *T. asperellum* and *B. amyloliquefaciens* was evaluated using a combination of *in vitro* dual culture assays and *planta* phytotron trials against the main soilborne garlic pathogens *F. proliferatum* and *S. cepivora*. In *vitro* assays provided a controlled environment to directly observe morphological interactions, inhibition kinetics, and antagonistic mechanisms, while *in planta* experiments assessed the ability of these biocontrol agents to mitigate pathogen-induced growth suppression under realistic plant–pathogen conditions. By integrating these two approaches, the study aimed to elucidate both the direct antifungal capacity of the antagonists and their broader protective effects on garlic seedlings, thus bridging the gap between laboratory observations and plant-level results.

In the *in vitro* dual-culture assays, *T. asperellum* consistently outperformed *B. amyloliquefaciens*. Against *F. proliferatum*, *T. asperellum* displayed rapid overgrowth of the pathogen, forming a well-defined confrontation zone characterised by hyphal melanization on the *Fusarium* margin. This melanization is a classical stress response to antagonistic organisms, typically induced by oxidative damage or antifungal metabolites secreted by *Trichoderma* spp. (Atanasova et al., 2013). The inhibition of *T. asperellum* reached 45.60% on Day 13, with radial growth stabilizing at 4.1 cm compared to 7.5 cm in the control. These observations are consistent with the well-documented mycoparasitic and competitive mechanisms of *Trichoderma* spp., which involve the secretion of cell wall–degrading enzymes (chitinases, glucanases) and secondary metabolites capable of lysing or inhibiting phytopathogenic fungi (Atanasova et al., 2013). Previous studies reported similar suppressive activity of *T. asperellum* against *Fusarium* spp., including significant mitigation of root rot in beans accompanied by enhanced plant growth (Elshahawy and Marrez, 2024).

In contrast, inhibition by *B. amyloliquefaciens* against *F. proliferatum* was more modest, peaking at 26.06 % by Day 10, characterized by the formation of a static inhibition zone without overgrowth or physical contact. This supports the predominance of antibiosis, rather than spatial competition. Indeed, the *B. amyloliquefaciens* strain QST 713 is known to secrete diffusible lipopeptides—iturins, fengycins, and surfactins—that disrupt fungal membranes and interfere with

pathogen metabolism (Cawoy et al., 2015). Comparable inhibition levels have been reported in other studies, where strains of *Bacillus subtilis* and *B. tequilensis* inhibited *F. proliferatum* in the range of 54–59%, while certain *Pseudomonas* isolates achieved up to 67% inhibition (El Barnossi et al., 2024). Thus, while *Bacillus* spp. is recognized as reliable BCAs, their *in vitro* effects often remain moderate relative to *Trichoderma* spp.

Similarly, when confronted with *S. cepivora*, *T. asperellum* induced a markedly stronger antagonistic response compared to *B. amyloliquefaciens*. The pathogen's radial growth plateaued at 1.7 cm by Day 8, resulting in a high inhibition rate of 77.4 % by Day 14. Morphologically, *T. asperellum* rapidly encircled and overgrew *S. cepivora*, forming a wide inhibition halo and completely suppressing the expansion completely consistent with mycoparasitism and secretion of potent antifungal metabolites. These findings parallel previous reports showing that *Trichoderma* spp. effectively controls garlic white rot under laboratory conditions (Elshahawy et al., 2019). On the contrary, *B. amyloliquefaciens* achieved only 26.0 % inhibition of *S. cepivora* on Day 10. The presence of melanised hyphae along the confrontation margin with *Bacillus* spp. indicated a stress-induced fungal defence reaction to bacterial metabolites, but without notable pathogen regression. Therefore, the overall antagonistic rank *in vitro* was *T. asperellum* > *B. amyloliquefaciens*, with the greatest disparity evident against *S. cepivora*.

Although the *in vitro* inhibition provides valuable preliminary insights, it does not always directly predict *in plant* efficacy. Indeed, several studies have highlighted cases where moderate *in vitro* inhibition is correlated with strong suppression in the greenhouse or field due to additional mechanisms such as root colonisation and induced systemic resistance (Kara et al., 2023, Nájera et al., 2022). In this study, the trials of phytotrons *in planta* reflected both direct pathogen suppression and plant-mediated responses.

In the absence of biocontrol agents, *F. proliferatum* inoculation caused severe stunting (5.05 cm by Week 3) and typical symptoms of vascular colonization such as wilting and chlorosis. Co-application of *T. asperellum* (TF) significantly mitigated these effects, restoring plant height to 10.30 cm by Week 3 and reducing symptom severity. By contrast, *B. amyloliquefaciens* (BF) provided partial recovery (8.12 cm by Week 3), while the combined treatment (TBF) produced similar or slightly better restoration (8.50 cm by Week 3) than *T. asperellum* alone. These outcomes support the hypothesis that *T. asperellum* acts through multiple mechanisms in planta: direct pathogen suppression, niche competition, and elicitation of plant defense pathways. Previous studies have shown that *Trichoderma* spp. primes host systemic defenses, leading to enhanced resistance against soilborne pathogens (Atanasova et al., 2013). *B. amyloliquefaciens* likely contributed via lipopeptide antibiosis in the rhizosphere and by triggering induced systemic

resistance (ISR) through salicylic acid and ethylene-mediated signaling pathways, as reported for other *Bacillus* spp. (Cawoy et al., 2015, Lugtenberg and Kamilova, 2009). Similar findings were observed in beans, where *T. asperellum* dramatically improved germination and yield under *Fusarium* infection (Elshahawy and Marrez, 2024).

Stromatinia cepivora exhibited strong pathogenicity, fully suppressing seedling emergence in untreated controls. The limited emergence observed in biocontrol-treated groups suggests partial mitigation of disease pressure. Notably, the dual application of *T. asperellum* and *B. amyloliquefaciens* was more effective than single-agent treatments, indicating a potential synergistic effect in reducing disease severity and enhancing early growth. This suggests a synergistic or at least complementary effect between *T. asperellum* and *B. amyloliquefaciens*: the former directly attacked the pathogen through overgrowth and enzymatic degradation, while the latter likely enhanced plant resilience by priming host immunity. However, even the combined treatment failed to fully counteract the necrotrophic virulence of *S. cepivora*, emphasizing the difficulty of managing white rot under high inoculum pressure. Comparable synergistic effects have been documented in other microbial consortia, where combining fungal and bacterial BCAs provided better disease suppression than single agents alone (Vargas Baquero and Cotes, 2024, Guetsky et al., 2002, Guetsky et al., 2001).

When contextualized within the broader literature, these findings corroborate the established biocontrol hierarchy where *Trichoderma* spp. exhibit stronger antagonism than *Bacillus*-based agents in direct fungal confrontation. Nevertheless, *Bacillu*s spp. contributes valuable ISR effects that complement fungal antagonism in planta. For example, *T. asperellum* and *T. harzianum* isolated from Allium rhizospheres have been reported to strongly inhibit *S. cepivora* (>50% *in vitro*) (Rivera-Méndez, 2016), while *B. subtilis* strains inhibited garlic white and basal rot pathogens by up to 94% *in vitro* (El-Sheshtawi et al., 2009, Mohy et al., 2024). Moreover, *Trichoderma virens* has been shown to suppress onion wilt in greenhouse conditions to a level comparable to chemical fungicides despite modest *in vitro* inhibition (~33.3%) (Nájera et al., 2022). These reports highlight that plant-associated mechanisms—colonization, nutrient competition, ISR—often amplify BCA performance beyond what static plate assays reveal.

Together, the quantitative correspondence between *in vitro* inhibition and *in planta* efficacy observed here (*T. asperellum* > *B. amyloliquefaciens*; TBS > single treatments) reinforces the rationale for combining multiple BCAs. *Trichoderma asperellum* provides robust direct suppression of both *F. proliferatum* and *S. cepivora*, while *Bacillus amyloliquefaciens* offers additional, though more limited, benefits through antibiosis and plant-mediated ISR. This integration is especially valuable against highly virulent pathogens like *S. cepivora*, where single

agent treatments remain insufficient under high disease pressure. Therefore, the data support a dual-strategy biocontrol approach for the sustainable management of garlic soilborne diseases.

In conclusion, *T. asperellum* emerged as the most effective antagonist under both laboratory and controlled phytotron conditions, confirming its potential as a primary biocontrol agent. *B. amyloliquefaciens* provided complementary, although weaker, protection and its combination with *T. asperellum* yielded additive effects, particularly under severe pathogen pressure. These results are consistent with the broader literature on Allium biocontrol, affirming the integration of microbial consortiums as a promising alternative to chemical fungicides for the management of *Fusarium proliferatum* and *Stromatinia cepivora* in garlic cultivation (Atanasova et al., 2013, El-Sheshtawi et al., 2009, Cawoy et al., 2015). At the same time, our findings also indicate that even the most effectile biocontrol combination did not completely protect garlic from white rot where disease symptoms still occurred. This suggests that while biocontrol can significantly reduce disease severity, it may need to be integrated with other strategies such as cultivating resistant varieties for full disease control. In fact, the absolute resistance of the 'Elephant' cultivar to both pathogens highlights the value of breeding or deploying resistant garlic lines. A resistant cultivar, when combined with effective BCAs like *T. asperellum* and *B. amyloliquefaciens* could provide a much more reliable and durable defense against these soil-borne diseases.

5.5. Enzymatic defense responses in garlic and okra under pathogen challenge and biocontrol treatments

The enzymatic profiling of guaiacol peroxidase (POX) and polyphenol oxidase (PPO) in garlic and okra seedlings revealed distinct and treatment-specific oxidative defense responses. These variations align with the well-documented role of these enzymes in mediating structural and biochemical resistance against fungal pathogens.

In garlic, the co-inoculation of biocontrol agents with pathogens resulted in significantly elevated POX activity compared to single-pathogen treatments. For example, the combination of *B. amyloliquefaciens* with *F. proliferatum* induced the highest POX levels, followed by *Trichoderma asperellum* with *F. proliferatum*. Similarly, dual treatments involving *T. asperellum* and *S. cepivora* were among the most effective in enhancing POX activity. These findings are consistent with previous reports that *Trichoderma* spp. can enhance host peroxidase responses and thereby strengthen structural defense mechanisms, such as lignification and cell wall reinforcement (Shalaby et al., 2013). In contrast, single-pathogen inoculations with either *S. cepivora* or *F. proliferatum* elicited the lowest POX activities, suggesting that these pathogens alone triggered only moderate oxidative responses.

PPO activity in garlic showed a different pattern, with the highest levels observed under *T. asperellum* + *S. cepivora* co-inoculation and in single *S. cepivora* infections, highlighting a pathogen-specific activation of phenolic metabolism. The reduction of PPO in treatments combining *B. amyloliquefaciens* with *S. cepivora* suggests that the BCA may modulate PPO differently depending on the pathogen context, a variability also noted in other studies where *Bacillus* spp. affected oxidative enzymes in a strain- and host-dependent manner (Saleh et al., 2024). *Bacillus*-induced systemic resistance (ISR) may selectively activate certain defense pathways—such as peroxidase—while suppressing others like polyphenol oxidase (PPO). The observed reduction in PPO activity could indicate a lower perception of tissue damage due to the partial suppression of *S. cepivora* by *B. amyloliquefaciens*. In addition, *Bacillus*-derived metabolites or enzymes may interfere with PPO-related responses by scavenging reactive oxygen species or modulating hormonal crosstalk (Alexis et al., 2021). These mechanisms suggest a finely regulated host response, in which *Bacillus* mitigates excessive phenolic oxidation that could otherwise harm plant tissues, while still maintaining effective defense through alternative pathways.

In okra, POX activity was most strongly induced by *Rhizoctonia solani*, either alone or in combination with *T. asperellum*. This suggests that *R. solani* is a potent elicitor of cell wall–associated defenses, a response consistent with reports that necrotrophic pathogens can trigger peroxidase-mediated lignification in plant tissues (Sagitov et al., 2011, Yang et al., 2024b). By contrast, *Sclerotinia sclerotiorum* alone elicited only minimal POX activity. Importantly, combining *R. solani* with *B. amyloliquefaciens* significantly reduced POX levels, supporting the idea that *Bacillus* spp. metabolites can interfere with peroxidase induction under certain conditions, particularly when host stress is moderate or when ISR pathways are preferentially activated over local oxidative responses, as also suggested for other host-pathogen interactions (Alexis et al., 2021).

For PPO in okra, the strongest induction was observed under dual-pathogen stress (*S. sclerotiorum* + *R. solani*), followed by treatments involving *T. asperellum*. The markedly low PPO activity in *S. sclerotiorum* single infections reflects this pathogen's limited stimulation of phenolic metabolism, a trend similarly noted in garlic where PPO induction was pathogen-specific. The enhancement of PPO in the presence of *T. asperellum* supports its established role in priming phenolic pathways and boosting systemic resistance (Shalaby et al., 2013).

The consistent enhancement of oxidative enzyme activity by *T. asperellum* in both garlic and okra reinforces its role as a broad-spectrum elicitor of host antioxidant defenses. This aligns with evidence that *Trichoderma* spp. can upregulate defense-related enzymes across diverse host plants.

In contrast, the variable response elicited by *B. amyloliquefaciens* in enhancing POX activity in garlic but reducing it in okra suggests a mode of action influenced by both host species and the co-infecting pathogen. Such specificity may reflect differential priming of immune pathways or metabolic trade-offs in how each host allocates defense resources, as also noted by Saleh et al. (2024).

Overall, these results confirm that pathogen identity, dual infections, and biocontrol agents distinctly modulate oxidative defenses, with POX primarily associated with structural reinforcement and PPO linked to phenolic oxidation. The consistent enhancement by *T. asperellum* suggests its potential as a reliable biocontrol agent for priming oxidative defenses, whereas the variable responses to *B. amyloliquefaciens* underline the need for careful host–pathogen–agent matching in biocontrol strategies. These findings provide a conservative but well-supported biochemical basis for optimizing integrated disease management in garlic and okra.

5.6. Cross-crop analysis of biocontrol-induced defence pathways in garlic and okra

The divergent responses of garlic and okra to biological control agents in this study underscore how host physiology, pathogen lifestyle and microbial antagonists jointly shape plant defence. While both crops rely on oxidative enzymes such as guaiacol peroxidase and polyphenol oxidase to restrict pathogen ingress, the timing and intensity of enzyme induction proved crop-specific. In garlic, co-application of *T. asperellum* and *B. amyloliquefaciens* was necessary to maintain elevated peroxidase and polyphenol oxidase activities; treatments with Bacillus alone often produced lower enzyme levels than pathogen-only controls. Okra, by contrast, mounted rapid and robust oxidative responses to both necrotrophic pathogens and *T. asperellum*, yet *B. amyloliquefaciens* occasionally suppressed peroxidase activity. These findings suggest that okra possesses a more plastic oxidative defence system, whereas garlic depends more heavily on non-enzymatic antioxidants and secondary metabolites.

Situating these results within the broader literature reveals that fungal biocontrol agents typically elicit stronger oxidative responses than their bacterial counterparts. Previous studies have shown that Trichoderma spp. can prime host peroxidases and chitinases in Allium crops, and that combinations of *Trichoderma* spp. with *Bacillus* spp. enhance peroxidase and polyphenol oxidase activities while reducing white-rot symptoms (Shalaby et al., 2013). Our observations mirror these patterns: *T. asperellum* consistently elevated oxidative enzymes in both crops, whereas the effects of *B. amyloliquefaciens* were context-dependent. The strong oxidative bursts observed in okra following infection are reminiscent of responses to elicitors such as chitosan or potassium salts, which trigger concurrent increases in peroxidase, polyphenol oxidase and β-1,3-glucanase

activities (Soliman and El-Mohamedy, 2017). Similarly, seed priming with entomopathogenic fungi has been reported to enhance peroxidase, catalase and ascorbate peroxidase activities while suppressing disease in okra (Mimma et al., 2023); these trends parallel the benefits conferred by *T. asperellum* in the present study.

The variable performance of *B. amyloliquefaciens* likely reflects differences in root exudates and signalling pathways between the two crops. Bacillus-induced systemic resistance is mediated predominantly through jasmonic acid and ethylene (Miljaković et al., 2020), pathways that may interact differently with garlic's and okra's innate defences. In garlic, the bacterium may have shifted defence towards phenylpropanoid or phytoalexin synthesis rather than oxidative pathways, whereas in okra the same treatment sometimes dampened peroxidase induction. These observations highlight the importance of tailoring biocontrol strategies to specific host–pathogen systems and suggest that combining fungal and bacterial antagonists can provide complementary defence activation.

Looking forward, integrative approaches that couple enzyme assays with metabolomic and transcriptomic profiling could unravel the regulatory networks governing these divergent responses. Standardized cross-crop experiments would clarify whether the observed differences stem from intrinsic host physiology or experimental variables. Moreover, dissecting the temporal interplay between salicylic, jasmonic and ethylene signalling pathways may explain why garlic relies more on chemical antioxidants while okra responds vigorously via oxidative enzymes. Such insights will guide the development of disease management strategies that leverage the strengths of both fungal and bacterial biocontrol agents and accommodate the unique defence hierarchies of individual crops.

CHAPTER 6: CONCLUSIONS

This dissertation investigated the interactions between soil-borne fungal pathogens, host plants, and biocontrol agents using garlic (*Allium sativum* L.) as primary host. The work focused on accurately identifying key pathogens, characterising their interactions, evaluating cultivar-level resistance, and assessing the performance of biological control agents. Additionally, it examined the responses of oxidative enzymes in garlic, with okra included as a comparative model to provide information on the host's defensive physiology.

Pathogen identification confirmed *Fusarium proliferatum* (causing dry rot) and *Stromatinia cepivora* (white rot) as the main threats. These findings, established through morphology and ITS sequencing, provided a reliable etiological basis for subsequent experiments. Dual culture assays revealed that *F. proliferatum* and *S. cepivora* exhibit mutual inhibition *in vitro*. However, *in planta* co-infection led to synergistic pathogenicity, with earlier symptom onset and greater disease severity compared to single infections. This shift highlights the limitations of *in vitro* models in predicting real-world pathogenic dynamics and emphasises the importance of studying interactions within the host context.

Among the eleven garlic cultivars tested, susceptibility was generally high under dual infection, with disease incidence exceeding 96%. However, the cultivar 'Elephant' showed complete resistance to both pathogens, even under co-inoculation. This unique resistance, absent in other cultivars, represents a significant finding with practical implications for breeding. It suggests that genetic resistance to complex pathogen interactions is achievable, although field validation and genetic characterisation remain necessary.

The performance of biocontrol agents was the second cornerstone of the study. *Trichoderma asperellum* and *Bacillus amyloliquefaciens* were isolated, confirmed through molecular identification, and their antagonism. *In vitro*, *T. asperellum* exhibited aggressive mycoparasitism, while *B. amyloliquefaciens* produced clear inhibition zones indicative of antibiosis. In phytotron trials, *T. asperellum* significantly suppressed *F. proliferatum*-related disease and restored seedling vigour, with *B. amyloliquefaciens* providing an additive but smaller benefit. When used together, both agents further improved plant health, though not significantly beyond *Trichoderma* alone for *Fusarium* suppression.

In the case of *S. cepivora, the* disease pressure was more severe. Neither biocontrol agent alone could prevent complete seedling death, but their combined application achieved measurable protection, allowing some replicates to survive and grow. However, even the best outcomes under

dual biocontrol fell short of restoring complete plant health, underscoring the difficulty of managing white rot with biocontrol alone.

Defence enzyme profiling revealed that different combinations of pathogen-biocontrol activated distinct physiological responses. In garlic, *F. proliferatum* paired with biocontrol agents triggered the highest peroxidase (POX) activity, particularly when *B. amyloliquefaciens* was present. On the contrary, polyphenol oxidase (PPO) activity was more elevated under *S. cepivora* infection, especially when combined with *T. asperellum*. These divergent activation patterns indicate that host responses are pathway-specific and context-dependent. The findings suggest that biocontrol agents not only suppress pathogens directly, but also induce host resistance mechanisms, providing a dual mode of protection.

Parallel okra assays supported the broader relevance of these mechanisms. In response to *Rhizoctonia solani* and *Sclerotinia sclerotiorum*, okra displayed distinct enzyme response profiles: POX increased with *R. solani*, while PPO increased under dual-pathogen stress and biocontrol treatment. These patterns reinforce the idea that defence induction is crop-specific but that the general principles of pathogen-induced stress and biocontrol-mediated priming apply across plant systems.

Methodologically, this work combined classical and molecular techniques to ensure experimental precision and reproducibility. Controlled phytotron conditions and replicated trials allowed high-confidence comparisons between treatments.

'Elephant' garlic emerges as a promising candidate for breeding disease resistant cultivars. *T. asperellum* shows consistent value as a biocontrol agent, particularly against *Fusarium*, and its combination with *B. amyloliquefaciens* may offer partial protection against more aggressive pathogens such as *S. cepivora*. The demonstrated capacity of these agents to trigger plant defences supports their integration into IPM strategies.

In summary, this dissertation advances understanding of plant-microbe interactions under co-infection pressure, identifies key resistance traits in garlic, validates biocontrol strategies, and reveals mechanistic insights into induced defences. Future work should focus on field validation, molecular dissection of resistance traits (especially in 'Elephant'), expanded biocontrol screening, and system-level profiling of host responses. The inclusion of okra as a secondary model affirms the broader applicability of the findings and sets the stage for comparative pathosystem studies. This work contributes both applied and conceptual tools to the ongoing pursuit of sustainable, biologically grounded plant disease management.

NEW SCIENTIFIC FINDINGS

- **Co-infection of *Fusarium proliferatum* and *Stromatinia cepivora* in garlic synergistically intensified disease *in planta* despite competitive coexistence *in vitro*.** Dual culture assays showed stable inhibition without dominance, with mutual suppression of 25.39% (*F. proliferatum*) and 28.61% (*S. cepivora*) by Day 14.
- **Garlic variety 'Elephant' was completely resistant to both pathogens under single and dual inoculation**, marking the first report of broad-spectrum resistance to *Fusarium* bulb rot and white rot in garlic under controlled conditions.
- ***Trichoderma asperellum* exhibited stronger antagonism than *Bacillus amyloliquefaciens*.** *T. asperellum* fully overgrew *S. cepivora* (77.4% inhibition) and suppressed *F. proliferatum* (45.6%), while *B. amyloliquefaciens* acted mainly through antibiosis, achieving 26.06% inhibition of *F. proliferatum* and 26.0% against *S. cepivora*.
- ***In planta* assays showed *S. cepivora* caused complete emergence failure, whereas *F. proliferatum* severely stunted growth.** *T. asperellum* restored seedling height most effectively, and combined *T. asperellum* + *B. amyloliquefaciens* treatments showed synergistic improvement over single applications.
- **Oxidative enzyme responses were pathogen- and treatment-specific.** In garlic, POX was maximally induced by *B. amyloliquefaciens* + *F. proliferatum*, while PPO peaked with *T. asperellum* + *S. cepivora*. In okra, *R. solani* strongly triggered POX, *S. sclerotiorum* suppressed it, and PPO peaked under dual stress, with *T. asperellum* restoring enzyme activity and *B. amyloliquefaciens* showing variable effects.
- **Combined biocontrol treatments provided superior suppression**, particularly against *S. cepivora*, improving emergence, reducing severity, and enhancing enzymatic defense more effectively than single agents.

SUMMARY

Garlic (*Allium sativum* L.), a globally essential crop, suffers severe losses from soil-borne fungal pathogens such as *Fusarium proliferatum* (*Fusarium* bulb rot) and *Stromatinia cepivora* (white rot). In May 2023, garlic fields near Makó City, Hungary, exhibited sporadic yellowing, wilting, and basal rot. Symptomatic cloves were incubated in humid chambers, cultured in PDA, purified via hyphal-tip isolation, and confirmed as *F. proliferatum* and *S. cepivora* through ITS1-2 sequencing and morphological identification. This study investigated pathogen–pathogen interactions under *in vitro* conditions, evaluated the resistance of eleven garlic cultivars to single and simultaneous infections, evaluated the antagonistic potential of *Trichoderma asperellum* and *Bacillus amyloliquefaciens in vitro* and in phytotron-controlled trials, and analysed oxidative enzyme responses in garlic to elucidate host defence activation under pathogen and biocontrol pressure. A secondary pathosystem using okra (*Abelmoschus esculentus* (L.) Moench), challenged with *Rhizoctonia solani* and *Sclerotinia sclerotiorum*, was included to validate and broaden the interpretation of induced defence responses.

The *in vitro* interaction between *F. proliferatum* and *S. cepivora* showed early competitive coexistence (inhibition 8.47% and 6.40% by Day 8), intensifying to 25.39% and 28.61% by Day 14. Resistance screening revealed high susceptibility in ‘Aulxito’, ‘Sabadrome’, ‘Arno’, ‘Garcua’, and ‘Makói Tavaszi’, while ‘Flavor’ and ‘Sabagold’ displayed mild tolerance; only ‘Elephant’ exhibited complete resistance even under simultaneous inoculation.

In dual culture assays, *T. asperellum* strongly antagonized both pathogens, overgrowing *F. proliferatum* (45.6% inhibition by Day 13) and markedly suppressing *S. cepivora* (77.4% inhibition by Day 14), suggesting competitive exclusion and mycoparasitism. *B. amyloliquefaciens* inhibited both fungi via antibiosis, forming stable halos with moderate suppression (~26%).

Under phytotron conditions, *F. proliferatum* significantly stunted garlic seedlings, limiting final height to 5.05 cm, whereas *S. cepivora* caused complete emergence failure. *T. asperellum* mitigated *F. proliferatum* infection, restoring height to 10.3 cm compared to 17.9 cm in the healthy control, while *B. amyloliquefaciens* achieved moderate recovery (8.1 cm). Against *S. cepivora*, partial emergence was possible: *T. asperellum* allowed 5.45 cm growth, *B. amyloliquefaciens* yielded 4.58 cm, and their combined application (TBS) provided the highest recovery (6.43 cm), outperforming single treatments but remaining below control growth.

Enzyme assays revealed pathogen-specific oxidative defense activation in garlic: guaiacol peroxidase (POX) was highest when *B. amyloliquefaciens* co-occurred with *F. proliferatum*, while

polyphenol oxidase (PPO) peaked with *T. asperellum* + *S. cepivora*. Single-pathogen infections induced only modest POX/PPO increases. In okra, *R. solani* strongly induced POX, whereas *S. sclerotiorum* suppressed it, but PPO was enhanced under dual stress (*S. sclerotiorum* + *R. solani*, 0.754) and restored by *T. asperellum*, while *B. amyloliquefaciens* variably modulated enzyme responses.

These findings reveal synergistic pathogen effects, highlight 'Elephant' as a resistant garlic cultivar, and demonstrate that *T. asperellum*, alone or with *B. amyloliquefaciens*, effectively suppresses garlic pathogens *F. proliferatum* and *S. cepivora* through direct inhibition and systemic defense priming, with parallels in broader host-pathogen systems.

REFERENCES

ABBA, J. F. 2019. Preliminary Studies on Fungus Associated with Storage Disease of Garlic (*Allium sativum* L.) in Nigeria. *Dutse J. Pure Appl. Sci,* 5**,** 161-168.

ABD-EL-KAREEM, F., SAIED, N. M., ELSHAHAWY, I. E. & ABD-ELGAWAD, M. 2023. Soil bio-solarization and *Trichoderma asperellum* suppress black root rot disease and increase strawberry yield. doi: 10.21203/rs.3.rs-3096529/v1.

ABDULLAH, A. S., MOFFAT, C. S., LOPEZ-RUIZ, F. J., GIBBERD, M. R., HAMBLIN, J. & ZERIHUN, A. 2017. Host–multi-pathogen warfare: pathogen interactions in co-infected plants. *Frontiers in plant science,* 8**,** 1806. doi: 10.3389/fpls.2017.01806.

ABED, N. & FARHAN, T. 2023. Identification of Some Fungi Causing Okra Root Rot Disease from Different Regions of Anbar and Waist and Testing Pathogenicity. *IOP Conference Series: Earth and Environmental Science,* 1252**,** 012013. doi: 10.1088/1755-1315/1252/1/012013.

ADAMS, P. & PAPAVIZAS, G. 1971. Effect of inoculum density of *Sclerotium cepivorum* and some soil environmental factors on disease severity. *Phytopathology,* 61**,** 1253-1256. doi: 10.1094/Phyto-61-1253.

ADEBOOYE, O. & OPUTA, C. 1996. Effects of galex (r) on growth and fruit nutrient composition of okra (*Abelmoschus esculentus* (l.) Moench). *Ife Journal of Agriculture,* 18**,** 1-9.

ADETUYI, F., OSAGIE, A. & ADEKUNLE, A. 2008. Effect of postharvest storage techniques on the nutritional properties of benin indigenous okra *Abelmoschus esculentus* (L) Moench. *Pakistan journal of Nutrition,* 7**,** 652-657.

ADIAHA, M. S. 2017. Effect of Okra (*Abelmoschus esculentus* L. Moench) on human development and its impact on the economy of farmers in Obubra Rainforest Zone of Nigeria. *World News of Natural Sciences,* 10**,** 80-85.

AFROZ, T., AKTARUZZAMAN, M. & KIM, B.-S. 2019. First report of gray mold on okra caused by *Botrytis cinerea* in Korea. *Plant Disease,* 103**,** 1038-1038. doi: 10.1094/PDIS-10-18-1884-PDN.

AFZAL, M., ALI, M., THOMSON, M. & ARMSTRONG, D. 2000. Garlic and its medicinal potential. *Inflammopharmacology,* 8**,** 123-148.

AKTER, U. H., BEGUM, F., ISLAM, M. R., KHATUN, M. R. & ISLAM, M. M. 2021. Screening of Selected Garlic Varieties Against White Rot Disease Caused by *Sclerotium cepivorum* at Dhaka City of Bangladesh. *American Journal of Plant Biology,* 6**,** 53-59. doi: 10.11648/j.ajpb.20210603.13.

ALEXIS, Z. P., FOTSO, A., MARTIAL, T. T. & PIERRE-FRANÇOIS, D. 2021. Effect of soil amendment with *Trichoderma harzianum* and *Bacillus amyloliquefaciens* bioformulation on biochemical parameters and antioxidant activity in *Abelmoschus esculentus*. *International Journal of Innovation and Applied Studies,* 33**,** 522-535.

ALLISON, G. L., LOWE, G. M. & RAHMAN, K. 2006. Aged garlic extract may inhibit aggregation in human platelets by suppressing calcium mobilization. *The Journal of nutrition,* 136**,** 789S-792S.

AMADI, J., NNAMANI, C., OZOKONKWO, O. & EZE, C. 2014. Survey of the incidence and severity of okra (*Abelmoschus esculentus* L. Moench) Fruit rot in Awka South lga, Anambra state, Nigeria. *International Journal of Current Microbiology and Applied Sciences,* 3**,** 1114-1121.

AMARAKOON, S. & JAYASEKARA, D. 2017. A review on garlic (*Allium sativum* L.) as a functional food. *Journal of Pharmacognosy and Phytochemistry,* 6**,** 1777-1780.

AMIRA, O. C. & OKUBADEJO, N. U. 2007. Frequency of complementary and alternative medicine utilization in hypertensive patients attending an urban tertiary care centre in Nigeria. *BMC complementary and alternative medicine,* 7**,** 1-5.

ANDRADE, G. C. G., CARRER FILHO, R. & DA CUNHA, M. G. 2018. Soybean genotypes resistant to white mold in the field and in oxalic acid sensitivity tests. *Científica,* 46**,** 126-131. doi: 10.15361/1984-5529.2018v46n2p126-131.

ANEES, M., RASHMI, C., VARMA, Y. & GOVINDAN, M. 2016. Report on new foliar blight disease caused by *Rhizoctonia solani* on chilli, Brinjal and Okra from India. *Imperial Journal of Interdisciplinary Research,* 2**,** 182-183.

ANISIMOVA, O. K., KOCHIEVA, E. Z., SHCHENNIKOVA, A. V. & FILYUSHIN, M. A. 2022. Thaumatin-like protein (TLP) genes in garlic (*Allium sativum* L.): Genome-wide identification, characterization, and expression in response to *Fusarium proliferatum* infection. *Plants,* 11**,** 748. doi: 10.3390/plants11060748.

ARDESTANI, S. T., KHODAPARAST, S. A., MOGHADDAM, A. A., GHANAVATI, F. & DARSARAEI, H. 2020. First report of powdery mildew caused by *Golovinomyces bolayi* on okra (*Abelmoschus esculentus*). *Australasian Plant Disease Notes,* 15**,** 1-5. doi: 10.1007/s13314-020-00396-7.

ATANASOVA, L., CROM, S. L., GRUBER, S., COULPIER, F., SEIDL-SEIBOTH, V., KUBICEK, C. P. & DRUZHININA, I. S. 2013. Comparative transcriptomics reveals different strategies of *Trichoderma* mycoparasitism. *BMC genomics,* 14**,** 121. doi: 10.1186/1471-2164-14-121.

AVGERI, I., ZELIOU, K., PETROPOULOS, S. A., BEBELI, P. J., PAPASOTIROPOULOS, V. & LAMARI, F. N. 2020. Variability in bulb organosulfur compounds, sugars, phenolics, and pyruvate among greek garlic genotypes: Association with antioxidant properties. *Antioxidants,* 9**,** 967. doi: 10.3390/antiox9100967.

AWASTHI, L. 2015. *Recent advances in the diagnosis and management of plant diseases*, L. P. Awasthi. doi: 10.1007/978-81-322-2571-3.

BAKHSHI, B., MALLA, S. & LOKESH, S. 2023. Monitoring of Defense Enzymes (Phenylalanine Ammonia Lyase and Peroxidase) in Magnaporthe oryzae Infected Leaves after Treatment with Green Synthesized Silver Nanoparticles. *Indian J. Pharm. Educ. Res,* 57**,** 141-146. doi: 10.5530/001954642708.

BAKONYI, J., VAJNA, L., SZEREDI, A., TÍMÁR, E., KOVÁCS, G., CSŐSZ, M. & VARGA, A. 2011. First report of *Sclerotium cepivorum* causing white rot of garlic in Hungary. *New Disease Reports,* 23**,** 2044-0588.2011. doi: 10.5197/j.2044-0588.2011.023.005.

BALA, S., ASTHIR, B. & BAINS, N. 2016. Syringaldazine peroxidase stimulates lignification by enhancing polyamine catabolism in wheat during heat and drought stress. *Cereal Research Communications,* 44**,** 561-571. doi: 10.1556/0806.44.2016.028.

BALOGUN, O. & BABATOLA, J. 1999. Effect of plant age and injury on the pathogenicity of *Choanephora cucurbitarum* in okra *Abelmoschus esculentus* Moench. *Agrosearch,* 5**,** 62-69.

BECKMAN, C. H. 1987. *The nature of wilt diseases of plants*, APS press.

BEHIRY, S. I., AL-ASKAR, A. A., SOLIMAN, S. A., ALOTIBI, F. O., BASILE, A., ABDELKHALEK, A., ELSHARKAWY, M. M., SALEM, M. Z., HAFEZ, E. E. & HEFLISH, A. A. 2022. Plantago lagopus extract as a green fungicide induces systemic resistance against *Rhizoctonia* root rot disease in tomato plants. *Frontiers in Plant Science,* 13**,** 966929. doi: 10.3389/fpls.2022.966929.

BELL, D., WELLS, H. & MARKHAM, C. 1982. *In vitro* antagonism of *Trichoderma* species against six fungal plant pathogens. *Phytopathology,* 72**,** 379-382.

BENKEBLIA, N. 2005. Free-radical scavenging capacity and antioxidant properties of some selected onions (*Allium cepa* L.) and garlic (*Allium sativum* L.) extracts. *Brazilian archives of biology and technology,* 48**,** 753-759. doi: 10.1590/S1516-89132005000600011.

BOLIE, H., NDONGO, B., NGATSI, P. Z., KUATE, W. N. T., DIDA, S. L. L., ESSOGUE ETAME, A., ESSOMÉ, C. S. & TONFACK, L. B. 2021. Antifungal activity of *Annona muricata* seed extracts against *Cercospora malayensis*, causal agent of cercospora leaf spot disease of okra (*Abelmoschus esculentus* L.). *International Journal of Pathogen Research,* 6**,** 12-24. doi: 10.9734/ijpr/2021/v6i430167.

BOLTON, M. D., THOMMA, B. P. & NELSON, B. D. 2006. *Sclerotinia sclerotiorum* (Lib.) de Bary: biology and molecular traits of a cosmopolitan pathogen. *Molecular plant pathology,* 7**,** 1-16. doi: 10.1111/j.1364-3703.2005.00316.x.

BORGES, N. O., DA SILVA SOLINO, A. J., FRANSCISCHINI, R., CAMPOS, H. D., OLIVEIRA, J. S. B. & SCHWAN-ESTRADA, K. R. F. 2022. Induction of soybean resistance mechanisms to anthracnose by biocontrol agents. *Revista Caatinga,* 35**,** 265-275. doi: 10.1590/1983-21252022v35n203rc.

BROWN, W. 1924. II. A method of isolating single strains of fungi by cutting out a hyphal tip. *Annals of Botany,* 38**,** 402-404.

ÇALıŞıR, S., ÖZCAN, M., HACıSEFEROĞULLARı, H. & YıLDıZ, M. U. 2005. A study on some physico-chemical properties of Turkey okra (*Hibiscus esculenta* L.) seeds. *Journal of Food Engineering,* 68**,** 73-78. doi: 10.1016/j.jfoodeng.2004.05.023.

CANIHOS, Y., PEEVER, T. & TIMMER, L. 1999. Temperature, leaf wetness, and isolate effects on infection of *Minneola tangelo* leaves by *Alternaria* sp. *Plant Disease,* 83**,** 429-433. doi: 10.1094/PDIS.1999.83.5.429.

CAO, F., LIU, F., GUO, H., KONG, W., ZHANG, C. & HE, Y. 2018. Fast detection of *Sclerotinia sclerotiorum* on oilseed rape leaves using low-altitude remote sensing technology. *Sensors,* 18**,** 4464. doi: 10.3390/s18124464.

CAWOY, H., DEBOIS, D., FRANZIL, L., DE PAUW, E., THONART, P. & ONGENA, M. 2015. Lipopeptides as main ingredients for inhibition of fungal phytopathogens by *B acillus subtilis/amyloliquefaciens*. *Microbial biotechnology,* 8**,** 281-295. doi: 10.1111/1751-7915.12238.

CHAMBERLIN, K. D. & PUPPALA, N. 2018. Genotyping of the Valencia peanut core collection with a molecular marker associated with *Sclerotinia* blight resistance. *Peanut Science,* 45**,** 12-18. doi: 10.3146/ps17-15.1.

CHANCE, B. & MAEHLY, A. C. 1955. Assay of catalases and peroxidases. *Methods in Enzymology.* doi: 10.1016/S0076-6879(55)02300-8.

CHANG, H. X., SANG, H., WANG, J., MCPHEE, K. E., ZHUANG, X., PORTER, L. D. & CHILVERS, M. I. 2018. Exploring the genetics of lesion and nodal resistance in pea (*Pisum sativum* L.) to *Sclerotinia sclerotiorum* using genome-wide association studies and RNA-Seq. *Plant Direct,* 2**,** e00064. doi: 10.1002/pld3.64.

CHARRIER, A. 1984. Genetic resources of the genus *Abelmoschus* Med.(Okra). *IBPGR (Rome, Italy)*.

CHO, J. & MOON, B. 1980. The occurrence of strawberry black leaf spot caused by *Alternaria alternata* (Fr.) Keissler in Korea. *Korean Journal of Plant Protection,* 19**,** 221-227.

CHOI, I.-Y., KIM, J.-H., KIM, J., HAN, K.-S., GALEA, V. & SHIN, H.-D. 2017. Confirmation of *Sclerotinia sclerotiorum* as the causal agent of stem rot of stock in Korea. *Australasian Plant Disease Notes,* 12**,** 22. doi: 10.1007/s13314-017-0247-4.

COLEY-SMITH, J. 1987. *Sclerotium cepivorum* Berk. *European Handbook of Plant Diseases,(eds IM Smith, J. Dunez DH, Phillips RA Lelliot and SA Archer) Blackwell Scientific Publications***,** 446-447.

COLEY-SMITH, J. & ENTWISTLE, A. 1988. Susceptibility of cultivars of garlic to *Sclerotium cepivorum*. *Plant pathology,* 37**,** 261-264. doi: 10.1111/j.1365-3059.1988.tb02071.x.

COŞKUNTUNA, A. & ÖZER, N. 2008. Biological control of onion basal rot disease using *Trichoderma harzianum* and induction of antifungal compounds in onion set following seed treatment. *Crop protection,* 27**,** 330-336. doi: 10.1016/j.cropro.2007.06.002.

CROWE, F. 2000. Management of Fungal Diseases in Onion and Garlic. *1PM in Oregon: Achievements and Future Directions***,** 172.

CROWE, F., HALL, D., GREATHEAD, A. & BAGHOTT, K. 1980. Inoculum density of *Sclerotium cepivorum* and the incidence of white rot of onion and garlic. *Phytopathology,* 70**,** 64-69.

CUI, W., HE, P., MUNIR, S., HE, P., HE, Y., LI, X., YANG, L., WANG, B., WU, Y. & HE, P. 2019. Biocontrol of soft rot of Chinese cabbage using an endophytic bacterial strain. *Frontiers in microbiology,* 10**,** 1471. doi: 10.3389/fmicb.2019.01471.

DAHIVELKAR, P., ATRE, G., GAWANDE, P. & MATE, G. 2017. Management of powdery mildew of okra caused by *Erysiphe cichoracearum*. *Int. J. Curr. Microbiol. App. Sci,* 6**,** 3183-3189. doi: 10.20546/ijcmas.2017.606.380.

DE SANTIS, D., GARZOLI, S. & VETTRAINO, A. M. 2021. Effect of gaseous ozone treatment on the aroma and clove rot by *Fusarium proliferatum* during garlic postharvest storage. *Heliyon,* 7. doi: 10.1016/j.heliyon.2021.e06634.

DELGADILLO-SÁNCHEZ, F., HEREDIA-ZEPEDA, A., ZAVALETA-MEJÍA, E., GONZÁLEZ-HERNÁNDEZ, V., TORRES-PACHECO, I., NIETO-ÁNGEL, D. & OSADA-KAWASOE, S. 2001. Susceptibility of different garlic (*Allium sativum* L.) types to *Sclerotium cepivorum* Berk. *Revista Chapingo Serie Horticultura,* 7**,** 171-176. doi: 10.5154/r.rchsh.1999.09.060.

DELGADO-ORTIZ, J. C., OCHOA-FUENTES, Y. M., CERNA-CHÁVEZ, E., BELTRÁN-BEACHE, M., RODRÍGUEZ-GUERRA, R., AGUIRRE-URIBE, L. A. & VÁZQUEZ-MARTÍNEZ, O. 2016. *Fusarium* species associated with basal rot of garlic in North Central Mexico and its pathogenicity. *Revista Argentina de Microbiología,* 48**,** 222-228. doi: 10.1016/j.ram.2016.04.003.

DERBYSHIRE, M. & DENTON-GILES, M. 2016. The control of sclerotinia stem rot on oilseed rape (*Brassica napus*): current practices and future opportunities. *Plant Pathology,* 65**,** 859-877. doi: 10.1111/ppa.12517.

DESJARDINS, A. 2006. Fusarium mycotoxins: chemistry, genetics and biology. *The Journal of Agricultural Science,* 145. doi: 10.1017/S0021859607007162.

DILBO, C., ALEMU, M., LENCHO, A. & HUNDUMA, T. 2015. Integrated management of garlic white rot (*Sclerotium cepivorum* Berk) using some fungicides and antifungal *Trichoderma* species. *Journal of Plant Pathology & Microbiology,* 6**,** 1. doi: 10.4172/2157-7471.1000251.

DING, Y., MEI, J., CHAI, Y., YANG, W., MAO, Y., YAN, B., YU, Y., DISI, J. O., RANA, K. & LI, J. 2020. *Sclerotinia sclerotiorum* utilizes host-derived copper for ROS detoxification and infection. *PLoS Pathogens,* 16**,** e1008919. doi: 10.1371/journal.ppat.1008919.

EL-SHESHTAWI, M., EL-GAZZAR, T. & SAAD, A. S. 2009. Comparative study between chemical and non-chemical control against *Sclerotium cepivorum*, the casual white rot of onion under Egyptian conditions. *Journal of Plant Protection and Pathology,* 34**,** 2169-2182.

EL BARNOSSI, A., MOUBCHIR, T., BENIAICH, G., SAGHROUCHNI, H., ALLALI, A. & HOUSSEINI, A. I. 2024. Isolation, conventional and molecular identification of *Fusarium proliferatum* responsible to bulb rot of garlic and potential biological control by new bacterial strains. *Journal of Biology and Biomedical Research (ISSN: 3009-5522),* 1**,** 1-9. doi: 10.69998/j2br.v1i1.5.

ELENANY, A. M., ATIA, M. M. M., ABBAS, E. E., MOUSTAFA, M., ALSHAHARNI, M. O., NEGM, S. & ELNAHAL, A. S. M. A. 2024. Nanoparticles and chemical inducers: A sustainable shield against onion white rot. *Biology,* 13**,** 219. doi: 10.3390/biology13040219.

ELSHAHAWY, I., SAIED, N., ABD-EL-KAREEM, F. & MORSY, A. 2019. Effect of inoculum density of *Stromatinia cepivora* on the amount of white rot reduced by *Trichoderma* species in garlic. *Bulletin of the National Research Centre,* 43**,** 27. doi: 10.1186/S42269-019-0064-3.

ELSHAHAWY, I. E. & MARREZ, D. A. 2024. Antagonistic activity of *Trichoderma asperellum* against *Fusarium* species, chemical profile and their efficacy for management of *Fusarium*-root rot disease in dry bean. *Pest Management Science,* 80**,** 1153-1167. doi: 10.1002/ps.7846.

ELSHAHAWY, I. E., OSMAN, S. A. & ABD-EL-KAREEM, F. 2021. Protective effects of silicon and silicate salts against white rot disease of onion and garlic, caused by *Stromatinia cepivora*. *Journal of Plant Pathology,* 103**,** 27-43. doi: 10.1007/s42161-020-00685-1.

ELSHAHAWY, I. E. & SAIED, N. M. 2021. Reduced sclerotial viability of *Stromatinia cepivora* and control of white rot disease of onion and garlic by means of soil bio-solarization. *European Journal of Plant Pathology,* 160**,** 519-540. doi: 10.1007/s10658-021-02260-5.

EPPO (EUROPEAN AND MEDITERRANEAN PLANT PROTECTION ORGANIZATION). nd. *EPPO Global Database* [Online]. Available: https://gd.eppo.int/ [Accessed August 11 2024].

ESLER, G. & COLEY-SMITH, J. 1984. Resistance to *Sclerotium cepivorum* in *Allium* and other genera. *Plant pathology,* 33**,** 199-204. doi: 10.1111/j.1365-3059.1984.tb02640.x.

ESTÉVEZ-GEFFRIAUD, V., VICENTE, R., VERGARA-DÍAZ, O., NARVÁEZ REINALDO, J. J. & TRILLAS, M. I. 2020. Application of *Trichoderma asperellum* T34 on maize (Zea mays) seeds protects against drought stress. *Planta,* 252**,** 8. doi: 10.1007/s00425-020-03404-3.

FAN, H., YANG, W., NIE, J., ZHANG, W., WU, J., WU, D. & WANG, Y. 2021. A novel effector protein SsERP1 inhibits plant ethylene signaling to promote *Sclerotinia sclerotiorum* infection. *Journal of Fungi,* 7**,** 825. doi: 10.3390/jof7100825.

FANG, X.-L., ZHANG, C.-X. & NAN, Z.-B. 2019. Research advances in *Fusarium* root rot of alfalfa (*Medicago sativa*). *Acta Prataculturae Sinica,* 28**,** 169. doi: 10.3389/fmicb.2021.664385.

FANG, X., ZHANG, C., WANG, Z., DUAN, T., YU, B., JIA, X., PANG, J., MA, L., WANG, Y. & NAN, Z. 2021. Co-infection by soil-borne fungal pathogens alters disease responses among diverse alfalfa varieties. *Frontiers in microbiology,* 12**,** 664385. doi: 10.3389/fmicb.2021.664385.

FAOSTAT. 2021. *Crop data* [Online]. Available: http://www.fao.org/faostat/en/ [Accessed May 12 2024].

FAOSTAT. 2022. *Production: Crops and livestock products: World, Production Quantity, Okra, 2022 (from pick lists)* [Online]. Food and Agriculture Organization. Available: https://www.fao.org/faostat/en/#data/QCL [Accessed 19 September 2024].

FAOSTAT. 2023. *Crops and livestock products (garlic)* [Online]. Available: https://www.fao.org/faostat/en/ [Accessed 09 March 2025].

FILYUSHIN, M. A., ANISIMOVA, O. K., KOCHIEVA, E. Z. & SHCHENNIKOVA, A. V. 2021. Genome-wide identification and expression of chitinase class I genes in garlic (*Allium sativum* L.) cultivars resistant and susceptible to *Fusarium proliferatum*. *Plants,* 10**,** 720. doi: 10.3390/plants10040720.

FILYUSHIN, M. A., ANISIMOVA, O. K., SHCHENNIKOVA, A. V. & KOCHIEVA, E. Z. 2023. Genome-wide identification, expression, and response to *Fusarium* infection of the SWEET gene family in garlic (*Allium sativum* L.). *International Journal of Molecular Sciences,* 24**,** 7533. doi: 10.3390/ijms24087533.

FONG, H. H. 2002. Integration of herbal medicine into modern medical practices: issues and prospects. *Integrative cancer therapies,* 1**,** 287-293.

FRADIN, E. F. & THOMMA, B. P. 2006. Physiology and molecular aspects of *Verticillium* wilt diseases caused by V. dahliae and *V. albo-atrum*. *Molecular plant pathology,* 7**,** 71-86.

FRITSCH, R. & FRIESEN, N. 2002. Evolution, domestication and taxonomy. *Allium crop science: recent advances.* CABI publishing Wallingford UK.

FUGRO, P. 1999. A new disease of okra (*Abelmoschus esculentus* L.) in India. *Journal of Mycology and Plant Pathology,* 29**,** 264.

FULLERTON, R. & STEWART, A. 1991. Chemical control of onion white rot (*Sclerotium cepivorum* Berk.) in the Pukekohe district of New Zealand. *New Zealand journal of crop and horticultural science,* 19**,** 121-127. doi: 10.1080/01140671.1991.10421789.

GÁLVEZ, L. & PALMERO, D. 2021. Incidence and etiology of postharvest fungal diseases associated with bulb rot in garlic (*Alllium sativum*) in Spain. *Foods,* 10**,** 1063. doi: 10.3390/foods10051063.

GÁLVEZ, L. & PALMERO, D. 2022. Fusarium dry rot of garlic bulbs caused by *Fusarium proliferatum*: A review. *Horticulturae,* 8**,** 628. doi: 10.3390/horticulturae8070628.

GAPPA-ADACHI, R. 2018. Studies on the taxonomy and ecology of pathogenic microorganisms related to the generation of an integrated pest management model for important horticultural crop diseases. *Journal of General Plant Pathology,* 84**,** 435-436. doi: 10.1007/s10327-018-0813-4.

GEORGIOU, C. D., PATSOUKIS, N., PAPAPOSTOLOU, I. & ZERVOUDAKIS, G. 2006. Sclerotial metamorphosis in filamentous fungi is induced by oxidative stress. *Integrative and comparative Biology,* 46**,** 691-712. doi: 10.1093/icb/icj034.

GHIASY-OSKOEE, M. & AGHAALIKHANI, M. 2025. Salt tolerance mechanisms in five *Asteraceae* species: seed germination and seedling growth, cellular damage, enzymatic and

non-enzymatic antioxidants. *Acta Physiologiae Plantarum,* 47**,** 33. doi: 10.1007/s11738-025-03785-6.

GORDON, T. R. 2017. *Fusarium oxysporum* and the *Fusarium* wilt syndrome. *Annual review of phytopathology,* 55**,** 23-39. doi: 10.1146/annurev-phyto-080615-095919.

GRUHLKE, M. C., HEMMIS, B., NOLL, U., WAGNER, R., LÜHRING, H. & SLUSARENKO, A. J. 2015. The defense substance allicin from garlic permeabilizes membranes of *Beta vulgaris*, *Rhoeo discolor*, *Chara corallina* and artificial lipid bilayers. *Biochimica et Biophysica Acta (BBA)-General Subjects,* 1850**,** 602-611. doi: 10.1016/j.bbagen.2014.11.020.

GUETSKY, R., SHTIENBERG, D., ELAD, Y. & DINOOR, A. 2001. Combining biocontrol agents to reduce the variability of biological control. *Phytopathology,* 91**,** 621-627. doi: 10.1094/PHYTO.2001.91.7.621.

GUETSKY, R., SHTIENBERG, D., ELAD, Y., FISCHER, E. & DINOOR, A. 2002. Improving biological control by combining biocontrol agents each with several mechanisms of disease suppression. *Phytopathology,* 92**,** 976-985. doi: 10.1094/PHYTO.2002.92.9.976.

GULATI, R. 2004. Incidence of *Tetranychus cinnabarinus* (Boisd.) Infestation in Different Varieties of *Abelmoschus esculentus* L. *Annals of Plant Protection Sciences,* 12**,** 45-47.

HAHN, D., SONNTAG, J. M., LÜCK, S., MAITZ, M. F., FREUDENBERG, U., JORDAN, R. & WERNER, C. 2021. Poly (2-alkyl-2-oxazoline)-Heparin Hydrogels—Expanding the Physicochemical Parameter Space of Biohybrid Materials. *Advanced Healthcare Materials,* 10**,** 2101327. doi: 10.1002/adhm.202101327.

HAKKAR, A. A., ROSMANA, A. & RAHIM, M. D. 2014. Pengendalian penyakit busuk buah *Phytophthora* pada kakao dengan cendawan endofit *Trichoderma asperellum*. *Jurnal Fitopatologi Indonesia,* 10**,** 139-139. doi: 10.14692/jfi.10.5.139.

HANCI, F. 2018. A comprehensive overview of onion production: Worldwide and Turkey. *Journal of Agriculture and Veterinary Science,* 11**,** 17-27. doi: 10.9790/2380-1109011727.

HAO, J. J., YANG, M. E. & DAVIS, R. M. 2009. Effect of soil inoculum density of *Fusarium oxysporum* f. sp. *vasinfectum* race 4 on disease development in cotton. *Plant disease,* 93**,** 1324-1328. doi: 10.1094/PDIS-93-12-1324.

HAYAT, S., AHMAD, H., ALI, M., HAYAT, K., KHAN, M. A. & CHENG, Z. 2018. Aqueous garlic extract as a plant biostimulant enhances physiology, improves crop quality and metabolite abundance, and primes the defense responses of receiver plants. *Applied Sciences,* 8**,** 1505. doi: 10.3390/app8091505.

HE, Y., PENG, J., JIA, N., WANG, X., MA, J., WANG, H., ZHANG, C., WANG, E., HU, D. & WANG, Z. 2023. *Bacillus velezensis* WSW007 Different Concentrations Volatile Organic Compounds Stimulated Tobacco Growth by Up-regulating the Expression of Genes Related to Plant Growth and Development. doi: 10.21203/rs.3.rs-2871463/v1.

HELGI LIBRARY. 2024. *Garlic Production* [Online]. Available: https://www.helgilibrary.com/indicators/garlic-production/ [Accessed 09 March 2025].

HENZ, G. P., LOPES, C. A. & REIS, A. 2007. A novel postharvest rot of okra pods caused by *Rhizoctonia solani* in Brazil. *Fitopatologia Brasileira,* 32**,** 237-240. doi: 10.1590/S0100-41582007000300008

HERNÁNDEZ-ORTEGA, H. A., FERRERA-CERRATO, R., LÓPEZ-DELGADO, H. A., SÁNCHEZ-RANGEL, J. C. & ALARCÓN, A. 2021. Nutrient status, hydrogen peroxide content and peroxidase activity of arbuscular mycorrhizal plants of *Melilotus albus* grown in diesel-contaminated substrate. *Scientia fungorum,* 51. doi: 10.33885/sf.2021.51.1298.

HERNANDEZ CASTILLO, F., BERLANGA PADILLA, A., GALLEGOS MORALES, G., CEPEDA SILLER, M., RODRIGUEZ HERRERA, R., AGUILAR GONZALES, C. & CASTILLO REYES, F. 2011. *In vitro* antagonist action of *Trichoderma* strains against *Sclerotinia sclerotiorum* and *Sclerotium cepivorum*. doi: 10.3844/ajabssp.2011.410.417.

HERRERA-TÉLLEZ, V. I., CRUZ-OLMEDO, A. K., PLASENCIA, J., GAVILANES-RUÍZ, M., ARCE-CERVANTES, O., HERNÁNDEZ-LEÓN, S. & SAUCEDO-GARCÍA, M. 2019. The protective effect of *Trichoderma asperellum* on tomato plants against *Fusarium oxysporum* and *Botrytis cinerea* diseases involves inhibition of reactive oxygen species production. *International journal of molecular sciences,* 20**,** 2007. doi: 10.3390/ijms20082007.

HONG, M.-K., KIM, K.-J. & YANG, Y.-J. 2007. Inhibitory Effect of β-glucosidase Inhibitor Isolated from *Bacillus lentimorbus* B-6 on the Polyphenol Oxidase Purified from Peeled Garlic. *Horticulture Environment and Biotechnology* 48**,** 349-353.

HOSSAIN, M. M., SULTANA, F., LI, W., TRAN, L.-S. P. & MOSTOFA, M. G. 2023. *Sclerotinia sclerotiorum* (Lib.) de Bary: Insights into the pathogenomic features of a global pathogen. *Cells,* 12**,** 1063. doi: 10.3390/cells12071063.

INFANTINO, A., TAITI, C., GROTTOLI, A., MANCUSO, S., COSTA, C. & GARZOLI, S. 2023. Examination of Volatile Signatures of *Fusarium* Bulb Rot in Garlic Using Proton-Transfer-Reaction Time-of-Flight Mass Spectrometry and Solid-Phase Microextraction Gas Chromatography/Mass Spectrometry. *Separations,* 10**,** 556. doi: 10.3390/separations10110556.

JANNATUN, N., FATEMA, B., MD, R., HABIBA, U. & MORSHED, M. 2020. Screening of selected garlic varieties against *Fusarium* rot caused by *Fusarium proliferatum*. *SSRG Int J Agric Environ Sci,* 7**,** 23-32.

JI, H., YU, R., LIU, H., ZHANG, H., WANG, X., CHEN, J. & LI, Y. 2023. Metabolic features of a novel *Trichoderma asperellum* YNQJ1002 with potent antagonistic activity against *Fusarium graminearum*. *Metabolites,* 13**,** 1144. doi: 10.3390/metabo13111144.

JISKANI, M. 2006. Okra diseases and IPDM. *J. Plant Pathol,* 4**,** 32.

JUKTE, S., BADGUJAR, S., SURYAWANSHI, A., UTPAL, D. & KULDHAR, D. 2016. Symptomatology, isolation, identification and pathogenicity test of damping off disease in okra. *International Journal of Plant Protection,* 9**,** 358-361.

KAR, M. & MISHRA, D. 1976. Catalase, peroxidase, and polyphenoloxidase activities during rice leaf senescence. *Plant physiology,* 57**,** 315-319. doi: 10.1104/pp.57.2.315.

KARA, M., SOYLU, S., GÜMÜŞ, Y., SOYLU, E. M., UYSAL, A. & KURT, Ş. 2023. Determination of *in Vitro* Biocontrol Potentials of Antagonist Bacterial Isolates Against Onion Basal and Root Rot Disease Agent *Fusarium proliferatum*. *Int. J. Innov. Approaches Agric. Res,* 7**,** 487-497. doi: 10.29329/ijiaar.2023.630.10.

KARSOU, B. & SAMARA, R. 2021. Plant extracts inducing enzyme activity in grains against loose smut disease. doi: 10.2478/sab-2021-0006.

KELTY, M. T., MIRON-OCAMPO, A. & BEATTIE, S. R. 2024. A series of pyrimidine-based antifungals with anti-mold activity disrupt ER function in *Aspergillus fumigatus*. *Microbiology spectrum,* 12**,** e01045-24. doi: 10.1128/spectrum.01045-24.

KENDALL, C. W. & JENKINS, D. J. 2004. A dietary portfolio: maximal reduction of low-density lipoprotein cholesterol with diet. *Current atherosclerosis reports,* 6**,** 492-498. doi: 10.1007/s11883-004-0091-9.

KHORRAMI, S. K., JAMEI, R. & KOUPAEI, S. J. T. 2014. UV radiation induced changes of Phenolic compounds and antioxidant enzymes in Okra (*Hibiscus esculents* L.) seedlings. *J. Plant Physiol. Breed.,* 4**,** 23-33.

KING, J. & COLEY-SMITH, J. 1969. Production of volatile alkyl sulphides by microbial degradation of synthetic alliin and alliin-like compounds, in relation to germination of sclerotia of *Sclerotium cepivorum* Berk. *Annals of Applied Biology,* 64**,** 303-314. doi: 10.1111/j.1744-7348.1969.tb02880.x.

KOCHLAR, S. 1986. *Tropical crops*, McMillian Publisher Ltd., London and Basingtone.

KOSTELAC, A., TABORDA, A., MARTINS, L. O. & HALTRICH, D. 2024. Evolution and separation of actinobacterial pyranose and C-glycoside-3-oxidases. *Applied and Environmental Microbiology,* 90**,** e01676-23. doi: 10.1128/aem.01676-23.

KOVAROVIČ, J., BYSTRICKA, J., VOLLMANNOVÁ, A., TÓTH, T. & BRINDZA, J. 2019. Biologically valuable substances in garlic (*Allium sativum* L.)–A review. *Journal of Central European Agriculture,* 20**,** 292-304. doi: 10.5513/JCEA01/20.1.2304.

KUMAR, A., KUMAR, P. & NADENDLA, R. 2013. A review on: *Abelmoschus esculentus* (Okra). *International Research Journal of Pharmaceutical and Applied Sciences,* 3**,** 129-132.

KUMAR, R., PATIL, M., PATIL, S. R. & PASCHAPUR, M. S. 2009. Evaluation of *Abelmoschus esculentus* mucilage as suspending agent in paracetamol suspension. *International Journal of PharmTech Research,* 1**,** 658-665.

KUMAR, S., DAGNOKO, S., HAOUGUI, A., RATNADASS, A., PASTERNAK, N. & KOUAME, C. 2010. Okra (*Abelmoschus* spp.) in West and Central Africa: Potential and progress on its improvement. *African Journal of Agricultural Research,* 5**,** 3590-3598.

LAMICHHANE, J. R. & VENTURI, V. 2015. Synergisms between microbial pathogens in plant disease complexes: a growing trend. *Frontiers in plant science,* 6**,** 141048. doi: 10.3389/fpls.2015.00385.

LE, D., AUDENAERT, K. & HAESAERT, G. 2021. *Fusarium* basal rot: profile of an increasingly important disease in *Allium* spp. *Tropical Plant Pathology,* 46**,** 241-253. doi: 10.1007/s40858-021-00421-9.

LEE, S.-Y., LEE, S.-B., KIM, Y. & HWANG, S. J. 2006. Biological control of garlic white rot accused by *Sclereotium cepivorum* and *Sclereotium* sp. using *Bacillus subtilis* 122 and *Trichoderma harzianum* 23. *Res Plant Dis,* 12**,** 81-84. doi: 10.5423/RPD.2006.12.2.081.

LEE, S. H., KIM, I. S. & KIM, Y. C. 2014. Identification and characterization of novel biocontrol bacterial strains. *Research in Plant Disease,* 20**,** 182-188. doi: 10.5423/rpd.2014.20.3.182.

LENGSFELD, C., TITGEMEYER, F., FALLER, G. & HENSEL, A. 2004. Glycosylated compounds from okra inhibit adhesion of *Helicobacter pylori* to human gastric mucosa. *Journal of Agricultural and Food Chemistry,* 52**,** 1495-1503.

LESLIE, J. F. & SUMMERELL, B. A. 2006. *The Fusarium laboratory manual*, John Wiley & Sons. doi: 10.1002/9780470278376.

LEYRONAS, C., CHRÉTIEN, P. L., TROULET, C., DUFFAUD, M., VILLENEUVE, F., MORRIS, C. E. & HUNYADI, H. 2018. First report of *Fusarium proliferatum* causing garlic clove rot in France. *Plant Dis,* 102**,** 2658. doi: 10.1094/PDIS-06-18-0962-PDN.

LI, T., GONG, L., WANG, Y., CHEN, F., GUPTA, V. K., JIAN, Q., DUAN, X. & JIANG, Y. 2017. Proteomics analysis of *Fusarium proliferatum* under various initial pH during fumonisin production. *Journal of proteomics,* 164**,** 59-72. doi: 10.1016/j.jprot.2017.05.008.

LIN, Y.-C., LIU, H.-H., TSENG, M.-N. & CHANG, H.-X. 2023. Heritability and gene functions associated with sclerotia formation of *Rhizoctonia solani* AG-7 using whole genome sequencing and genome-wide association study. *Microbial Genomics,* 9**,** 000948. doi: 10.1099/mgen.0.000948.

LISZKA, J., DYMIŃSKA, L., ŁABA, W. & WRÓBEL-KWIATKOWSKA, M. 2025. The Influence of the Non-Pathogenic *Fusarium oxysporum* Fo47 Strain on Flax Resistance to Pathogens. *International Journal of Molecular Sciences,* 26**,** 4396. doi: 10.3390/ijms26094396.

LIU, I.-M., LIOU, S.-S., LAN, T.-W., HSU, F.-L. & CHENG, J.-T. 2005. Myricetin as the active principle of *Abelmoschus moschatus* to lower plasma glucose in streptozotocin-induced diabetic rats. *Planta medica,* 71**,** 617-621. doi: 10.1055/s-2005-871266.

LIU, J., ZHOU, T., HE, D., LI, X.-Z., WU, H., LIU, W. & GAO, X. 2011. Functions of lipopeptides bacillomycin D and fengycin in antagonism of *Bacillus amyloliquefaciens* C06 towards *Monilinia fructicola*. *Journal of Molecular Microbiology and Biotechnology,* 20**,** 43-52. doi: 10.1159/000323501.

LLAMAS, D. P., PATÓN, L. G., DÍAZ, M. G., SERNA, J. G. & SÁEZ, S. B. 2013. The effects of storage duration, temperature and cultivar on the severity of garlic clove rot caused by *Fusarium proliferatum*. *Postharvest Biology and Technology,* 78**,** 34-39. doi: 10.1016/j.postharvbio.2012.12.003.

LOURENÇO JR, V., VIEIRA, B. S., LOPES, E. A. & VILLALTA, O. N. 2018. Etiology, epidemiology, and management of white rot on onion and garlic: Current knowledge and future directions for Brazil. *Científica,* 46**,** 241-256. doi: 10.15361/1984-5529.2018V46N3P241-256.

LUGTENBERG, B. & KAMILOVA, F. 2009. Plant-growth-promoting rhizobacteria. *Annual review of microbiology,* 63**,** 541-556. doi: 10.1146/annurev.micro.62.081307.162918.

MA, Y., LI, Y., YANG, S., LI, Y. & ZHU, Z. 2023. Biocontrol potential of *Trichoderma asperellum* strain 576 against *Exserohilum turcicum* in *Zea mays*. *Journal of Fungi,* 9**,** 936. doi: 10.3390/jof9090936.

MAIA, F. G. M., DE PAULA FREITAS, M., MAIA, J. B., ARMESTO, C. & DA COSTA GONTIJO, P. 2024. Reaction of *Coffea arabica* seedlings to colonization by wild *Colletotrichum gloeosporioides* and transformed with gfp. *REVISTA DE AGRICULTURA NEOTROPICAL,* 11. doi: 10.32404/rean.v11i4.8365.

MAMOUEI, Z., ALQARIHI, A., SINGH, S., XU, S., MANSOUR, M. K., IBRAHIM, A. S. & UPPULURI, P. 2018. Alexidine dihydrochloride has broad-spectrum activities against diverse fungal pathogens. *Msphere,* 3. doi: 10.1128/msphere.00539-18.

MANANDHAR, H. K., TIMILA, R. D., SHARMA, S., JOSHI, S., MANANDHAR, S., GURUNG, S. B., STHAPIT, S., PALIKHEY, E., PANDEY, A. & JOSHI, B. 2016. A field guide for identification and scoring methods of diseases in the mountain crops of Nepal. *Bioversity International***,** 186.

MARCHETTO, K. M. & POWER, A. G. 2018. Coinfection timing drives host population dynamics through changes in virulence. *The American Naturalist,* 191**,** 173-183. doi: 10.1086/695316.

MARTINS, N., PETROPOULOS, S. & FERREIRA, I. C. 2016. Chemical composition and bioactive compounds of garlic (*Allium sativum* L.) as affected by pre-and post-harvest conditions: A review. *Food chemistry,* 211**,** 41-50. doi: 10.1016/j.foodchem.2016.05.029.

MATSUURA, H. 2001. Saponins in garlic as modifiers of the risk of cardiovascular disease. *The Journal of nutrition,* 131**,** 1000S-1005S. doi: 10.1093/jn/131.3.1000S.

MATUO, T., MIYAGAWA, M. & SAITO, H. 1986. *Fusarium oxysporum* f. sp. garlic nf sp. causing basal rot of garlic. *Japanese Journal of Phytopathology,* 52**,** 860-864. doi: 10.3390/horticulturae8070628.

MAYER, Z., DUC, N. H., SASVÁRI, Z. & POSTA, K. 2017. How arbuscular mycorrhizal fungi influence the defense system of sunflower during different abiotic stresses. *Acta Biologica Hungarica,* 68**,** 376-387. doi: 10.1556/018.68.2017.4.4.

MEDINA, Á., GONZÁLEZ-JARTÍN, J. M. & SAINZ, M. J. 2017. Impact of global warming on mycotoxins. *Current Opinion in Food Science,* 18**,** 76-81. doi: 10.1016/j.cofs.2017.11.009.

MEENA, R., GHASOLIA, R., CHAND, K., BUNKER, R. R. & YADAV, S. L. 2024a. Management of Root Rot (*Rhizoctonia solani*) of Okra Through Novel Combined

Formulations of Fungicides. *Journal of Experimental Agriculture International,* 46**,** 474-484. doi: 10.9734/jeai/2024/v46i102971.

MEENA, R., GHASOLIA, R., GODIKA, S., CHAND, K., BUNKER, R. R. & YADAV, P. D. 2024b. Reaction of Okra (*Abelmoschus esculentus*) Genotypes against Rhizoctonia solani Inciting Root Rot Disease. *Journal of Experimental Agriculture International,* 46**,** 436-441. doi: 10.9734/jeai/2024/v46i102966.

MILJAKOVIĆ, D., MARINKOVIĆ, J. & BALEŠEVIĆ-TUBIĆ, S. 2020. The significance of *Bacillus* spp. in disease suppression and growth promotion of field and vegetable crops. *Microorganisms,* 8**,** 1037. doi: 10.3390/microorganisms8071037.

MIMMA, A. A., AKTER, T., HAQUE, M. A., BHUIYAN, M. A. B., CHOWDHURY, M. Z. H., SULTANA, S. & ISLAM, S. M. N. 2023. Effect of *Metarhizium anisopliae* (MetA1) on growth enhancement and antioxidative defense mechanism against *Rhizoctonia* root rot in okra. *Heliyon,* 9. doi: 10.1016/j.heliyon.2023.e18978.

MISHRA, R., ADHOLEYA, A. & SARDANA, H. 2012. *Integrated Pest Management: strategies for onion and garlic*, The Energy and Resources Institute (TERI).

MISHRA, R., JAISWAL, R., KUMAR, D., SAABALE, P. & SINGH, A. 2014. Management of major diseases and insect pests of onion and garlic: A comprehensive review. *Journal of Plant Breeding and Crop Science,* 6**,** 160-170. doi: 10.5897/JPBCS2014.0467.

MOHAMMADI, M. & KAZEMI, H. 2002. Changes in peroxidase and polyphenol oxidase activities in susceptible and resistant wheat heads inoculated with *Fusarium graminearum* and induced resistance. *Plant Science,* 162**,** 491-498. doi: 10.1016/S0168-9452(01)00538-6.

MOHARAM, M. H., ASRAN, M. R. & GHANEM, S. A. 2023. Factors affecting the infection by *Fusarium oxysporum* and *F. proliferatum* and the progress of garlic clove rot disease during storage. *Journal of Sohag Agriscience (JSAS),* 8**,** 77-84. doi: 10.21608/jsasj.2023.316186.

MOHARAM, M. H., FARRAG, E. S. & MOHAMED, M. D. 2013. Pathogenic fungi in garlic seed cloves and first report of *Fusarium proliferatum* causing cloves rot of stored bulbs in upper Egypt. *Archives of Phytopathology and Plant Protection,* 46**,** 2096-2103. doi: 10.1080/03235408.2013.785122.

MOHY, S., ELAMEEN, T., KHALAPHALLAH, R. & HASSAN, N. M. 2024. Biological control of garlic white and basal rot pathogens in vitro and under field conditions. *SVU-International Journal of Agricultural Sciences,* 6**,** 12-23. doi: 10.21608/svuijas.2024.319563.1393.

MONDANI, L., CHIUSA, G. & BATTILANI, P. 2021. Fungi associated with garlic during the cropping season, with focus on *Fusarium proliferatum* and *F. oxysporum*. *Plant health progress,* 22**,** 37-46. doi: 10.1094/PHP-06-20-0054-RS.

MONDANI, L., CHIUSA, G. & BATTILANI, P. 2022. Efficacy of chemical and biological spray seed treatments in preventing garlic dry rot. *Phytopathologia Mediterranea,* 61**,** 27-37. doi: 10.36253/phyto-13103.

MU, F., XIA, J., JIA, J., JIANG, D., ZHANG, B., FU, Y., CHENG, J. & XIE, J. 2025. Exploring the interaction between endornavirus and *Sclerotinia sclerotiorum*: mechanisms of phytopathogenic fungal virulence and antivirus. *mBio,* 16**,** e03365-24. doi: 10.1128/mbio.03365-24.

NÁJERA, J. F. D., SERNA, S. A., HERNÁNDEZ, M. V., VELÁZQUEZ, A. D. S., APARICIO, C. M. C. & MALDONADO, G. A. E. 2022. Effectiveness of biological, botanical and synthetic products in the control of onion (*Allium cepa*) wilt caused by *Fusarium* sp. Resources for integrated management. *Steviana,* 14**,** 44-54. doi: 10.56152/StevianaFacenV14N1A4_2022.

NAVEED, A., KHAN, A. A. & KHAN, I. A. 2009. Generation mean analysis of water stress tolerance in okra (*Abelmoschus esculentu*s L.). *Pak. J. Bot,* 41**,** 195-205.

NDOYE FOE, F. M.-C., TCHINANG, T. F. K., NYEGUE, A. M., ABDOU, J.-P., YAYA, A. J. G., TCHINDA, A. T., ESSAME, J.-L. O. & ETOA, F.-X. 2016. Chemical composition, in vitro antioxidant and anti-inflammatory properties of essential oils of four dietary and medicinal plants from Cameroon. *BMC complementary and alternative medicine,* 16**,** 1-12. doi: 10.1186/s12906-016-1096-y.

NIU, G., ANNAMALAI, T., WANG, X., LI, S., MUNGA, S., NIU, G., TSE-DINH, Y.-C. & LI, J. 2020. A diverse global fungal library for drug discovery. *PeerJ,* 8**,** e10392. doi: 10.7717/peerj.10392.

OSMAN, H. E., NEHELA, Y., ELZAAWELY, A. A., EL-MORSY, M. H. & EL-NAGAR, A. 2023. Two bacterial bioagents boost onion response to *Stromatinia cepivora* and promote growth and yield via enhancing the antioxidant Defense System and Auxin Production. *Horticulturae,* 9**,** 780. doi: 10.3390/horticulturae9070780.

OUNIS, S., TURÓCZI, G. & KISS, J. 2025. Co-Occurrence of *Stromatinia cepivora* and *Fusarium proliferatum* Fungi on Garlic: *In Vitro* Investigation of Pathogen–Pathogen Interactions and *In Planta* Screening for Resistance of Garlic Cultivars. *Plants,* 14**,** 440. doi: 10.3390/plants14030440.

PALMERO, D., DE CARA, M., IGLESIAS, C., MORENO, M., GONZALEZ, N. & TELLO, J. 2010. First report of *Fusarium proliferatum* causing rot of garlic bulbs in Spain. *Plant disease,* 94**,** 277-277. doi: 10.1094/PDIS-94-2-0277C.

PALMERO, D., DE CARA, M., NOSIR, W., GÁLVEZ, L., CRUZ, A., WOODWARD, S., GONZÁLEZ-JAÉN, M. T. & TELLO, J. C. 2012. *Fusarium proliferatum* isolated from garlic in Spain: Identification, toxigenic potential and pathogenicity on related *Allium* species. *Phytopathologia Mediterranea***,** 207-218. doi: 10.14601/PHYTOPATHOL_MEDITERR-10341.

PARK, J. H., CHO, S. E., CHOI, I. Y. & SHIN, H. D. 2015. First Report of C*hoanephora* Rot of Okra Caused by *Choanephora cucurbitarum* in Korea. *Journal of Phytopathology,* 163**,** 503-506. doi: 10.1111/jph.12295.

PEARSON, C., SCHWENK, F., CROWE, F. & KELLEY, K. 1984. Colonization of soybean roots by *Macrophomina phaseolina*. *Plant Disease,* 68**,** 1086-1088.

PERINCHERRY, L., LALAK-KAŃCZUGOWSKA, J. & STĘPIEŃ, Ł. 2019. *Fusarium*-produced mycotoxins in plant-pathogen interactions. *Toxins,* 11**,** 664. doi: 10.3390/toxins11110664.

PETROPOULOS, S. A., DI GIOIA, F., POLYZOS, N. & TZORTZAKIS, N. 2020. Natural antioxidants, health effects and bioactive properties of wild *Allium* species. *Current pharmaceutical design,* 26**,** 1816-1837. doi: 10.2174/1381612826666200203145851.

PLANTWISEPLUS KNOWLEDGE BANK. 2021. *Stromatinia cepivora (white rot of onion and garlic)* [Online]. Available: https://doi.org/10.1079/pwkb.species.49145 [Accessed 19 July 2025].

POROMARTO, S., PUTRI, H. & WIDONO, S. 2022. Effectiveness and compatibility of *Bacillus* and *Trichoderma* in increasing disease tolerance of garlic to basal rot caused by *Fusarium oxysporum* f. sp. *cepae*. *IOP Conference Series: Earth and Environmental Science,* 1018**,** 012009. doi: 10.1088/1755-1315/1018/1/012009.

PROVA, A., AKANDA, A. M., ISLAM, S. & MOTAHER HOSSAIN, M. 2017. First report of *Sclerotinia sclerotiorum* causing pod rot disease on okra in Bangladesh. *Canadian journal of plant pathology,* 39**,** 72-76. doi: 10.1080/07060661.2017.1278723.

PUVAČA, N., LJUBOJEVIĆ, D., LUKAČ, D., BEUKOVIĆ, M., KOSTADINOVIĆ, L., TEODOSIN, S. & STANAĆEV, V. Bioactive compounds of garlic, black pepper and hot red pepper. Proceedings of the XVI International Symposium,"Feed Technology", Novi Sad, Serbia, 2014. 28-30. doi: 10.13140/2.1.1833.9526.

RAHMAN, K. & LOWE, G. M. 2006. Garlic and cardiovascular disease: a critical review. *The Journal of nutrition,* 136**,** 736S-740S. doi: 10.1093/jn/136.3.736S.

RAJENDRAN, K. & RANGANATHAN, K. 1996. Biological control of onion basal rot (*Fusarium oxysporum* f. sp. *cepae*) by combined application of fungal and bacterial antagonists. *Journal of Biological Control***,** 97-102.

RAMÍREZ, V., MUNIVE, J.-A., CORTES, L., MUÑOZ-ROJAS, J., PORTILLO, R. & BAEZ, A. 2020. Long-chain hydrocarbons (C21, C24, and C31) released by Bacillus sp. MH778713 break dormancy of mesquite seeds subjected to chromium stress. *Frontiers in microbiology,* 11**,** 741. doi: 10.3389/fmicb.2020.00741.

RANA, K., DING, Y., BANGA, S. S., LIAO, H., ZHAO, S., YU, Y. & QIAN, W. 2021. *Sclerotinia sclerotiorum* Thioredoxin1 (SsTrx1) is required for pathogenicity and oxidative stress tolerance. *Molecular plant pathology,* 22**,** 1413-1426. doi: 10.1111/mpp.13127.

RANJAN, A., JAYARAMAN, D., GRAU, C., HILL, J. H., WHITHAM, S. A., ANÉ, J. M., SMITH, D. L. & KABBAGE, M. 2018. The pathogenic development of *Sclerotinia sclerotiorum* in soybean requires specific host NADPH oxidases. *Molecular plant pathology,* 19**,** 700-714. doi: 10.1111/mpp.12555.

RASBAK. 2009. *Sclerotinia sclerotiorum at Phaseolus vulgaris bushbean* [Online]. Wikimedia Commons. Available: https://commons.wikimedia.org/wiki/File:Sclerotinia_sclerotiorum_at_Phaseolus_vulgaris,_scleroti%C3%ABnrot_stamsperzieboon.jpg [Accessed 19 July 2025].

RENGWALSKA, M. & SIMON, P. 1986. Laboratory evaluation of pink root and *Fusarium* basal rot resistance in garlic. *Plant disease,* 70**,** 670-672.

RIVERA-MÉNDEZ, W. 2016. Molecular identification of *Trichoderma* spp. in garlic and onion fields and *in vitro* antagonism trials on *Sclerotium cepivorum*. *Revista Brasileira de Ciência do Solo,* 40**,** e0150454. doi: 10.1590/18069657rbcs20150454.

ROSLAN, H. A., HUSAINI, A., LIHAN, S. & KOTA, M. F. 2020. Partial purification and characterization of antifungal peptides produced by *Bacillus amyloliquefaciens* PEP3 against *Phytophthora capsici*. *Applied Science and Engineering Progress,* 13**,** 56-66. doi: 10.14416/j.asep.2020.01.004.

SAGITOV, A., EL-HABBAA, G. & EL-FIKI, I. 2011. Studies on tomato wilt caused by *Fusarium oxysporum* f. sp. *lycopersici* in Kazachestan. 2: Effect of exogenous application of plant extracts and safe chemicals as resistance inducer treatments on the activity of the oxidative enzymes. *Исследования Результаты (КазНАУ), г. Алматы,* 1**,** 107-113.

SALEH, A. A., ELSHEIKH, M. H., EL-NAKIEB, F. A., SOBHY, S. E., KABEIL, S. S. & HAFEZ, E. E. 2024. New perspectives into the application of Effective Microorganism (EM) on phytopathogenic fungi: *in-vitro* antioxidant capacity, bioactive substances and fungicidal efficacy. *Biotechnology & Biotechnological Equipment,* 38**,** 2387190. doi: 10.1080/13102818.2024.2387190.

SALVALAGGIO, A. & RIDAO, A. D. C. 2013. First report of *Fusarium proliferatum* causing rot on garlic and onion in Argentina. *Plant Disease,* 97**,** 556-556. doi: 10.1094/PDIS-05-12-0507-PDN.

SAMMOUR, R. H., YEHIA, A.-G. M., MUSTAFA, A. & ALHOZIEM, R. 2011. Biology, controlling and genetic variability in *Sclerotium cepivorum* Berk; the causal agent of *Allium* white rot disease. *Microbiology,* 7**,** 101-111.

SANTHOSHA, S. G., JAMUNA, P. & PRABHAVATHI, S. 2013. Bioactive components of garlic and their physiological role in health maintenance: A review. *Food bioscience,* 3**,** 59-74. doi: 10.1016/j.fbio.2013.07.001.

SANTOS, P. S. D., COSTA, I. F. D., MINUZZI, S. G., BELLE, C., REBELATTO, G., LOPES, A. N. & FURLANI, L. 2023. Response of Soybean Cultivars to Oxidative Stress caused by *Meloidogyne javanica*. *Anais da Academia Brasileira de Ciências,* 95**,** e20201328. doi: 10.1590/0001-3765202320201328.

SARPKAYA, K. 2025. Effect of Fusarium proliferatum infection on physiological, phytochemical, and nutrient responses in garlic. *PeerJ,* 13**,** e19601. doi: 10.7717/peerj.19601.

SAVELLO, P. A., MARTIN, F. W. & HILL, J. M. 1980. Nutritional composition of okra seed meal. *Journal of Agricultural and Food Chemistry,* 28**,** 1163-1166. doi: 10.1021/jf60232a021.

SCHNATHORST, W. & MATHRE, D. 1966. Host range and differentiation of a severe form of *Verticillium albo-atrum* in cotton. *Phytopathology,* 56**,** 1155-1161.

SCHWARTZ, H. F. & GENT, D. H. 2008. Downy mildew. *Compendium of onion and garlic diseases and pests, 2nd edn. The American Phytopathological Society Press, Minnesota***,** 32-35.

SEEFELDER, W., GOSSMANN, M. & HUMPF, H.-U. 2002. Analysis of fumonisin B1 in *Fusarium proliferatum*-infected asparagus spears and garlic bulbs from Germany by liquid chromatography− electrospray ionization mass spectrometry. *Journal of Agricultural and Food Chemistry,* 50**,** 2778-2781. doi: 10.1021/jf0115037.

SHAHOVEISI, F., RIAHI MANESH, M. & DEL RÍO MENDOZA, L. 2022. Modeling risk of *Sclerotinia sclerotiorum*-induced disease development on canola and dry bean using machine learning algorithms. *Scientific Reports,* 12**,** 864. doi: 10.1038/s41598-021-04743-1.

SHALABY, M. E., GHONIEM, K. E. & EL-DIEHI, M. A. 2013. Biological and fungicidal antagonism of *Sclerotium cepivorum* for controlling onion white rot disease. *Annals of microbiology,* 63**,** 1579-1589. doi: 10.1007/s13213-013-0621-1.

SHARMA, S. 2015. Pathogenicity of root-knot nematode, *Meloidogyne incognita* and root-rot fungus, *Rhizoctonia solani* on okra [*Abelmoshcus esculentus* L.]. *e-Journal of Science & Technology (e-JST)* 97-102.

SHI, Y.-X., ZHANG, X.-H., ZHAO, Q. & LI, B.-J. 2019. First report of *Colletotrichum gloeosporioides* causing anthracnose on okra in China. *Plant Disease,* 103**,** 1023-1023. doi: 10.1094/PDIS-05-18-0878-PDN.

SIMAY, E. 1990. Garlic rot caused by *Fusarium proliferatum* (Matsushima) Nirenferg var. *minus* Nirenferg in Hungary. *Növényvédelem***,** 397-399.

SIMO, C., DJOCGOUE, P. F., MINYAKA, E. & OMOKOLO, N. 2018. Guaiacol Peroxidase heritability in tolerance of cocoa (*Theobroma cacao* L.) to Phytophthora megakarya, agent of cocoa black pod disease. *International Journal of Agricultural Policy and Research,* 6**,** 7-20. doi: 10.15739/ijapr.18.002.

SOLIMAN, M. H. & EL-MOHAMEDY, R. S. 2017. Induction of defense-related physiological and antioxidant enzyme response against powdery mildew disease in okra (*Abelmoschus esculentus* L.) plant by using chitosan and potassium salts. *Mycobiology,* 45**,** 409-420. doi: 10.5941/MYCO.2017.45.4.409.

SOLIMAN, S. A., KHALEIL, M. M. & METWALLY, R. A. 2022. Evaluation of the antifungal activity of *Bacillus amyloliquefaciens* and B. *velezensis* and characterization of the bioactive secondary metabolites produced against plant pathogenic fungi. *Biology,* 11**,** 1390. doi: 10.3390/biology11101390.

STANKOVIC, S., LEVIC, J., PETROVIC, T., LOGRIECO, A. & MORETTI, A. 2007. Pathogenicity and mycotoxin production by *Fusarium proliferatum* isolated from onion and garlic in Serbia. *European Journal of Plant Pathology,* 118**,** 165-172. doi: 10.1007/s10658-007-9126-8.

SUSI, H., BARRÈS, B., VALE, P. F. & LAINE, A.-L. 2015. Co-infection alters population dynamics of infectious disease. *Nature communications,* 6**,** 5975. doi: 10.1038/ncomms6975.

TANTAWY, I., ABDALLA, R. M., EL-ASHMONY, R. & GALAL, A. 2020. Effectiveness of Peroxy Acetic Aacid (PAA), Perbicarbonate (PB) and Potassium Silicate (PS) on Okra Growth, Yield and Resistance to Powdery Mildew. *Journal of Plant Production,* 11**,** 1417-1425. doi: 10.21608/jpp.2020.149814.

TEBBETS, B., YU, Z., STEWART, D., ZHAO, L.-X., JIANG, Y., XU, L.-H., ANDES, D., SHEN, B. & KLEIN, B. 2013. Identification of antifungal natural products via *Saccharomyces cerevisiae* bioassay: insights into macrotetrolide drug spectrum, potency and mode of action. *Sabouraudia,* 51**,** 280-289. doi: 10.3109/13693786.2012.710917.

THIPPESWAMY, B., KRISHNAPPA, M., CHAKRAVARTHY, C., SATHISHA, A., JYOTHI, S. & KUMAR, K. 2007. Pathogenicity and management of brown lesion and leaf spot in okra caused by *Macrophomina phaseolin*a and *Alternaria alternata*. *Journal of Plant Disease Sciences,* 2**,** 43-47.

TINDALL, H. D. 1983. *Vegetables in the Tropics*, Macmillan Press Ltd. doi: 10.1007/978-1-349-17223-8.

TINI, F., BECCARI, G., TERZAROLI, N., BERNA, E., COVARELLI, L. & QUAGLIA, M. 2024. Phytosanitary problems in elephant garlic (*Allium ampeloprasum* var. *holmense*) in the" Val di Chiana" area (Central Italy), and evaluation of potential control strategies. *Phytopathologia Mediterranea,* 63. doi: 10.36253/phyto-14911.

TOLLENAERE, C., SUSI, H. & LAINE, A.-L. 2016. Evolutionary and epidemiological implications of multiple infection in plants. *Trends in plant science,* 21**,** 80-90. doi: 10.1016/j.tplants.2015.10.014.

TONG, P. 2016. Okra (*Abelmoschus esculentus*)–a popular crop and vegetable. *UTAR Agriculture Science Journal (UASJ),* 2**,** 39-42.

TONTI, S., PRÀ, M. D., NIPOTI, P., PRODI, A. & ALBERTI, I. 2012. First Report of *Fusarium proliferatum* Causing Rot of Stored Garlic Bulbs (*Allium sativum* L.) in Italy. *Journal of Phytopathology,* 160**,** 761-763. doi: 10.1111/jph.12018.

VARGAS BAQUERO, C. D. & COTES, A. M. 2024. Microbial consortia as an option for biocontrol of *Stromatinia cepivora*. *Canadian Journal of Plant Pathology,* 46**,** 1-10. doi: 10.1080/07060661.2023.2262959.

VITULLO, D., DI PIETRO, A., ROMANO, A., LANZOTTI, V. & LIMA, G. 2012. Role of new bacterial surfactins in the antifungal interaction between *Bacillus amyloliquefaciens* and *Fusarium oxysporum*. *Plant Pathology,* 61**,** 689-699. doi: 10.1111/j.1365-3059.2011.02561.x.

WANG, H., MA, S., XIA, Q., ZHAO, Z., CHEN, X., SHEN, X., YIN, C. & MAO, Z. 2022. The interaction of the pathogen *Fusarium proliferatum* with *Trichoderma asperellum* characterized by transcriptome changes in apple rootstock roots. *Physiological and Molecular Plant Pathology,* 121**,** 101894. doi: 10.1016/j.pmpp.2022.101894.

WERNER, M. 1987. Necrotic leaf spot of apple caused by fungi of the genus *Alternaria*. *Ochrona Roslin (Poland),* 31**,** 6-7.

WILLE, L., MESSMER, M. M., STUDER, B. & HOHMANN, P. 2019. Insights to plant–microbe interactions provide opportunities to improve resistance breeding against root diseases in grain legumes. *Plant, cell & environment,* 42**,** 20-40. doi: 10.1111/pce.13214.

WILLIAMS, B., KABBAGE, M., KIM, H.-J., BRITT, R. & DICKMAN, M. B. 2011. Tipping the balance: *Sclerotinia sclerotiorum* secreted oxalic acid suppresses host defenses by manipulating the host redox environment. *PLoS pathogens,* 7**,** e1002107.

WORKNEH, Y. Y., LEGESSE, N. H., SHIFERAW, H. K. & ASHENAFI, B. D. 2024. Management of garlic white rot (*Stromatinia cepivora*) with fungicides and host resistance in North Shewa, central highland of Ethiopia. *Journal of Plant Pathology,* 106**,** 1335-1345. doi: 10.1007/s42161-024-01690-4.

WU, B. M., DAVIS, M. & TURINI, T. Developing New Integrated Strategies for Controlling White Rot in Garlic. Third Annual Symposium Spotlights Research Spring. California Garlic & Onion Research Advisory Board, 2010.

XU, L., LI, G., JIANG, D. & CHEN, W. 2018a. *Sclerotinia sclerotiorum*: an evaluation of virulence theories. *Annual Review of Phytopathology,* 56**,** 311-338. doi: 10.1146/annurev-phyto-080417-050052.

XU, T., LI, J., YU, B., LIU, L., ZHANG, X., LIU, J., PAN, H. & ZHANG, Y. 2018b. Transcription factor SsSte12 was involved in mycelium growth and development in *Sclerotinia sclerotiorum*. *Frontiers in Microbiology,* 9**,** 2476. doi: 10.3389/fmicb.2018.02476.

XU, Z., SHAO, J., LI, B., YAN, X., SHEN, Q. & ZHANG, R. 2013. Contribution of bacillomycin D in *Bacillus amyloliquefaciens* SQR9 to antifungal activity and biofilm formation. *Applied and environmental microbiology,* 79**,** 808-815. doi: 10.1128/aem.02645-12.

YANG, L., MA, X., WANG, L., YANG, G., ZHOU, L., ZHANG, Z. & LI, X. 2024a. *In vitro* antifungal activity and mechanism of action of carvacrol against *Sclerotinia sclerotiorum* (Lib.) de Bary. *Plant Protection Science,* 60. doi: 10.17221/121/2023-pps.

YANG, X., ZHANG, W., LV, H., GAO, Y., KANG, Y., WU, Y., WANG, F., ZHANG, W. & LIANG, H. 2024b. Lignin synthesis pathway in response to *Rhizoctonia solani* Kühn infection in potato (*Solanum tuberosum* L.). *Chemical and Biological Technologies in Agriculture,* 11**,** 135. doi: 10.1186/s40538-024-00663-0.

YANG, Y., CHEN, S., WU, X., PENG, L., VÍLCHEZ, J. I., KAUSHAL, R., LIU, X., SINGH, S. K., HE, D. & YUAN, F. 2022. Plant latent defense response to microbial non-pathogenic factors antagonizes compatibility. *National Science Review,* 9**,** nwac109. doi: 10.1093/nsr/nwac109.

YUAN, X. & CHEN, F. 2021. Cocultivation study of *Monascus* spp. and *Aspergillus niger* inspired from Black-Skin-Red-Koji by a double-sided petri dish. *Frontiers in Microbiology,* 12**,** 670684. doi: 10.3389/fmicb.2021.670684.

ZAFAR, I., PERVEZ, M. T., RATHER, M. A., BABAR, M. E., RAZA, M. A. & IFTIKHAR, R. 2020. Genome-wide identification and expression analysis of PPOs and POX gene families in the selected plant species. *Biosciences Biotechnology Research Asia,* 17**,** 301-318. doi: 10.13005/bbra/2834.

ZHANG, C., WANG, W., XUE, M., LIU, Z., ZHANG, Q., HOU, J., XING, M., WANG, R. & LIU, T. 2021. The combination of a biocontrol agent *Trichoderma asperellum* SC012 and hymexazol reduces the effective fungicide dose to control *Fusarium* wilt in cowpea. *Journal of Fungi,* 7**,** 685. doi: 10.3390/jof7090685.

ZHANG, Y., HUAI, D., YANG, Q., CHENG, Y., MA, M., KLIEBENSTEIN, D. J. & ZHOU, Y. 2015. Overexpression of three glucosinolate biosynthesis genes in *Brassica napus* identifies enhanced resistance to *Sclerotinia sclerotiorum* and *Botrytis cinerea*. *PLoS One,* 10**,** e0140491. doi: 10.1371/journal.pone.0140491.

ZHANG, Y., TIAN, C., XIAO, J., WEI, L., TIAN, Y. & LIANG, Z. 2020. Soil inoculation of *Trichoderma asperellum* M45a regulates rhizosphere microbes and triggers watermelon resistance to *Fusarium* wilt. *Amb Express,* 10**,** 189.

ACKNOWLEDGMENTS

Above all, I am grateful to Almighty God for granting me the strength, patience, and perseverance to see this PhD journey through to completion. His guidance and blessings gave me the ability to overcome the challenges along the way.

I am deeply grateful to my supervisor, Dr. György Turóczi, for his constant support, understanding, and exceptional guidance throughout my research. His advice, encouragement, and insightful discussions helped me stay focused and move forward, even during the most challenging moments. I truly appreciate his patience and the time he devoted to helping me shape this work.

My sincere thanks also go to Prof. Dr. József Kiss, Head of the Department of Integrated Plant Protection, for giving me the opportunity to pursue this research. His valuable advice and scientific insights enriched my work and provided direction whenever I needed clarity. I am especially thankful for his trust and the opportunity to be part of this academic environment.

I would like to thank Ms. Nagy Andrea, Ms. Edit Simáné Dolányi, International Coordinator at the Doctoral and Habilitation Centre, Ms. Tallárомné Czingili Judit, Institutional Coordinator at the International Relations Centre, and Ms. Zsuzsanna Tassy, International Coordinator at the Centre for International Education for their assistance, patience, kindness, and continuous support with all the administrative and practical aspects of this journey.

A very special thanks goes to my father, Abdelhafid, and brother, Safieddine, for their invaluable academic and scientific insights, which guided my thinking and improved the quality of my work. Beyond intellect, my family has been my rock and my biggest source of emotional strength, lifting me up when experiments failed, celebrating when they succeeded, and never doubting me through the most challenging moments. For their unwavering faith and love, I am profoundly grateful.

Finally, to the friends and dear ones I had the privilege of meeting throughout this journey, thank you for your unwavering support, heartfelt kindness, and for bringing lightness and meaning to the path. I am deeply grateful to each of you—for the laughter, the late-night conversations, and above all, for the enduring sense of belonging you have given me